

\$5

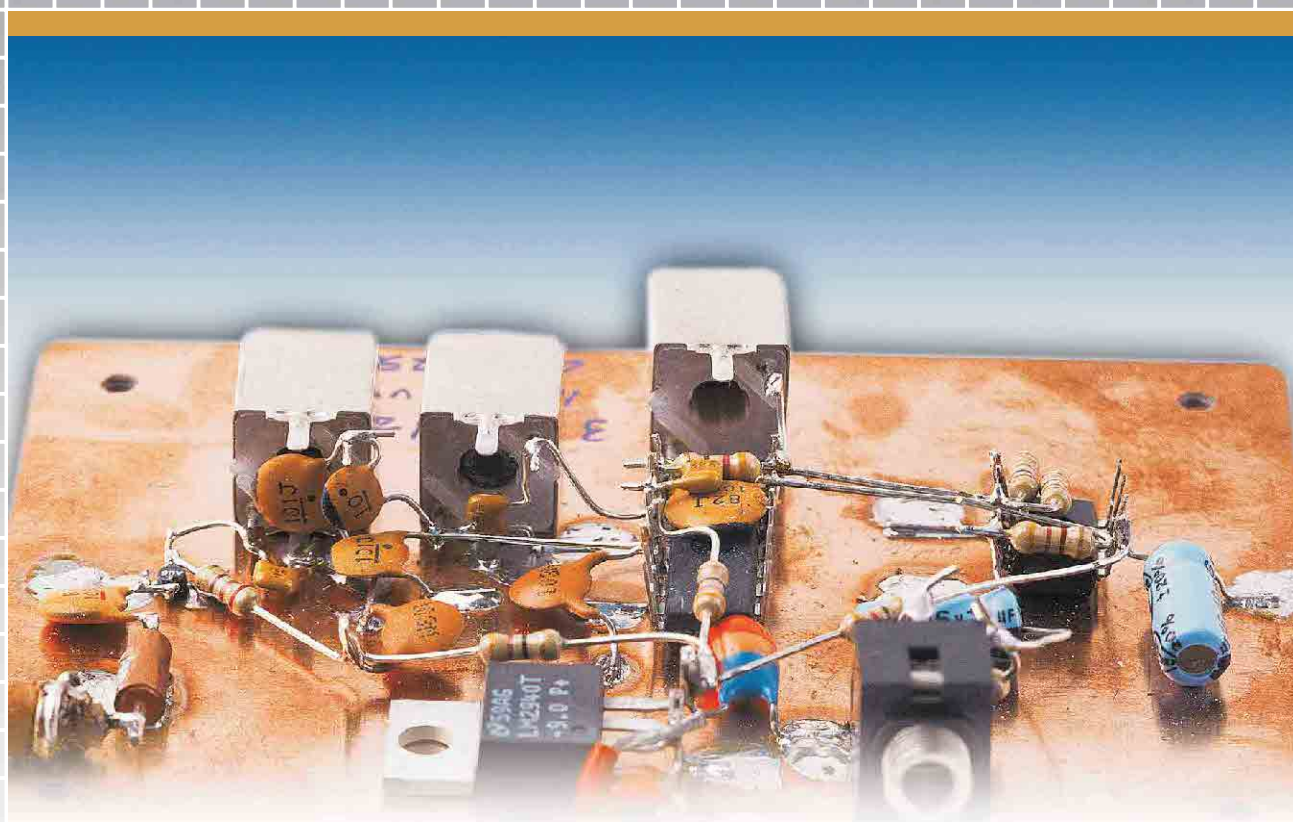


QEX

INCLUDING:
COMMUNICATIONS
QUARTERLY

Forum for Communications Experimenters

July/August 2002



This month in RF: **W1VT** presents a simple
24-GHz Wide-Band FM Transceiver

ARRL *The national association for*
AMATEUR RADIO

225 Main Street
Newington, CT USA 06111-1494



RSGB PRODUCTS

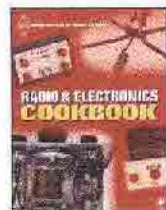
Imported by ARRL— from the Radio Society of Great Britain



Radio Communication Handbook

One of the most comprehensive guides to the theory and practice of Amateur Radio communication. Find the latest technical innovations and techniques, from LF (including a new chapter for LowFERS!) to the GHz bands. For professionals and students alike. 820 pages.

ARRL Order No. 5234—\$53



Radio & Electronics Cookbook

Build up your electronics skills and knowledge with this unique collection of electronic projects. Ideal for all levels of experimenters. Quick, rewarding construction projects. 319 pages.

ARRL Order No. RREC—\$28



RSGB Technical Compendium

A collection of proven and experimental radio equipment designs, and practical advice (articles from 12 editions of *RadCom* 1999). 288 pages.

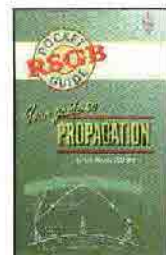
ARRL Order No. RTCP—\$30



Backyard Antennas

With a variety of simple techniques, you can build high performance antennas. Create compact multi-band antennas, end-fed and center-fed antennas, rotary beams, loops, tuning units, VHF/UHF antennas, and more! 208 pages.

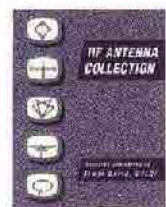
ARRL Order No. RBYA—\$32



Your Guide to Propagation

This handy, easy-to-read guide takes the mystery out of radio wave propagation. It will benefit anyone who wants to understand how to get better results from their station.

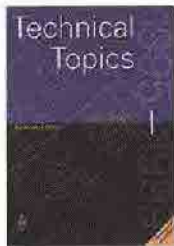
ARRL Order No. 7296—\$17



HF Antenna Collection

Articles from RSGB's *RadCom* magazine. Single- and multi-element horizontal and vertical antennas, very small transmitting and receiving antennas, feeders, tuners and more. 240 pages.

ARRL Order No. 3770—\$18



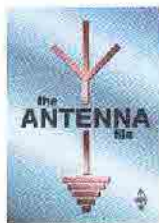
Technical Topics Scrapbook

Invaluable collections of experimental HF/VHF antennas, circuit ideas, radio lore, general hints and comments—all from the popular *RadCom* magazine column, *Technical Topics*.

1985-1989 edition, Order No. RT85—\$18

1990-1994 edition, Order No. 7423—\$25

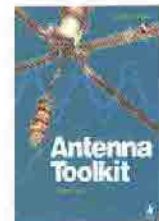
1995-1999 edition, Order No. RT95—\$25



The Antenna File

The best work from the last ten years of RSGB's *RadCom* magazine. 50 HF antennas, 14 VHF/UHF/SHF, 3 on receiving, 6 articles on masts and supports, 9 on tuning and measuring, 4 on antenna construction, 5 on design and theory. Beams, wire antennas, verticals, loops, mobile whips and more. 288 pages.

ARRL Order No. 8558—\$34.95



Antenna Toolkit 2

The complete solution for understanding and designing antennas. Book includes a powerful suite of antenna design software (CD-ROM requires *Windows*). Select antenna type and frequency for quick calculations. 256 pages.

ARRL Order No. 8547—\$43.95



HF Antennas for All Locations

Design and construction details for hundreds of antennas, including some unusual designs. Don't let a lack of real estate keep you off the air! 322 pages.

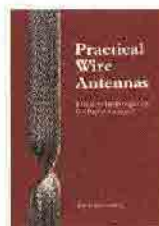
ARRL Order No. 4300—\$15



The Antenna Experimenter's Guide

Build and use simple RF equipment to measure antenna impedance, resonance and performance. General antenna construction methods, how to test theories, and using a computer to model antennas. 158 pages.

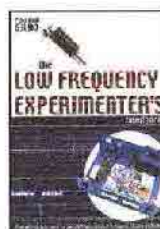
ARRL Order No. 6087—\$30



Practical Wire Antennas

The practical aspects of HF wire antennas: how the various types work, and how to buy or build one that's right for you. Marconis, Windoms, loops, dipoles and even underground antennas! The final chapter covers matching systems. 100 pages.

Order No. R878—\$17



The Low Frequency Experimenter's Handbook

Invaluable reference and techniques for transmitting and receiving between 50 and 500 kHz. 112 pages.

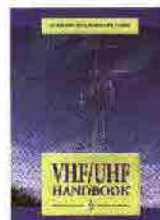
ARRL Order No. RLFS—\$32



RadCom 2001 on CD-ROM

All twelve editions of *RadCom* magazine, published in 2001, with a fully searchable index.

ARRL Order No. 8742—\$33



VHF/UHF Handbook

The theory and practice of VHF/UHF operating and transmission lines. Background on antennas, EMC, propagation, receivers and transmitters, and construction details for many projects. Plus, specialized modes such as data and TV. 317 pages.

ARRL Order No. 6559—\$35

Order Toll Free
1-888-277-5289
www.arrl.org/shop

Shipping: US orders add \$5 for one item, plus \$1 for each additional item (\$10 max.). International orders add \$2.00 to US rate (\$12.00 max.). US orders shipped via UPS.



The VHF/UHF DX Book

Assemble a VHF/UHF station, and learn about VHF/UHF propagation, operating techniques, transmitters, power amplifiers and EMC. Includes designs for VHF and UHF transverters, power supplies, test equipment and much more. 448 pages.

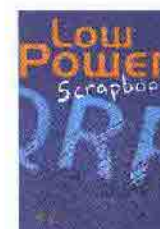
Order No. 5668—\$35



RSGB IOTA Directory—11th Edition

An essential guide to participating in the IOTA (Islands on the Air) award program.

ARRL Order No. 8745—\$16



Low Power Scrapbook

Build it yourself! Low power transmitters, simple receivers, accessories, circuit and construction hints and antennas. Projects from the G-QRP Club's magazine *Sprat*. 320 pages.

ARRL Order No. LPSB—\$19.95

ARRL

225 Main St.,
Newington, CT 06111-1494

tel: 860-594-0355 fax: 860-594-0303

e-mail: pubsales@arrl.org

www.arrl.org/

OEX 7/2002



INCLUDING: COMMUNICATIONS
QUARTERLY

QEX (ISSN: 0886-8093) is published bimonthly in January, March, May, July, September, and November by the American Radio Relay League, 225 Main Street, Newington CT 06111-1494. Yearly subscription rate to ARRL members is \$24; nonmembers \$36. Other rates are listed below. Periodicals postage paid at Hartford, CT and at additional mailing offices.

POSTMASTER: Send address changes to: QEX, 225 Main St, Newington, CT 06111-1494 Issue No 213

Mark J. Wilson, K1RO
Publisher

Doug Smith, KF6DX
Editor

Robert Schetgen, KU7G
Managing Editor

Lori Weinberg, KB1EIB
Assistant Editor

Peter Bertini, K1ZJH
Zack Lau, W1VT

Ray Mack, WD5IFS
Contributing Editors

Production Department

Steve Ford, WB8IMY
Publications Manager

Michelle Bloom, WB1ENT
Production Supervisor

Sue Fagan
Graphic Design Supervisor

David Pingree, N1NAS
Technical Illustrator

Joe Shea
Production Assistant

Advertising Information Contact:

Hanan Al-Rayyashi, KB1AFX, *Advertising Supervisor*
860-594-0207 direct
860-594-0200 ARRL
860-594-4285 fax

Circulation Department

Debra Jahnke, *Circulation Manager*
Kathy Capodicasa, *Senior Fulfillment Supervisor*
Cathy Stepina, *QEX Circulation*

Offices

225 Main St, Newington, CT 06111-1494 USA
Telephone: 860-594-0200
Telex: 650215-5052 MCI
Fax: 860-594-0259 (24 hour direct line)
e-mail: qex@arrl.org

Subscription rate for 6 issues:

In the US: ARRL Member \$24,
nonmember \$36;

US by First Class Mail:
ARRL member \$37, nonmember \$49;

Elsewhere by Surface Mail (4-8 week delivery):
ARRL member \$31, nonmember \$43;

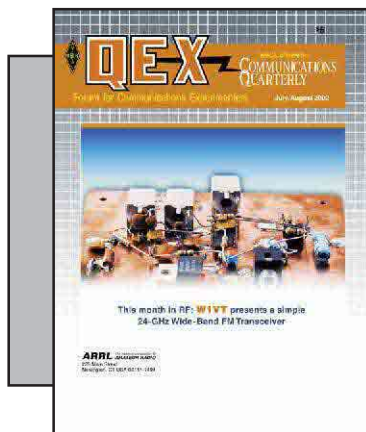
Canada by Airmail: ARRL member \$40,
nonmember \$52;

Elsewhere by Airmail: ARRL member \$59,
nonmember \$71.

Members are asked to include their membership control number or a label from their QST wrapper when applying.

In order to ensure prompt delivery, we ask that you periodically check the address information on your mailing label. If you find any inaccuracies, please contact the Circulation Department immediately. Thank you for your assistance.

Copyright ©2002 by the American Radio Relay League Inc. For permission to quote or reprint material from QEX or any ARRL publication, send a written request including the issue date (or book title), article, page numbers and a description of where you intend to use the reprinted material. Send the request to the office of the Publications Manager (permission@arrl.org)



About the Cover

W1VT's description of a simple 24-GHz Wide-Band FM Transceiver begins on p 54.



Features

3 The Dirodyne: A New Radio Architecture?

By Rod Green, VK6KRG

13 A Software-Defined Radio for the Masses, Part 1

By Gerald Youngblood, AC5OG

22 Notes on the OWA Yagi

By L. B. Cebik, W4RNL

35 A High-Performance Digital-Transceiver Design, Part 1

By James Scarlett, KD7O

46 Improved Dynamic-Range Testing

By Doug Smith, KF6DX

Columns

53 Tech Notes

55 RF *By Zack Lau, W1VT*

61 Letters to the Editor

64 Next Issue in QEX

Jul/Aug 2002 QEX Advertising Index

American Radio Relay League: 60,
Cov II, Cov III

Atomic Time, Inc.: 54

Down East Microwave Inc.: 34

HAL Communications Corp.: 45, Cov IV

Roy Lewallen, W7EL: 34

Nemal Electronics International, Inc.: 34
Palomar: 21

Teri Software: 12

Tucson Amateur Packet Radio Corp: 44,
64

Universal Radio, Inc.: 52

THE AMERICAN RADIO RELAY LEAGUE



The American Radio Relay League, Inc. is a noncommercial association of radio amateurs, organized for the promotion of interests in Amateur Radio communication and experimentation, for the establishment of networks to provide communications in the event of disasters or other emergencies, for the advancement of radio art and of the public welfare, for the representation of the radio amateur in legislative matters, and for the maintenance of fraternalism and a high standard of conduct.

ARRL is an incorporated association without capital stock chartered under the laws of the state of Connecticut, and is an exempt organization under Section 501(c)(3) of the Internal Revenue Code of 1986. Its affairs are governed by a Board of Directors, whose voting members are elected every two years by the general membership. The officers are elected or appointed by the Directors. The League is noncommercial, and no one who could gain financially from the shaping of its affairs is eligible for membership on its Board.

"Of, by, and for the radio amateur," ARRL numbers within its ranks the vast majority of active amateurs in the nation and has a proud history of achievement as the standard-bearer in amateur affairs.

A bona fide interest in Amateur Radio is the only essential qualification of membership; an Amateur Radio license is not a prerequisite, although full voting membership is granted only to licensed amateurs in the US.

Membership inquiries and general correspondence should be addressed to the administrative headquarters at 225 Main Street, Newington, CT 06111 USA.

Telephone: 860-594-0200
Telex: 650215-5052 MCI
MCIMAIL (electronic mail system) ID: 215-5052
FAX: 860-594-0259 (24-hour direct line)

Officers

President: JIM D. HAYNIE, W5JBP
3226 Newcastle Dr., Dallas, TX 75220-1640
Executive Vice President: DAVID SUMNER, K1ZZ

The purpose of QEX is to:

- 1) provide a medium for the exchange of ideas and information among Amateur Radio experimenters,
- 2) document advanced technical work in the Amateur Radio field, and
- 3) support efforts to advance the state of the Amateur Radio art.

All correspondence concerning QEX should be addressed to the American Radio Relay League, 225 Main Street, Newington, CT 06111 USA. Envelopes containing manuscripts and letters for publication in QEX should be marked Editor, QEX.

Both theoretical and practical technical articles are welcomed. Manuscripts should be submitted on IBM or Mac format 3.5-inch diskette in word-processor format, if possible. We can redraw any figures as long as their content is clear. Photos should be glossy, color or black-and-white prints of at least the size they are to appear in QEX. Further information for authors can be found on the Web at www.arrl.org/qex/ or by e-mail to qex@arrl.org.

Any opinions expressed in QEX are those of the authors, not necessarily those of the Editor or the League. While we strive to ensure all material is technically correct, authors are expected to defend their own assertions. Products mentioned are included for your information only; no endorsement is implied. Readers are cautioned to verify the availability of products before sending money to vendors.

Empirical Outlook

New Technology and the Old Struggle for Dynamic Range

There is much excitement about what's just around the corner in Amateur Radio. This year's Dayton Hamvention saw a Digital Voice Forum that documented remarkable progress and demonstrated some formats that produce astonishingly good audio quality. Steve Bible, N7HPR, of TAPR graciously recorded the audio from the forum. He put the audio together with the presentation slides and the whole thing is on the Web. Visit www.tapr.org and www.arrl.org/tis/info/digivoice.html to check it out.

The ARRL Digital Voice Working Group (DVWG) has been joined by a Software-Defined Radio Working Group (SDRWG) and a High-Speed Multimedia Working Group (HSMMWG). These groups are tasked with making recommendations to the League's Technology Task Force (TTF) about incorporating contemporary technologies into Amateur Radio. We have learned that many of you are ready to try those new things and that you look forward to enjoying the benefits of them.

So-called software-defined radio (SDR) is a hot topic these days. We are happy to have several articles in this issue describing how some are getting involved. We also note renewed support for a universal application-programming interface (API) for computer control of transceivers. Such an API standard would allow programmers to write generic software for rig control. Translation between a standard set of commands and rig-specific protocols would be handled by the API, which in turn would be compiled by the rig's manufacturer. That way, writing application software for various transceivers would be made easier and programmers would not have to scramble much every time a new rig or feature is introduced.

SDRs have been around for a while now. It is time for us to further exploit their possibilities. Those possibilities include access to digital signals and algorithms, digital networking and other features that would help Amateur Radio fulfill its purposes. Radios that have some of these features are starting to appear. As they become more widely available, we shall begin to experience new chances for experimentation. It is important that we lay

the groundwork for that revival.

Receiver dynamic range is a key issue in the design of SDRs. In fact, it is the central issue for SDR designers today. Data-converter development has just about reached the point where signals may be digitally sampled directly from the antenna. It is important that we learn such digital-signal-processing techniques so that we can continue to build our legacy of innovation. We suspect that similar groundbreaking advances in analog circuits also lie close at hand, waiting to be discovered.

Some friends suggest that QEX is the logical place for discussion of proposed and ongoing research projects and of unfinished ideas for the future. We agree and make a call for articles and letters about that sort of thing. Please write us with your suggestions and comments.

In This Issue

Rod Green, VK6KRG, puts forth a significant modification of the Tayloe design. He shows how chaining two Tayloe detectors achieves significant advantages. Rod explains what is possible with that configuration.

Gerald Youngblood, AC5OG, is a member of the SDRWG. He contributes Part 1 of a series on his designs. Central to his work is the Tayloe detector, an invention of Dan Tayloe, N7VE. Gerald includes references to prior art.

L. B. Cebik presents an analysis of optimized wide-band antennas (OWAs). He describes very interesting ways to design broadband directional arrays having maximum side- and back-lobe suppression. It is intriguing what you can achieve.

Jim Scarlett, KD7O, has also been homebrewing and he details his recent efforts. Jim has paid particular attention to the dynamic range required by HF receivers and he lets us in on his thinking during the design process.

I have a few comments on dynamic-range testing and ways to improve accuracy. Many thanks to Ed Hare, W1RFI, and the ARRL laboratory staff for their assistance on this one. In *Tech Notes*, Peter Bertini, K1ZJH, brings us another piece by Rick Littlefield, N1BQT. In *RF*, Zack Lau, W1VT, presents a 24-GHz transceiver. Build the thing and jump on the microwave bandwagon—73, Doug Smith, KF6DX, kf6dx@arrl.org. □□

The Dirodyne: A New Radio Architecture?

Multiple Tayloe detectors simultaneously perform filtering and frequency-translation duties.

By Rod Green, VK6KRG

The superheterodyne principle has been a mainstay of commercial and most Amateur Radio receivers and transceivers since its inception in the 1920s. This, despite its relative complexity, has generally better performance than any other type. My new receiver has, in my opinion, much to offer and has the potential to outperform most “superhets.” This article is designed to give the reader sufficient information to get started and to build a basic prototype. Although the relative newcomer can attempt this receiver, it is mainly for those amateurs who wish to experiment and add to the as-yet-small pool

of knowledge regarding this technology.

Some History

After developing the Bedford receiver,¹ a reader of *QEX*, Harold, W4ZCB, informed me via e-mail of the existence of the Tayloe Detector, invented by Dan Tayloe, N7VE.^{2,3,4} He had used it in place of the NE602 in his version of the Bedford front end. I received a copy of Dan Tayloe’s original circuit from Harold. I reasoned that the four-phase audio outputs from the detector were not unlike those appearing from an audio phase shifter to generate SSB using the phasing method. Thus, I felt that the audio from a Tayloe detector could be re-modulated to any conven-

nient IF as an SSB signal without the use of audio phase-shift networks. This indeed is just what happened: The *Dirodyne* was born. I have subsequently applied for a patent with the Australian Patent Office.

I then contacted Dan Tayloe. I described what I had done and that a patent application had been lodged. To my surprise, Dan had also built a similar receiver, but for a variety of reasons, did not go ahead with a patent application.

The Dirodyne is, as far as I am aware, a new receiver architecture. It is based on what I call a Tayloe filter, which in turn consists of two Tayloe detectors back to back. See [Fig 1](#) for a block diagram of a Tayloe detector. This detector consists of four mixers on a single IC, and it is fed with

106 Rosebery St
Bedford, Western Australia 6052
rodagreen@bigpond.com

¹Notes appear on [page 12](#).

quadrature VFO signals. The mixer has four baseband (audio) outputs in quadrature. In the Tayloe filter, these outputs feed into a Tayloe detector in the reverse direction. That is, the four baseband outputs from the first mixer feed into the four (normally output but now input) ports of a second Tayloe detector. The single combined port (normally the input) becomes the output. The result of doing this is what I call the Tayloe filter. See Fig 2.

If the carrier frequency fed to the first mixer is the same as that fed to the second, a filtering action takes place. The filter acts as a tuned circuit with a center frequency equal to one-quarter of the local oscillator frequency. It can have staggering Q factor: See Fig 3, which shows a -6 -dB bandwidth of approximately 2.4 kHz. A 6-dB bandwidth of 200 Hz is easily possible at even 30 MHz. The actual Q value is set with one resistor, and the bandwidth—once set—is constant at all frequencies. I have done a spectrum sweep of the filter and its bandwidth is almost the same at 3.5 MHz as at 30 MHz. The stop-band attenuation is around 30 dB on the prototype and this adds very significantly to front-end performance. The 6-dB bandwidth is a simple calculation and is

$$BW = \frac{1}{\left(\frac{\pi R_{in}}{4}\right)C} \quad (\text{Eq 1})$$

The Tayloe filter has yet another feature that makes it particularly useful in a receiver front end. If the carrier oscillator frequency to the first mixer were variable and that feeding the second mixer in the pair were fixed, a filter with fixed output frequency and with variable input frequency would result. Therefore, if the second mixer were fed with 1820 kHz, (4×455 kHz) and the first mixer fed with a frequency equal to $4 \times$ that of the operating frequency, say 4×3.5 MHz, the resulting Tayloe filter would be a sharply tuned filter at 3.5 MHz with an output frequency of 455 kHz. The output could then be fed to a conventional IF/product-detector chain. This is the Dirodyne principle. In its basic form, the Tayloe filter is reversible and thus can be used in the transmitting direction by simply using the output as its input and taking the output from the input. Thus, a 455-kHz SSB signal would be directly translated to 3.5 MHz in the preceding filter.

Circuitry to do all of this is amazingly

simple, but the actual theory of operation can be quite mind-bending. Fig 4 shows a basic block diagram of how a Dirodyne receiver might look. Keep in mind that everything in this article is new and experimental. As such, this work is possibly describing the equivalent of the model-T Ford of many years ago. The field is wide open for your additions, criticisms and comments.

There are many questions I hear you asking already, such as, “What happened to the audio image?” “Does it ring, as a high- Q filter would normally do?” “How does the thing work?” Don’t worry too much about these questions at this point, as all will be revealed as you read on. Fittingly, the first thing to do is to become familiar with the Tayloe detector.

The Tayloe Detector

I believe the Tayloe detector to be the most ingenious device to come out of the latter half of the last century. This mixer has had a very slow introduction to ham radio; but it is a truly amazing device and I recommend that readers study it in detail (see Note 2).

The Tayloe detector consists of four FET SPST switches on a single IC. These are operated one at a time such that only one switch is on at a time. See

the waveforms of Fig 1. Since the local oscillator operates at four times the input frequency, the switches complete one cycle of operation at the same rate as the antenna-input frequency. In Fig 1, the switches are combined on the input side and the other sides of the four switches are outputs. Since the switches operate in sequence continually, it is helpful to think of them as a single-pole, four-way rotary switch rotating once for each cycle of the antenna-input frequency. Thus, it can be seen that each switch samples a period of 90° , or one-quarter of each input cycle. The capacitor at each switch output, C1 to C4, charges via the input resistor R_{in} . Notice that this is not an actual resistor, but the resistance seen by the source and further shunted until the bandwidth is as desired. Thus, the impedance driving it determines the selectivity of the Tayloe detector. This, as it turns out, is a blessing in disguise, as you will see as you read on.

Each output would therefore sample the input waveform for the one-quarter cycle in which it is operated. If the input frequency is close to one quarter of the clock frequency, a beat note will appear on each mixer output. The frequency of this beat note will be the difference between one quarter of the

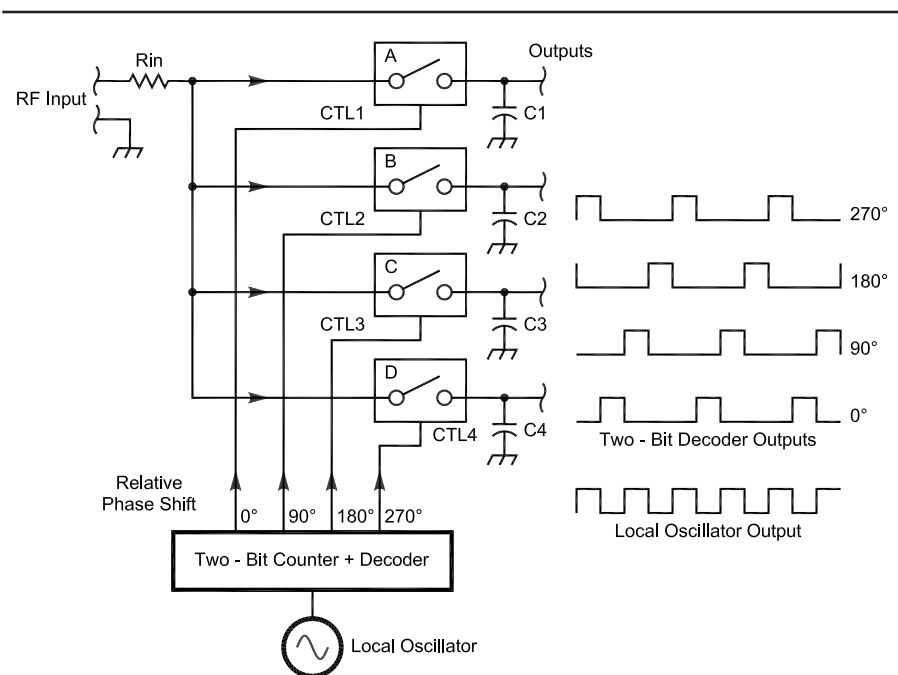


Fig 1—Basic Tayloe detector block diagram. R_{in} is the input resistor, see text. Lines CTL1 through CTL4 switch the input among the four outputs as shown in the waveforms. A through D are the mixer switches, 0° , 90° , 180° and 270° , respectively. C1 through C4 are the output filter capacitors. I through L are the outputs. The LO drives the two-bit counter to produce an output that drives CTL1 through CTL4 in the proper sequence.

local oscillator frequency and the input frequency. The sum frequency of the LO and the RF input is absorbed by the input resistor R_{in} and shunted to earth by the output capacitors and so does not appear at the output. Additionally, each of the four outputs will be 90° out of phase with its neighbor. When the input frequency crosses over from one side of zero beat to the other, the output phase relationships each reverse (change by 180°). Thus 0° , 90° , 180° and 270° become 180° , 270° , 0° and 90° , respectively. In fact, if these four outputs were to feed a 90° audio phase-shift network such as a polyphase network, we would have a conventional direct-conversion SSB receiver.

The Tayloe detector gets its high Q factor from the fact that the four capacitors are being charged via the common resistor R_{in} . At or near resonance, the capacitors are being charged and discharged a little at a time and thus taking only a little input current. However, well away from resonance, the capacitors are randomly charged and discharged, and the input impedance becomes very low. Thus, the input impedance of the Tayloe detector has a rapid upward change near resonance. The four outputs also follow a typical tuned-circuit curve. The circuit isn't actually resonant (like an LC filter), so it does not extend the noise pulses by ringing, as does a bell or LC circuit. There are many advantages to having a circuit of such high Q so close to the antenna. The sheer simplicity of obtaining good third-order-distortion performance is obvious.

At first sight, Tayloe detectors have a disadvantage of having high impedance at resonance. How does one measure input power, and thus sensitivity, in a 50- or 75- Ω system? In fact, I found it impossible to do such a measurement. To overcome this seeming shortcoming, I put a grounded-gate FET amplifier ahead of the mixer, terminating it with a resistor of value R_{in} . In this case, I used 220 Ω to give an approximate 3-kHz bandwidth. The grounded-gate amplifier has the characteristic of constant input impedance no matter what the load does. Further, the gain of such an amplifier is proportional to load impedance. Thus, the gain of the amplifier decreases away from resonance, because of the falling load impedance of the Tayloe detector, thereby even further improving out-of-band intermodulation distortion products, I think.

The Tayloe Filter

The phase reversal at resonance from the Tayloe detector mentioned above is pivotal to the operation of the Tayloe filter. In a phasing system for receiving SSB, this phase reversal at zero beat is what the audio phase shifter uses to cancel the unwanted sideband. Think about this: If two signals, differing in phase by 90° , were summed into a differential audio phase shifter of 90° , the output would be shifted a further 90° and thus have a phase difference of either 180° (cancellation when summed) or 0° (enhanced when summed). If all four phases were shifted in this manner, the result would be two paths of cancellation or enhancement.

Now to generate SSB, an audio signal is split with a differential phase shifter into two (or four) paths 90° apart at all frequencies of interest. These are then fed to balanced mixers and combined into a single output. The emerging signal is SSB with a suppressed carrier at the local-oscillator injection frequency. To change sidebands, the two (or four) audio paths are simply reversed in phase.

The Tayloe detector mentioned above already has quadrature audio outputs, so there is no need for an audio phase-shift network to regenerate SSB at the same or at any other frequency; so far, so good.

Now for the mind-bending bit: Suppose the Tayloe filter was gen-

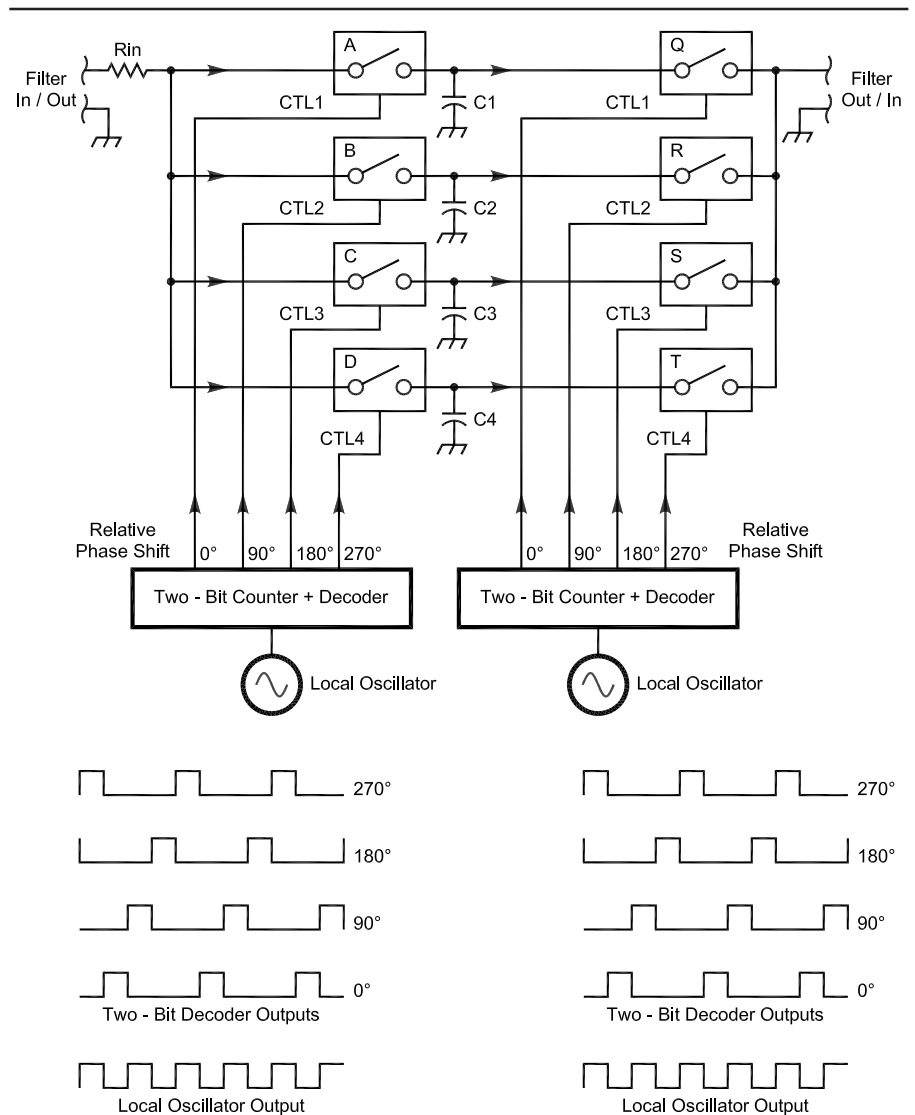


Fig 2—Basic Tayloe filter block diagram. R_{in} sets the bandwidth, see text. A through D are the first-mixer switches. C1 through C4 are the output filter capacitors. Q through T are the second-mixer switches. The LOs and two-bit counters function as in Fig 1, but the oscillators may operate at different frequencies.

erating upper sideband and the input frequency to the filter was falling toward zero-beat. The output of the filter would follow, dropping in frequency from some value above the second carrier toward the carrier frequency. As the first carrier hits zero-beat and crosses it, the four audio tones from the first Tayloe detector would zero beat, then climb up again with the four audio phases reversed, as previously described. This now causes the *lower* sideband to be generated by the second Tayloe detector. Thus, as the audio pitch would keep rising, the output frequency from the second Tayloe detector would keep falling below the second carrier frequency. The output frequency would follow the input frequency in direction, even if it were at a different frequency. Phew—a piece of cake!

A Tayloe filter does two things very well. Firstly, it has high selectivity; and secondly, it converts the input frequency to any desired IF even down to 10 kHz or lower. This one stage sidesteps many problems encountered with conventional “superhets.” The image frequency is strongly suppressed—to the tune of 60 dB in the prototype. It can be made to have high dynamic range as it is a switching mixer, and this is improved consider-

ably by its own selectivity.

A Prototype Receiver

Figs 5 and 6 are schematics of the prototype receiver. Fig 5 shows the front end and Fig 6 shows the circuit

from the IF amplifier onward. Each section is labeled for easy reference to the block diagram.

In Fig 5, connector P3 is the antenna input to a 3.5-4.0 MHz band-pass filter consisting of L3, L2 and compo-

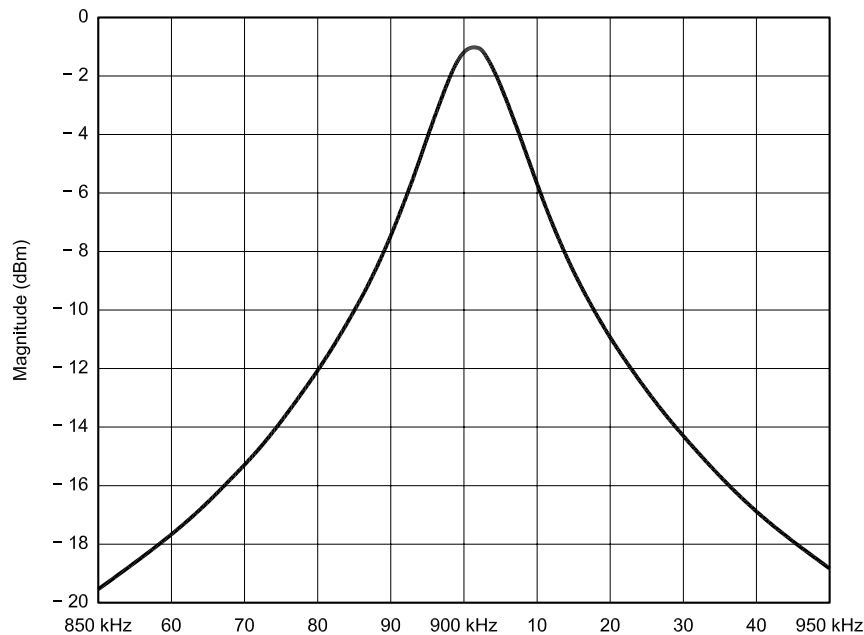


Fig 3—Tayloe filter prototype selectivity sweep.

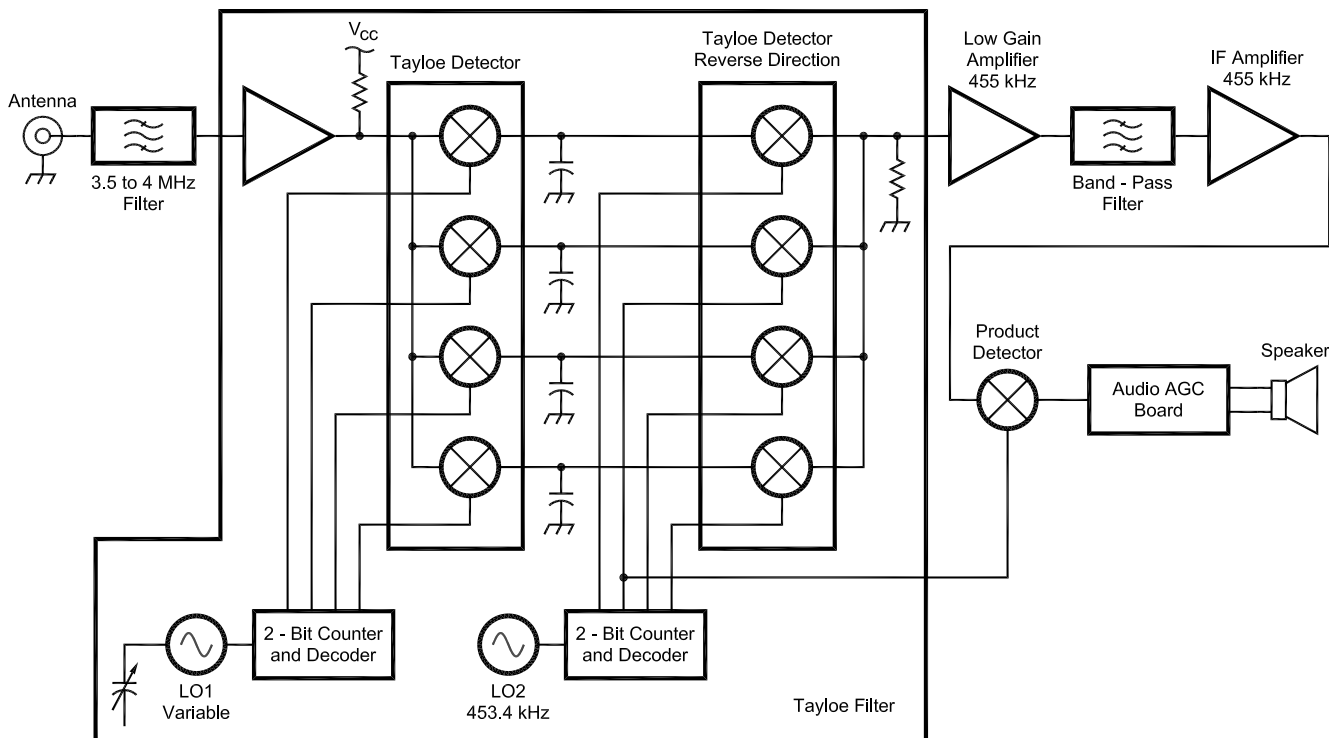


Fig 4—Dirdyne receiver block diagram.

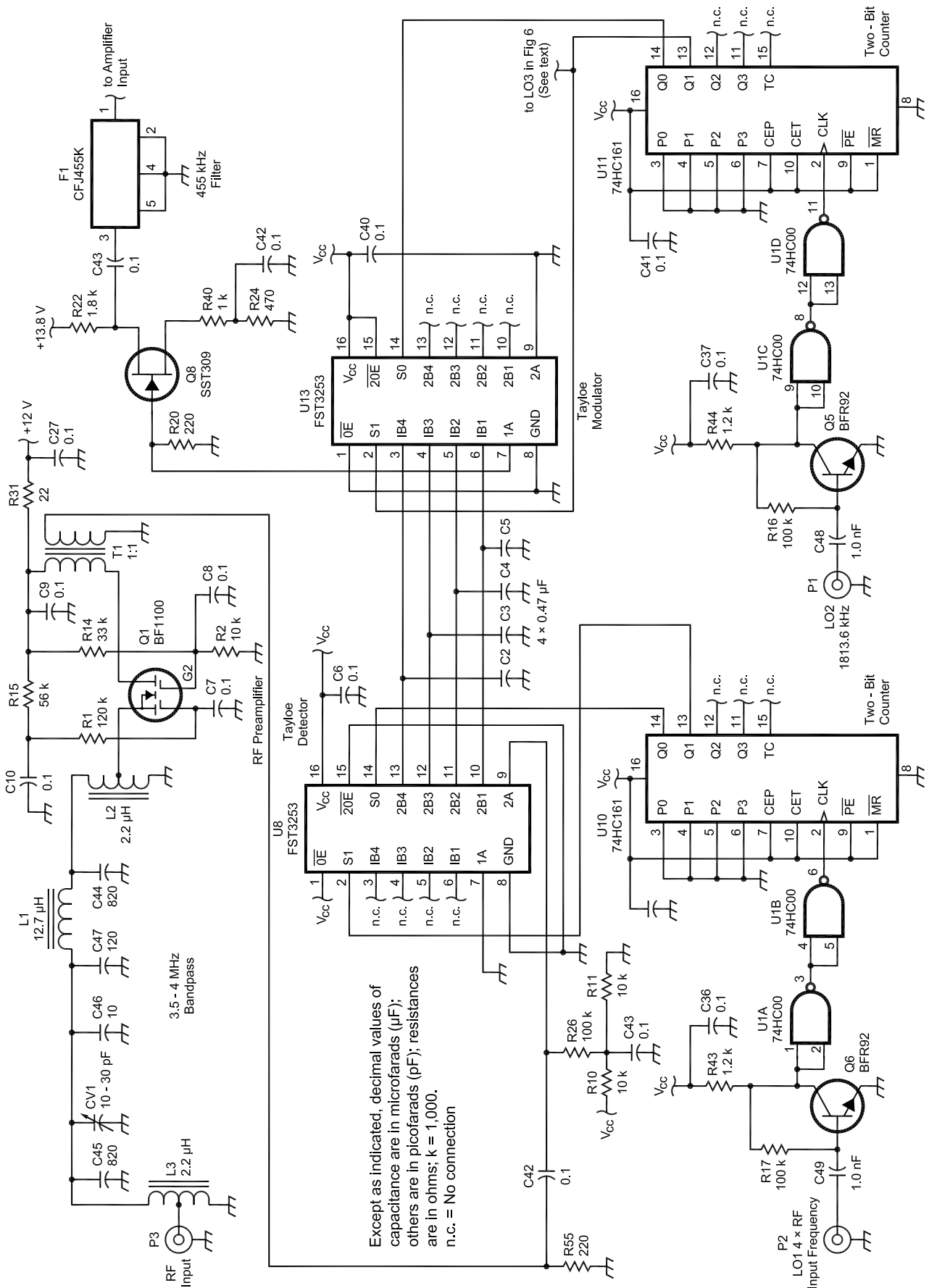


Fig 5—Dirodyne receiver front end schematic.

nents between them. Q1 is the grounded-gate preamplifier, a dual-gate MOSFET with its bias set such that the amplifier input impedance is close to 50 Ω. Transformer T2 is the output transformer, with a 1:1 ratio. Resistor R55 serves as the load resistance of the amplifier and the shunt resistor mentioned previously to set the bandwidth of the first Tayloe mixer. This consists of the mixer switch U8, which also contains the two-bit decoder of Fig 1 and capacitors C2 through C5. The two-bit counter of Fig 1 is represented by U10.

The local oscillator is fed to connector P2 and squared up by transistor Q6 and NAND gates U1A and U1B. The first mixer's output, now at baseband and in quadrature, directly feeds the reversed Tayloe mixer or modulator, U13. Similar to the first mixer, the second local oscillator is buffered by Q5, U1C and U1D. The second two-bit counter is U11. The second mixer output is the Tayloe filter's output and is terminated in resistor R20. Following the Tayloe filter is a low-gain amplifier Q8, the output of which matches the input impedance of the ceramic or crystal filter F1. This filter is terminated in R23 and a two-stage MOSFET amplifier boosts the signal. This amplifier has unusually low load resistors R26 and R25 to ensure that maximum gain is only 40 dB total for the pair. That is to ensure that the suppressed carrier emerging from the Tayloe filter is not amplified to the point that the IF amplifier clips or comes anywhere near to

doing so. Two stages are used so that excellent AGC performance may be achieved; however, only manual gain control is provided in the prototype.

The MOSFETs are Philips BF1100s and these are of the enhancement type. Most dual-gate MOSFETs are of the depletion type and require a negative AGC voltage to shut them off. The gain-control gate on the BF1100 need only go from 0-4 V for full gain-control range.

The IF amplifier feeds a product detector, consisting of CMOS switch U14B, op amp U15B and surrounding components. The clock signal is supplied by buffer U9E.

A Third Local Oscillator

The local oscillator input frequency to the product detector will normally be LO2/4. In this case, I used 453.4 kHz. This can be obtained from pin 13 of U11 in Fig 5. However, a separate, third local-oscillator input has been provided to enable future development, wherein the image frequency can be made an in-band frequency. In this case, the LO3 signal would need to be 455 kHz, the product detector would need to be a quadrature device and audio-phasing networks would be required. An audio notch filter would also be needed at the center of the audio passband. I include this as an as-yet-untried option.

Audio Amplifier and AGC circuits

The audio AGC unit used in the prototype receiver was taken from a previous direct-conversion receiver. Some

parts of it may not be required here, but they are included because this is quite a good general-purpose AGC unit. The schematic is shown in Fig 7. Audio from the product detector is passed via preset potentiometer R28, which enables this circuit to work with a wide range of input levels. The signal then passes through a 300-Hz high-pass filter around U1A and U1B. This IC was chosen for its low noise and relatively high output drive capability, because the next stage is a 600-Ω, 2.4-kHz low-pass elliptical filter. This is made up of components L1 through L3 and surrounding capacitors. Notice R5 in series with the output of U1B. That terminates the filter input. The output impedance of U1B is nearly zero, hence the need for this resistor.

Notice also R8. This is the filter's output termination. The filter output at T3 is designed to feed narrower active filters, such as for CW. If none is used, a link is placed between terminals T3 and T5, the input to the next stage. This is a noninverting stage around U2B that has a high input impedance to avoid undesired additional loading of the filters, if used. The output is coupled to a variable shunt attenuator made up of MOSFET Q1 and resistors R9 and R11. The gate voltage on Q1 controls the attenuator. The attenuator output feeds amplifier U2A, and it is rectified by transistors Q2 and Q3, whose output controls the FET attenuator loss.

A greater signal feeding into Q3 increases the voltage applied to the

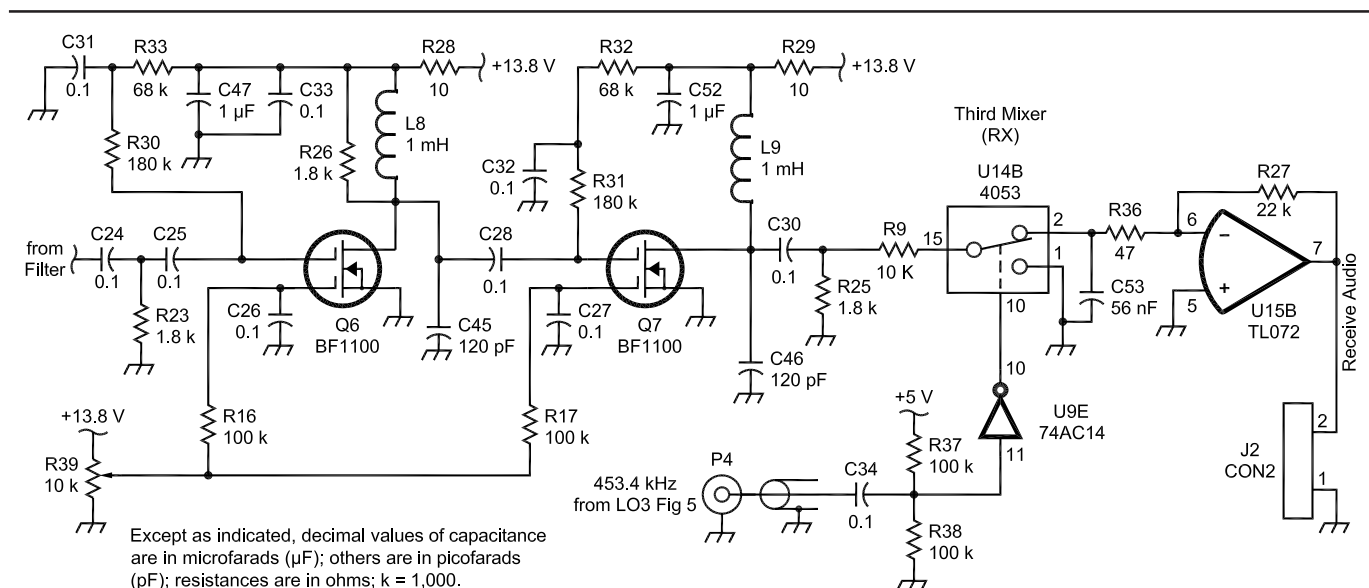
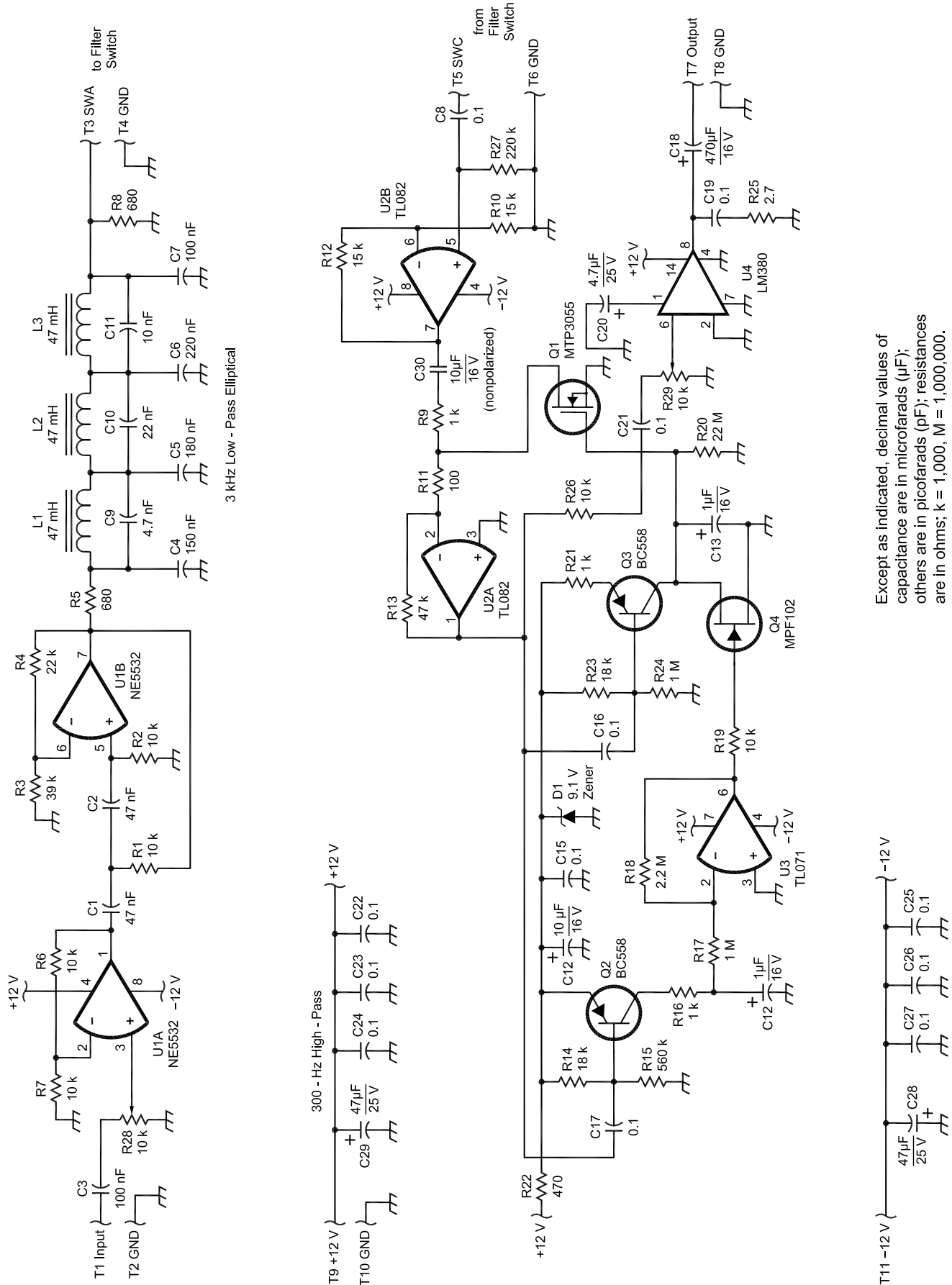


Fig 6—Dirodyne receiver IF-amplifier and product-detector schematic.



Except as indicated, decimal values of capacitance are in microfarads (μF); others are in picofarads (pF); resistances are in ohms; k = 1,000, M = 1,000,000.

Fig 7—Audio AGC unit schematic diagram.

gate of Q1 and thus, the attenuation. The effect is that for a 60-dB change in audio level from the product detector, the output rises by only about 1.5 dB. C13 holds the charge from the rectifier Q3 and takes around four seconds or so to discharge via R20. However, rectifier Q2 has a storage capacitor also: C12. The discharge time for C12 is around one second (it can be made shorter). The discharge path is via R17 and the virtual earth is at the summing junction of U3 pin 2. When there has been no signal for the one-second period mentioned above, JFET Q4's gate changes from being in cutoff with negative gate voltage supplied by U3, to being conductive due to reduced gate voltage. This rapidly discharges the AGC time-constant capacitor C13. This system is known as full-hang AGC, and it sounds unusual. However, it prevents the receiver from being in the low-gain state after receiving a strong signal for any longer than one second.

The audio signal feeds a standard power amplifier (LM380) that delivers a watt or two to the loudspeaker. The maximum gain of this system is around 80 dB.

Performance

I will keep the performance information here very general, as I have not

done a complete check at this point. However, there are a few points that may help, especially if you duplicate the circuit and want to be sure it is

working.

- Maximum usable sensitivity (20-dB SINAD): -80 dBm with a $50\text{-}\Omega$ source, no preamplifier (see the "Sen-

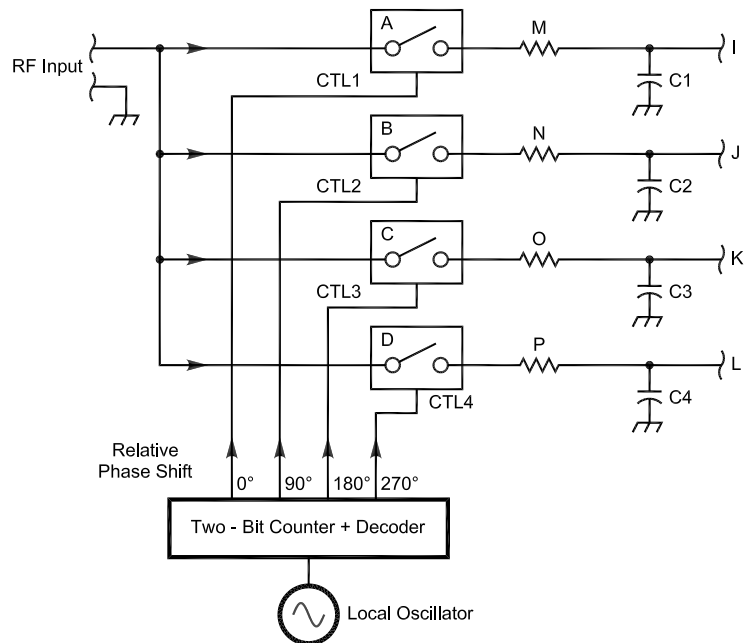


Fig 8—Block diagram of a Taylor detector modified for reduced noise. A through D are the mixer switches. Resistors M through P set the bandwidth. I through L are the output terminals.

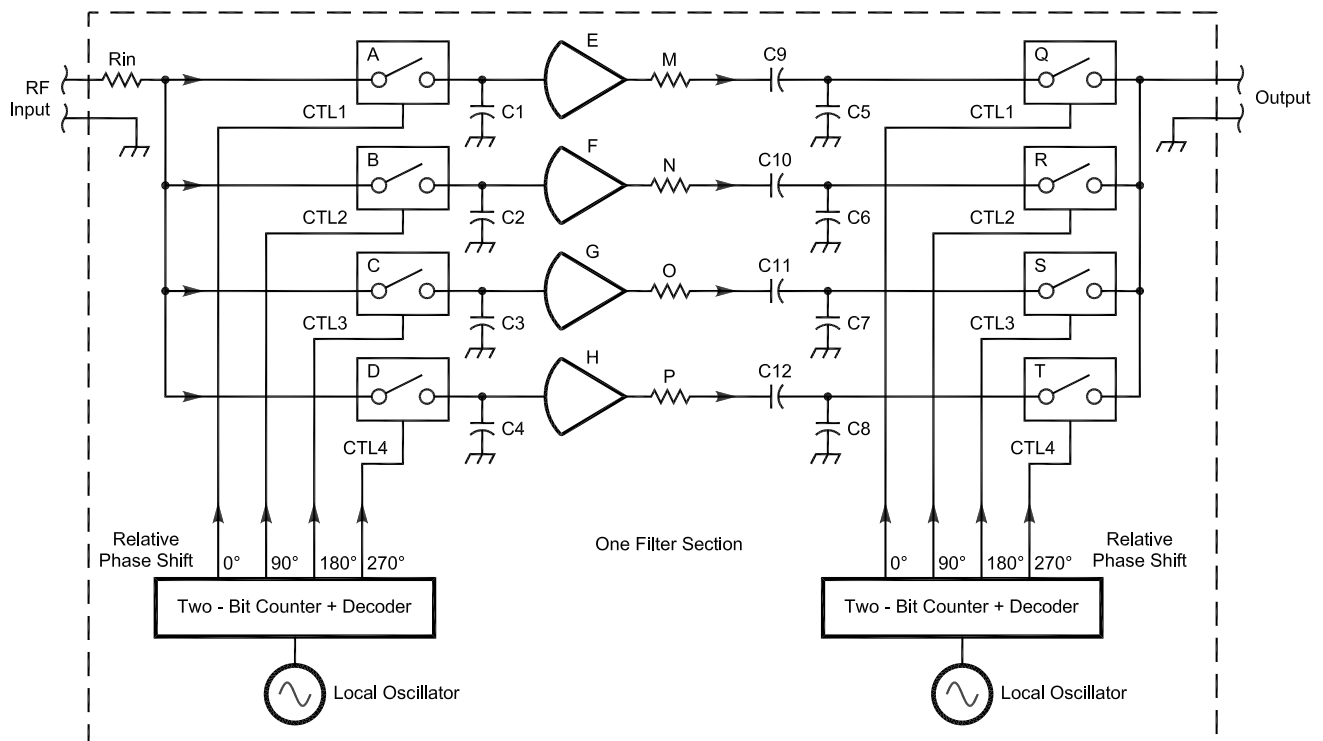


Fig 9—Block diagram of a Taylor filter with better carrier suppression. E through H are noninverting amplifiers. M through P are the input resistors for the second Taylor mixer. C9 through C12 are dc-blocking capacitors to reduce carrier feedthrough.

sitivity and Noise” heading).

- Unwanted sideband suppression: 60 dB.
- Blocking (ETS 300-373) method: 70 dB.
- Local oscillator feed-through (no preamplifier): -50 dBm, 50-Ω termination.

The above figures are the only reliable data for this early version.

Sensitivity and Noise

The sensitivity of the Tayloe detector can be quite poor despite its loss of about 1-2 dB. This means that the detector seems to be noisy. However, I believe this is not the case, as such; but it does have some local-oscillator feed-through to the antenna. Thus, the noise floor of the oscillator is of paramount importance. The noise caused by oscillator feed-through is quite complex and not yet fully understood. I have done several experiments in an attempt to find the exact cause of this LO noise. I have drawn some conclusions from my testing and include these below. The tests were done without a preamplifier and a terminated antenna input, no signal present.

The problem does not occur in the case of a single, doubly balanced mixer.

The tuning rate of the “birdies” is

much greater than that of the LO. To me, this indicates that a mixing process involving high-order harmonics of the LO mixing with LO spurs is involved—even very small ones. That effect appears in the antenna as a signal to be demodulated. However, I think the relationship is quite complex, as I deliberately introduced a spurious signal into the LO port using a 6-dB hybrid coupler. To even hear it, the level had to be only about 30 dB below the LO level. The LO signal I am using is very much better than this (HP 8640).

The most likely cause of the discrepancy lies where the mixers of the Tayloe filter are combined at the input. The LO noise sidebands do not have the same phase relationship at the mixer input as they do when they leave the oscillator. Normally, in a one-off mixer situation, the oscillator feed-through simply causes a small dc component in the mixer output because the oscillator signal at the antenna terminal is coherent. I’m only guessing here, but I think that the oscillator noise sidebands are cancelled as dc also. However, in the Tayloe case, the four mixers operate at four phase angles and the local oscillator cannot have a zero phase relationship with the four carriers simultaneously. Thus, if the oscillator has a

noise floor of say 90 dBc, and its output level is around +10 dBm (ball-park figures), then the noise sidebands and spurs will have a level of -80 dBm. This noise is an input signal!

Possible Noise Solutions

In the second-generation receiver, I modified the Tayloe detector as shown in Fig 8. The idea was to replace the input resistance with four resistors: one on the output of each switch and in series with its capacitor. The value of each resistor should be one-quarter of the original single-input resistor value. The detector was then fed from an emitter follower. This was done to avoid an input impedance across which noise voltage could develop. I also found that I needed to completely shield the RF amplifier. Otherwise, its inclusion made absolutely no difference to sensitivity whether it was on or off!

This indeed was effective to the extent that I could no longer detect LO-noise signals in the audio output. I subsequently found that the emitter-follower stage was not required. A side effect of moving the resistors and removing the emitter follower is that the mixer input impedance became flat with frequency (around 50 Ω in the

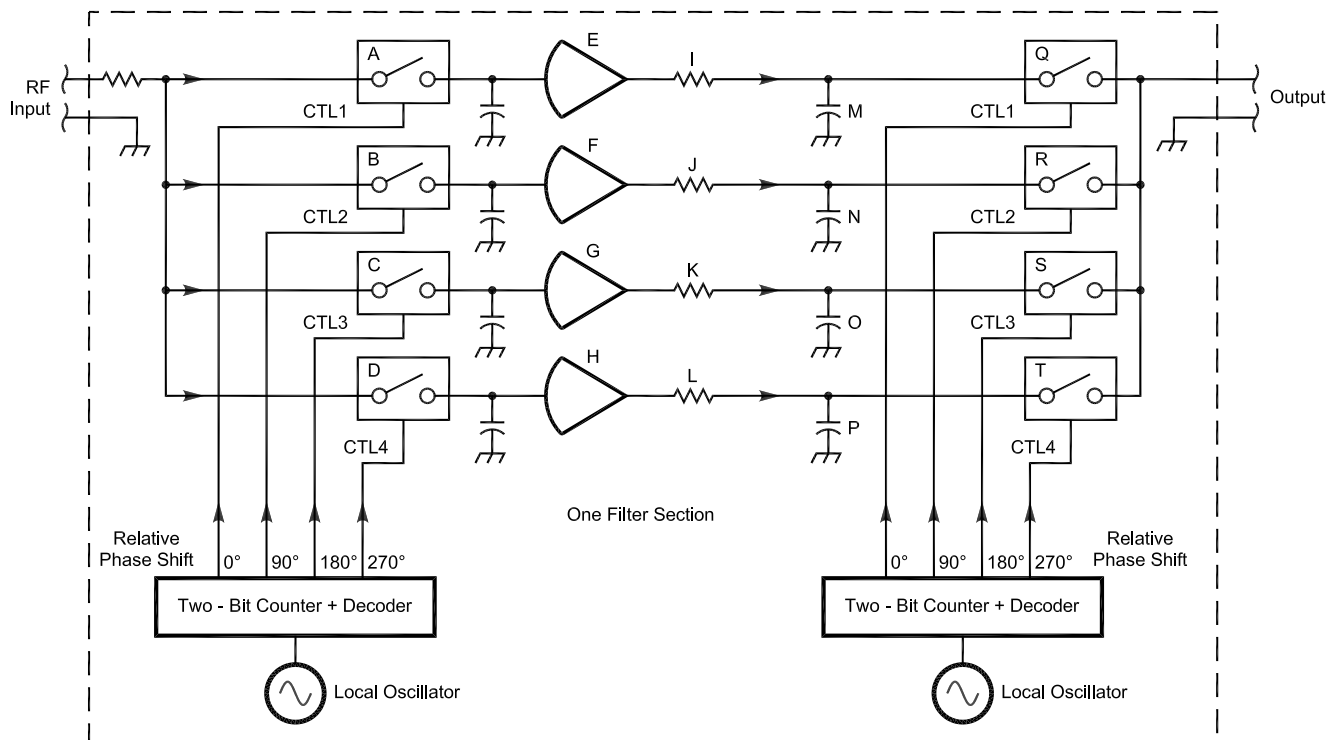


Fig 10—Block diagram of a Tayloe filter with interstage amplifiers. E through H are added noninverting amplifiers. I through L are amplifier-output isolating resistors. M through P are RF-bypass capacitors.

prototype), but it retained selectivity in the output.

I feel that the 0° and 180° inputs can remain combined, as can the 90° and 270° inputs; but there should be a split to isolate the two pairs of inputs and make two inputs instead of one. They could be fed from a combiner of some kind. This is untried at present.

Thirdly, I feel that a high-frequency harmonic shunt to ground, such as a parallel-tuned circuit on the operating frequency, connected to the combined input of the Tayloe switches in the standard Tayloe mixer, would be very useful. There would be an added benefit to this. The inductive or capacitive components of the tuned circuit could be configured to provide a match to 50 Ω at resonance. An input resistor (as an amplifier load) would not be needed if this were done. The tuned circuit would have a low impedance to ground at harmonics of the LO. The spurs associated with these appear to be the main source of LO noise. There may be many other possible options, and these may become obvious to experimenters in the light of increased knowledge about the exact nature of the LO-noise problem. Notice here that the second mixer is also subject to this problem, but it is easier to combat with a single-frequency clean oscillator.

I have been asked about reciprocal mixing in this receiver. This is a test to check the effect of noise sidebands from the LO on spurious input signal responses. I have as yet not had the opportunity to test for this; but if the LO is clean, the worst problem would be caused by signals close to the received signal.

Future Developments

There is actually no need to have four quadrature paths, as two are sufficient. Therefore, two double-balanced diode mixers—or for that matter, almost any pair of good mixers—will work in the front end. Care should be exercised, however, in correct mixer termination where appropriate. The Tayloe detectors provide an extremely simple solution to the balanced-mixer question.

I have been toying with the idea of having an IF of about 2.7 kHz or so and selecting the lower sideband (second

mixer). This could be the basis of a nearly direct-conversion receiver with most of the gain at audio frequencies. There would be no need for complex audio phase-shift networks. The AGC could be derived from the audio (high-level) feeding back to a spare mixer to be chopped and fed to a rectifier, thus we could hopefully avoid the clicks of audio-derived AGC. Please notice that this has not yet been tried.

Figs 9 and 10 have also been included as suggested improvements or changes to the Tayloe filter. These are currently being investigated as time permits.

Conclusion

I think that given a little time, the noise problem could be solved. I hope that many of you will take up this challenge. If this can be done, the amateur fraternity may be responsible for yet another major development in radio.

Notes

1. R. Green, VK6KRG, "The Bedford Receiver: A New Approach," *QEX*, Sep 1999, pp 9-24.
2. D. Tayloe, N7VE, regarding "Notes on 'Ideal' Commutating Mixers" (Nov/Dec 1999), *QEX*, Mar 2001, p 61.
3. D. Smith, KF6DX, "Notes on 'Ideal' Commutating Mixers," *QEX*, Nov 1999, pp 52-55.
4. US Patent No. 6230000

Rod Green, VK6KRG, has been interested in things scientific since early childhood. It's in his blood. His grandfather built neutrodyne radios in the early 1900s. Rod's technical training began in 1968, when he specialized in radio with the Australian Postmaster General's (PMG) Department. In the PMG, he worked mostly at TV transmitter and high-power broadcast transmitter sites for 20 years. Wherever Rod worked, he designed accessory equipment for the installation.

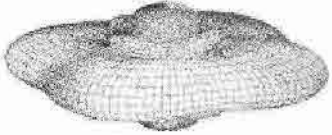
He received his first amateur station license in about 1976, and this was a technical-class license. He has very little commercial radio equipment, preferring instead to purchase good quality used test equipment and to homebrew wherever possible.

Beginning in 1988, Rod spent 10 years doing electronic and RF design with a local company, which produces 90% of Australia's broadcast studio equipment. In 1998, he joined Barrett

Communications as a senior R&D design technician. He was their chief RF designer in the absence of a qualified communications engineer. Since he joined Barrett, they have found one, much to Rod's relief! Barrett makes 100-W HF transceivers and related equipment for connection to the telephone network and so forth. At work, he must design to order; but Rod enjoys the challenge of designing something different at home. He has chosen to develop equipment based on the phasing method of RF processing, as he feels this is a well under-developed technology. He often teams up with Richard, VK6BRO, in a combined effort.

Rod holds no degrees other than his technician's certificate from long ago. Nonetheless, he has great experience and imagination for employment in the field of RF design and invention. He is currently looking for a backer to commercialize his techniques. □□

A picture is worth a thousand words...



With the all-new

ANTENNA MODEL™

wire antenna analysis program for Windows you get true 3D far field patterns that are far more informative than conventional 2D patterns or wire-frame pseudo-3D patterns.

Describe the antenna to the program in an easy-to-use spreadsheet-style format, and then with one mouse-click the program shows you the antenna pattern, front/back ratio, front/rear ratio, input impedance, efficiency, SWR, and more.

An optional Symbols window with formula evaluation capability can do your computations for you. A Match Wizard designs Gamma, T, or Hairpin matches for Yagi antennas. A Clamp Wizard calculates the equivalent diameter of Yagi element clamps. Yagi Optimization finds Yagi dimensions that satisfy performance objectives you specify. Major antenna properties can be graphed as a function of frequency.

There is no built-in segment limit. Your models can be as large and complicated as your system permits.

ANTENNA MODEL is only \$85US. This includes a Web site download and a permanent backup copy on CD-ROM. Visit our Web site for more information about ANTENNA MODEL.

Teri Software
P.O. Box 277
Lincoln, TX 78948

www.antennamodel.com
e-mail sales@antennamodel.com
phone 979-542-7852

A Software-Defined Radio for the Masses, Part 1

This series describes a complete PC-based, software-defined radio that uses a sound card and an innovative detector circuit. Mathematics is minimized in the explanation. Come see how it's done.

By Gerald Youngblood, AC5OG

A certain convergence occurs when multiple technologies align in time to make possible those things that once were only dreamed. The explosive growth of the Internet starting in 1994 was one of those events. While the Internet had existed for many years in government and education prior to that, its popularity had never crossed over into the general populace because of its slow speed and arcane interface. The development of the Web browser, the rapidly accelerating power and availability of the PC, and the availability of inexpensive and increasingly

speedy modems brought about the Internet convergence. Suddenly, it all came together so that the Internet and the worldwide Web joined the everyday lexicon of our society.

A similar convergence is occurring in radio communications through digital signal processing (DSP) software to perform most radio functions at performance levels previously considered unattainable. DSP has now been incorporated into much of the amateur radio gear on the market to deliver improved noise-reduction and digital-filtering performance. More recently, there has been a lot of discussion about the emergence of so-called software-defined radios (SDRs).

A software-defined radio is characterized by its flexibility: Simply modifying or replacing software programs

can completely change its functionality. This allows easy upgrade to new modes and improved performance without the need to replace hardware. SDRs can also be easily modified to accommodate the operating needs of individual applications. There is a distinct difference between a radio that internally uses software for some of its functions and a radio that can be completely redefined in the field through modification of software. The latter is a software-defined radio.

This SDR convergence is occurring because of advances in software and silicon that allow digital processing of radio-frequency signals. Many of these designs incorporate mathematical functions into hardware to perform all of the digitization, frequency selection, and down-conversion to base-

8900 Marybank Dr
Austin, TX 78750
gerald@sixthmarket.com

band. Such systems can be quite complex and somewhat out of reach to most amateurs.

One problem has been that unless you are a math wizard and proficient in programming C++ or assembly language, you are out of luck. Each can be somewhat daunting to the amateur as well as to many professionals. Two years ago, I set out to attack this challenge armed with a fascination for technology and a 25-year-old, virtually unused electrical engineering degree. I had studied most of the math in college and even some of the signal processing theory, but 25 years is a long time. I found that it really was a challenge to learn many of the disciplines required because much of the literature was written from a mathematician's perspective.

Now that I am beginning to grasp many of the concepts involved in software radios, I want to share with the Amateur Radio community what I have learned without using much more than simple mathematical concepts. Further, a software radio should have as little hardware as possible. If you have a PC with a sound card, you already have most of the required hardware. With as few as three integrated circuits you can be up and running with a Tayloe detector—an innovative, yet simple, direct-conversion receiver. With less than a dozen chips, you can build a transceiver that will outperform much of the commercial gear on the market.

Approach the Theory

In this article series, I have chosen to focus on practical implementation rather than on detailed theory. There are basic facts that must be understood to build a software radio. However, much like working with integrated circuits, you don't have to know how to create the IC in order to use it in a design. The convention I have chosen is to describe practical applications followed by references where appropriate for more detailed study. One of the easier to comprehend references I have found is *The Scientist and Engineer's Guide to Digital Signal Processing* by Steven W. Smith. It is free for download over the Internet at www.DSPGuide.com. I consider it required reading for those who want to dig deeper into implementation as well as theory. I will refer to it as the "DSP Guide" many times in this article series for further study.

So get out your four-function calculator (okay, maybe you need six or

seven functions) and let's get started. But first, let's set forth the objectives of the complete SDR design:

- Keep the math simple
- Use a sound-card equipped PC to provide all signal-processing functions
- Program the user interface and all signal-processing algorithms in *Visual Basic* for easy development and maintenance
- Utilize the Intel Signal Processing Library for core DSP routines to minimize the technical knowledge requirement and development time, and to maximize performance
- Integrate a direct conversion (D-C) receiver for hardware design simplicity and wide dynamic range
- Incorporate direct digital synthesis (DDS) to allow flexible frequency control
- Include transmit capabilities using similar techniques as those used in the D-C receiver.

Analog and Digital Signals in the Time Domain

To understand DSP we first need to understand the relationship between digital signals and their analog counterparts. If we look at a 1-V (pk) sine wave on an analog oscilloscope, we see that the signal makes a perfectly smooth curve on the scope, no matter how fast the sweep frequency. In fact, if it were possible to build a scope with an infinitely fast horizontal sweep, it would still display a perfectly smooth curve (really a straight line at that point). As such, it is often called a *continuous-time signal* since it is continuous in time. In other words, there are an infinite number of different voltages along the curve, as can be seen on the analog oscilloscope trace.

On the other hand, if we were to measure the same sine wave with a digital voltmeter at a sampling rate of four times the frequency of the sine wave, starting at time equals zero, we would read: 0 V at 0°, 1 V at 90°, 0 V at 180° and -1 V at 270° over one complete cycle. The signal could continue perpetually, and we would still read those same four voltages over and over again, forever. We have measured the voltage of the signal at discrete moments in time. The resulting voltage-measurement sequence is therefore called a *discrete-time signal*.

If we save each discrete-time signal voltage in a computer memory and we know the frequency at which we sampled the signal, we have a *discrete-time sampled signal*. This is what an analog-to-digital converter (ADC)

does. It uses a sampling clock to measure discrete samples of an incoming analog signal at precise times, and it produces a digital representation of the input sample voltage.

In 1933, Harry Nyquist discovered that to accurately recover all the components of a periodic waveform, it is necessary to use a sampling frequency of at least twice the bandwidth of the signal being measured. That minimum sampling frequency is called the *Nyquist criterion*. This may be expressed as:

$$f_s \geq 2f_{bw} \quad (\text{Eq 1})$$

where f_s is the sampling rate and f_{bw} is the bandwidth. See? The math isn't so bad, is it?

Now as an example of the Nyquist criterion, let's consider human hearing, which typically ranges from 20 Hz to 20 kHz. To recreate this frequency response, a CD player must sample at a frequency of at least 40 kHz. As we will soon learn, the maximum frequency component must be limited to 20 kHz through low-pass filtering to prevent distortion caused by false images of the signal. To ease filter requirements, therefore, CD players use a standard sampling rate of 44,100 Hz. All modern PC sound cards support that sampling rate.

What happens if the sampled bandwidth is greater than half the sampling rate and is not limited by a low-pass filter? An *alias* of the signal is produced that appears in the output along with the original signal. Aliases can cause distortion, beat notes and unwanted spurious images. Fortunately, alias frequencies can be precisely predicted and prevented with proper low-pass or band-pass filters, which are often referred to as *anti-aliasing* filters, as shown in Fig 1. There are even cases where the alias frequency can be used to advantage; that will be discussed later in the article.

This is the point where most texts on DSP go into great detail about what sampled signals look like above the Nyquist frequency. Since the goal of this article is practical implementation, I refer you to Chapter 3 of the DSP Guide for a more in-depth discussion of sampling, aliases, A-to-D and

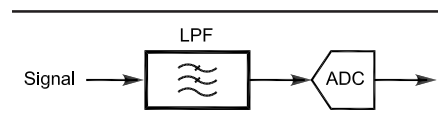


Fig 1—A/D conversion with antialiasing low-pass filter.

D-to-A conversion. Also refer to Doug Smith's article, "Signals, Samples, and Stuff: A DSP Tutorial."¹

What you need to know for now is that if we adhere to the Nyquist criterion in Eq 1, we can accurately sample, process and recreate virtually any desired waveform. The sampled signal will consist of a series of numbers in computer memory measured at time intervals equal to the sampling rate. Since we now know the amplitude of the signal at discrete time intervals, we can process the digitized signal in software with a precision and flexibility not possible with analog circuits.

From RF to a PC's Sound Card

Our objective is to convert a modulated radio-frequency signal from the frequency domain to the time domain for software processing. In the frequency domain, we measure amplitude versus frequency (as with a spectrum analyzer); in the time domain, we measure amplitude versus time (as with an oscilloscope).

In this application, we choose to use a standard 16-bit PC sound card that has a maximum sampling rate of 44,100 Hz. According to Eq 1, this means that the maximum-bandwidth signal we can accommodate is 22,050 Hz. With quadrature sampling, discussed later, this can actually be extended to 44 kHz. Most sound cards have built-in antialiasing filters that cut off sharply at around 20 kHz. (For a couple hundred dollars more, PC sound cards are now available that support 24 bits at a 96-kHz sampling rate with up to 105 dB of dynamic range.)

Most commercial and amateur DSP designs use dedicated DSPs that sample intermediate frequencies (IFs) of 40 kHz or above. They use traditional analog superheterodyne techniques for down-conversion and filtering. With the advent of very-high-speed and wide-bandwidth ADCs, it is now possible to directly sample signals up through the entire HF range and even into the low VHF range. For example, the Analog Devices AD9430 A/D converter is specified with sample rates up to 210 Msps at 12 bits of resolution and a 700-MHz bandwidth. That 700-MHz bandwidth can be used in under-sampling applications, a topic that is beyond the scope of this article series.

The goal of my project is to build a PC-based software-defined radio that uses as little external hardware as possible while maximizing dynamic range and flexibility. To do so, we will need to convert the RF signal to audio frequencies in a way that allows removal of the unwanted mixing products or images caused by the down-conversion process. The simplest way to accomplish this while maintaining wide dynamic range is to use D-C techniques to translate the modulated RF signal directly to baseband.

¹Notes appear on page 21.

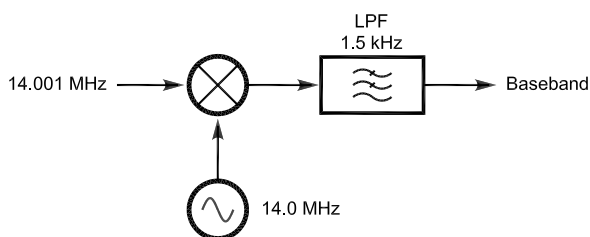


Fig 2—A direct-conversion real mixer with a 1.5-kHz low-pass filter.

We can mix the signal with an oscillator tuned to the RF carrier frequency to translate the bandwidth-limited signal to a 0-Hz IF as shown in Fig 2.

The example in the figure shows a 14.001-MHz carrier signal mixed with a 14.000-MHz local oscillator to translate the carrier to 1 kHz. If the low-pass filter had a cutoff of 1.5 kHz, any signal between 14.000 MHz and 14.0015 MHz would be within the passband of the direct-conversion receiver. The problem with this simple approach is that we would also simultaneously receive all signals between 13.9985 MHz and 14.000 MHz as unwanted images within the passband, as illustrated in Fig 3. Why is that?

Most amateurs are familiar with the concept of sum and difference frequencies that result from mixing two signals. When a carrier frequency, f_c , is mixed with a local oscillator, f_{lo} , they combine in the general form:

$$f_c f_{lo} = \frac{1}{2} [(f_c + f_{lo}) + (f_c - f_{lo})] \quad (\text{Eq 2})$$

When we use the direct-conversion mixer shown in Fig 2, we will receive these primary output signals:

$$\begin{aligned} f_c + f_{lo} &= 14.001 \text{ MHz} + 14.000 \text{ MHz} = 28.001 \text{ MHz} \\ f_c - f_{lo} &= 14.001 \text{ MHz} - 14.000 \text{ MHz} = 0.001 \text{ MHz} \end{aligned}$$

Note that we also receive the image frequency that "folds over" the primary output signals:

$$-f_c + f_{lo} = -14.001 \text{ MHz} + 14.000 \text{ MHz} = -0.001 \text{ MHz}$$

A low-pass filter easily removes the 28.001-MHz *sum frequency*, but the -0.001-MHz *difference-frequency* image will remain in the output. This unwanted image is the lower sideband with respect to the 14.000-MHz carrier frequency. This would not be a problem if there were no signals below 14.000 MHz to interfere. As previously stated, all undesired signals between 13.9985 and 14.000 MHz will translate into the passband along with the desired signals above 14.000 MHz. The image also results in increased noise in the output.

So how can we remove the image-frequency signals? It can be accomplished through *quadrature mixing*. Phasing or quadrature transmitters and receivers—also called Weaver-method or image-rejection mixers—have existed since the early days of single sideband. In fact, my first SSB transmitter was a used Central Electronics 20A exciter that incorporated a phasing design. Phasing systems lost favor in the early 1960s with the advent of relatively inexpensive, high-performance filters.

To achieve good opposite-sideband or image suppression, phasing systems require a precise balance of amplitude and phase between two samples of the signal that are 90° out

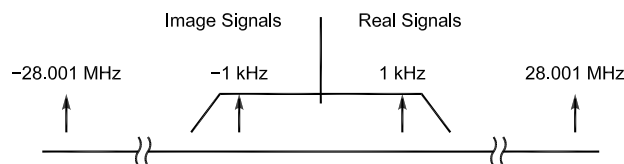


Fig 3—Output spectrum of a real mixer illustrating the sum, difference and image frequencies.

of phase or in quadrature with each other—"orthogonal" is the term used in some texts. Until the advent of digital signal processing, it was difficult to realize the level of image rejection performance required of modern radio systems in phasing designs. Since digital signal processing allows precise numerical control of phase and amplitude, quadrature modulation and demodulation are the preferred methods. Such signals in quadrature allow virtually any modulation method to be implemented in software using DSP techniques.

Give Me I and Q and I Can Demodulate Anything

First, consider the direct-conversion mixer shown in Fig 2. When the RF signal is converted to baseband audio using a single channel, we can visualize the output as varying in amplitude along a single axis as illustrated in Fig 4. We will refer to this as the *in-phase* or *I* signal. Notice that its magnitude varies from a positive value to a negative value at the frequency of the modulating signal. If we use a diode to rectify the signal, we would have created a simple envelope or AM detector.

Remember that in AM envelope detection, both modulation sidebands carry information energy and both are desired at the output. Only amplitude information is required to fully demodulate the original signal. The problem is that most other modulation techniques require that the phase of the signal be known. This is where quadrature detection comes in. If we delay a copy of the RF carrier by 90° to form a quadrature (*Q*) signal, we can then use it in conjunction with the original in-phase signal and the math we learned in middle school to determine the instantaneous phase and amplitude of the original signal.

Fig 5 illustrates an RF carrier with the level of the *I* signal plotted on the x-axis and that of the *Q* signal plotted on the y-axis of a plane. This is often referred to in the literature as a *phasor diagram* in the *complex plane*. We are now able to extrapolate the two signals to draw an arrow or phasor that represents the instantaneous magnitude and phase of the original signal.

Okay, here is where you will have to use a couple of those extra functions on the calculator. To compute the magnitude m_t or envelope of the signal, we use the geometry of right triangles. In a right triangle, the square of the hypotenuse is equal to the sum

of the squares of the other two sides—according to the Pythagorean theorem. Or restating, the hypotenuse as m_t (magnitude with respect to time):

$$m_t = \sqrt{I_t^2 + Q_t^2} \quad (\text{Eq 3})$$

The instantaneous phase of the signal as measured counterclockwise from the positive *I* axis and may be computed by the inverse tangent (or arctangent) as follows:

$$\phi_t = \tan^{-1}\left(\frac{Q_t}{I_t}\right) \quad (\text{Eq 4})$$

Therefore, if we measured the instantaneous values of *I* and *Q*, we would know everything we needed to know about the signal at a given moment in time. This is true whether we are dealing with continuous analog signals or discrete sampled signals. With *I* and *Q*, we can demodulate AM signals directly using Eq 3 and FM signals using Eq 4. To demodulate SSB takes one more step. Quadrature signals can be used analytically to remove the image frequencies and leave only the desired sideband.

The mathematical equations for quadrature signals are difficult but are very understandable with a little study.² I highly recommend that you read the online article, "Quadrature

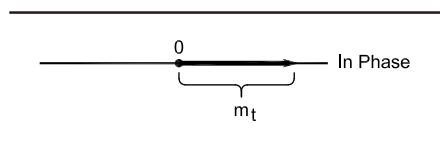


Fig 4—An in-phase signal (*I*) on the real plane. The magnitude, m_t , is easily measured as the instantaneous peak voltage, but no phase information is available from in-phase detection. This is the way an AM envelope detector works.

Signals: Complex, But Not Complicated," by Richard Lyons. It can be found at www.dspguru.com/info/tutor/quadsig.htm. The article develops in a very logical manner how quadrature-sampling *I/Q* demodulation is accomplished. A basic understanding of these concepts is essential to designing software-defined radios.

We can take advantage of the analytic capabilities of quadrature signals through a quadrature mixer. To understand the basic concepts of quadrature mixing, refer to Fig 6, which illustrates a quadrature-sampling *I/Q* mixer. First, the RF input signal is band-pass filtered and applied to the two parallel mixer channels. By delaying the local oscillator wave by 90°, we can generate a cosine wave that, in tandem, forms a *quadrature oscillator*. The RF carrier, $f_c(t)$, is mixed with the respective cosine and sine wave local oscillators and is subsequently low-pass filtered to create the in-phase, $I(t)$, and quadrature, $Q(t)$, signals. The $Q(t)$

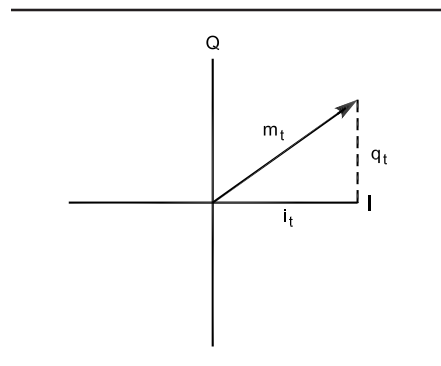


Fig 5— $I + jQ$ are shown on the complex plane. The vector rotates counterclockwise at a rate of $2\pi f_c$. The magnitude and phase of the rotating vector at any instant in time may be determined through Eqs 3 and 4.

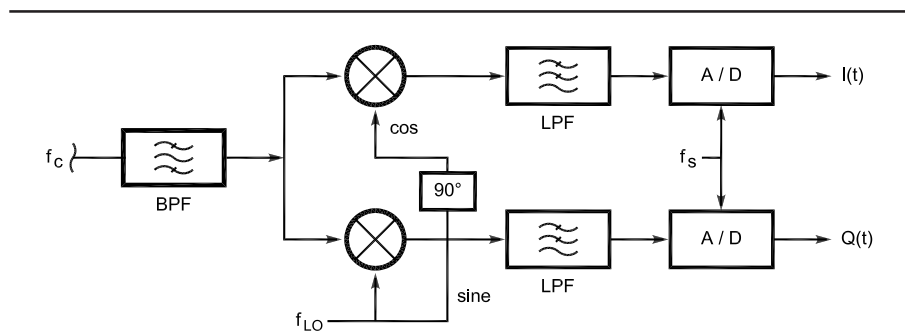


Fig 6—Quadrature sampling mixer: The RF carrier, f_c , is fed to parallel mixers. The local oscillator (Sine) is fed to the lower-channel mixer directly and is delayed by 90° (Cosine) to feed the upper-channel mixer. The low-pass filters provide antialias filtering before analog-to-digital conversion. The upper channel provides the in-phase ($I(t)$) signal and the lower channel provides the quadrature ($Q(t)$) signal. In the PC SDR the low-pass filters and A/D converters are integrated on the PC sound card.

channel is phase-shifted 90° relative to the $I(t)$ channel through mixing with the sine local oscillator. The low-pass filter is designed for cutoff below the Nyquist frequency to prevent aliasing in the A/D step. The A/D converts continuous-time signals to discrete-time sampled signals. Now that we have the I and Q samples in memory, we can perform the magic of digital signal processing.

Before we go further, let me reiterate that one of the problems with this method of down-conversion is that it can be costly to get good opposite-sideband suppression with analog circuits. Any variance in component values will cause phase or amplitude imbalance between two channels, resulting in a corresponding decrease in opposite-sideband suppression. With analog circuits, it is difficult to achieve better than 40 dB of suppression without much higher cost. Fortunately, it is straightforward to correct the analog imbalances in software.

Another significant drawback of direct-conversion receivers is that the noise increases as the demodulated signal approaches 0 Hz. Noise contributions come from a number of sources, such as $1/f$ noise from the semiconductor devices themselves, 60-Hz and 120-Hz line noise or hum, microphonic mechanical noise and local-oscillator phase noise near the carrier frequency. This can limit sensitivity since most people prefer their CW tones to be below 1 kHz. It turns out that most of the low-frequency noise rolls off above 1 kHz. Since a sound card can process signals all the way up to 20 kHz, why not use some of that bandwidth to move away from the low frequency noise? The PC SDR uses an 11.025-kHz, *offset-baseband IF* to reduce the noise to a manageable level. By offsetting the local oscillator by 11.025 kHz, we can now receive signals near the carrier

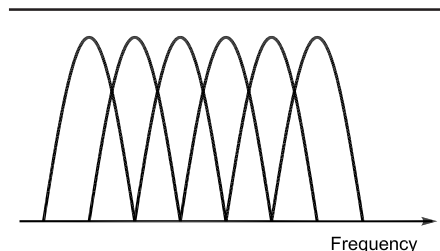


Fig 7—FFT output resembles a comb filter: Each bin of the FFT overlaps its adjacent bins just as in a comb filter. The 3-dB points overlap to provide linear output. The phase and magnitude of the signal in each bin is easily determined mathematically with Eqs 3 and 4.

frequency without any of the low-frequency noise issues. This also significantly reduces the effects of local-oscillator phase noise. Once we have digitally captured the signal, it is a trivial software task to shift the demodulated signal down to a 0-Hz offset.

DSP in the Frequency Domain

Every DSP text I have read thus far concentrates on time-domain filtering and demodulation of SSB signals using *finite-impulse-response (FIR)* filters. Since these techniques have been thoroughly discussed in the literature^{1, 3, 4} and are not currently used in my PC SDR, they will not be covered in this article series.

My PC SDR uses the power of the *fast Fourier transform (FFT)* to do almost all of the heavy lifting in the frequency domain. Most DSP texts use a lot of ink to derive the math so that one can write the FFT code. Since Intel has so helpfully provided the code in executable form in their signal-processing library,⁵ we don't care how to write an FFT: We just need to know how to use it. Simply put, the FFT converts the complex I and Q discrete-time signals into the frequency domain. The FFT output can be thought of as a large bank of very narrow band-pass filters, called *bins*, each one measuring the spectral energy within its respective bandwidth. The output resembles a *comb filter* wherein each bin slightly overlaps its adjacent bins forming a scalloped curve, as shown in Fig 7. When a signal is precisely at the center frequency of a bin, there will be a corresponding value only in that bin. As the frequency is offset from the bin's center, there will be a corresponding increase in the value of the

adjacent bin and a decrease in the value of the current bin. Mathematical analysis fully describes the relationship between FFT bins,⁶ but such is beyond the scope of this article.

Further, the FFT allows us to measure both phase and amplitude of the signal within each bin using Eqs 3 and 4 above. The complex version allows us to measure positive and negative frequencies separately. Fig 8 illustrates the output of a complex, or quadrature, FFT.

The bandwidth of each FFT bin may be computed as shown in Eq 5, where BW_{bin} is the bandwidth of a single bin, f_s is the sampling rate and N is the size of the FFT. The center frequency of each FFT bin may be determined by Eq 6 where f_{center} is the bin's center frequency, n is the bin number, f_s is the sampling rate and N is the size of the FFT. Bins zero through $(N/2)-1$ represent upper-sideband frequencies and bins $N/2$ to $N-1$ represent lower-sideband frequencies around the carrier frequency.

$$BW_{bin} = \frac{f_s}{N} \quad (\text{Eq 5})$$

$$f_{center} = \frac{nf_s}{N} \quad (\text{Eq 6})$$

If we assume the sampling rate of the sound card is 44.1 kHz and the number of FFT bins is 4096, then the bandwidth and center frequency of each bin would be:

$$BW_{bin} = \frac{44100}{4096} = 10.7666 \text{ Hz and}$$

$$f_{center} = n10.7666 \text{ Hz}$$

What this all means is that the receiver will have 4096, ~11-Hz-wide

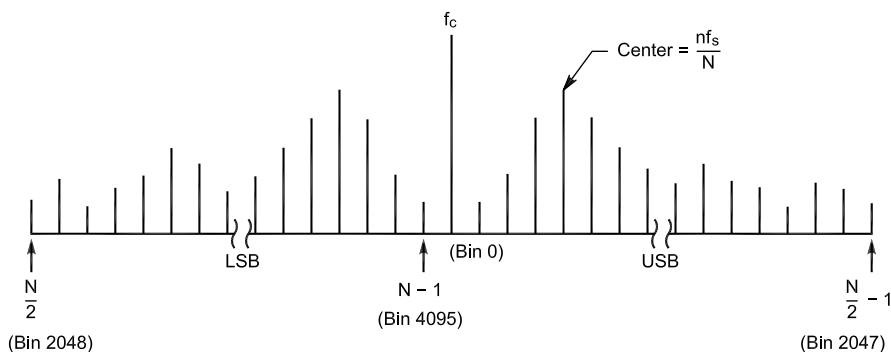


Fig 8—Complex FFT output: The output of a complex FFT may be thought of as a series of band-pass filters aligned around the carrier frequency, f_c , at bin 0. N represents the number of FFT bins. The upper sideband is located in bins 1 through $(N/2)-1$ and the lower sideband is located in bins $N/2$ to $N-1$. The center frequency and bandwidth of each bin may be calculated using Eqs 5 and 6.

band-pass filters. We can therefore create band-pass filters from 11 Hz to approximately 40 kHz in 11-Hz steps.

The PC SDR performs the following functions in the frequency domain after FFT conversion:

- Brick-wall fixed and variable band-pass filters
- Frequency conversion
- SSB/CW demodulation
- Sideband selection
- Frequency-domain noise subtraction
- Frequency-selective squelch
- Noise blanking
- Graphic equalization (“tone control”)
- Phase and amplitude balancing to remove images
- SSB generation
- Future digital modes such as PSK31 and RTTY

Once the desired frequency-domain processing is completed, it is simple to convert the signal back to the time domain by using an *inverse FFT*. In the PC SDR, only AGC and adaptive noise filtering are currently performed in the time domain. A simplified diagram of the PC SDR software architecture is provided in Fig 9. These concepts will be discussed in detail in a [future article](#).

Sampling RF Signals with the Tayloe Detector: A New Twist on an Old Problem

While searching the Internet for information on quadrature mixing, I ran across a most innovative and elegant design by Dan Tayloe, N7VE. Dan, who works for Motorola, has developed and patented (US Patent #6,230,000) what has been called the *Tayloe detector*.⁷ The beauty of the Tayloe detector is found in both its design elegance and its exceptional performance. It resembles other concepts in design, but appears unique in its high performance with minimal components.^{8, 9, 10, 11} In its simplest form, you can build a complete quadrature down converter with only three or four ICs (less the local oscillator) at a cost of less than \$10.

Fig 10 illustrates a single-balanced version of the Tayloe detector. It can be visualized as a four-position rotary switch revolving at a rate equal to the carrier frequency. The 50-Ω antenna impedance is connected to the rotor and each of the four switch positions is connected to a *sampling capacitor*. Since the switch rotor is turning at exactly the RF carrier frequency, each capacitor will track the carrier’s amplitude for exactly one-quarter of the cycle and will hold its value for the remainder of

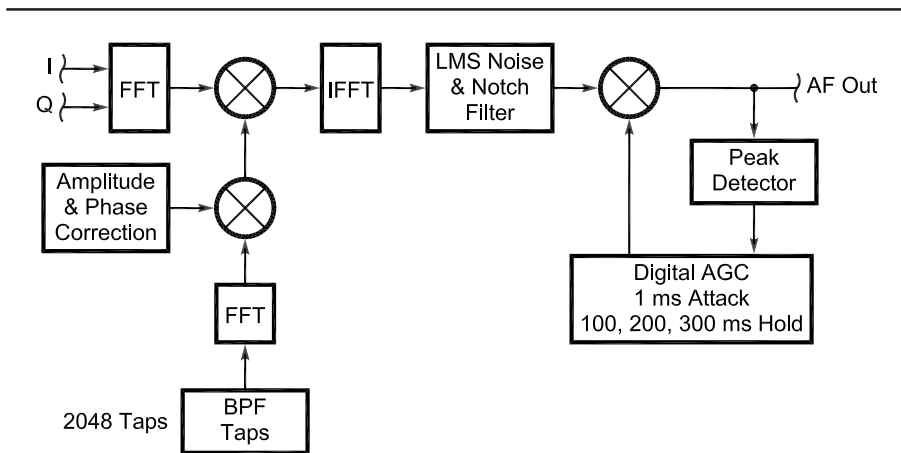


Fig 9—SDR receiver software architecture: The *I* and *Q* signals are fed from the sound-card input directly to a 4096-bin complex FFT. Band-pass filter coefficients are precomputed and converted to the frequency domain using another FFT. The frequency-domain filter is then multiplied by the frequency-domain signal to provide brick-wall filtering. The filtered signal is then converted to the time domain using the inverse FFT. Adaptive noise and notch filtering and digital AGC follow in the time domain.

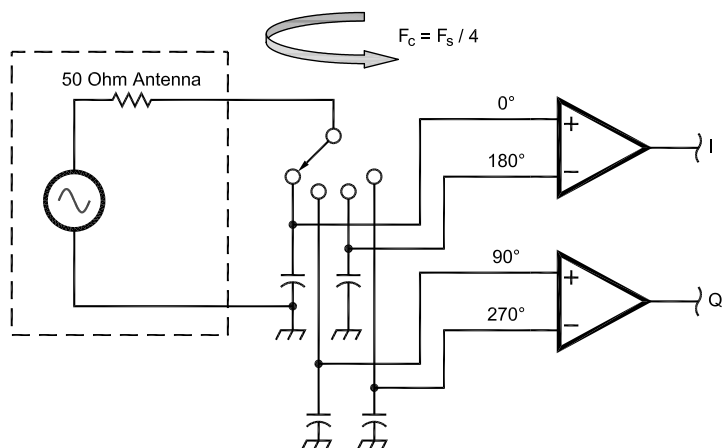


Fig 10—Tayloe detector: The switch rotates at the carrier frequency so that each capacitor samples the signal once each revolution. The 0° and 180° capacitors differentially sum to provide the in-phase (*I*) signal and the 90° and 270° capacitors sum to provide the quadrature (*Q*) signal.

the cycle. The rotating switch will therefore sample the signal at 0°, 90°, 180° and 270°, respectively.

As shown in Fig 11, the 50-Ω impedance of the antenna and the sampling capacitors form an R-C low-pass filter during the period when each respective switch is turned on. Therefore, each sample represents the integral or average voltage of the signal during its respective one-quarter cycle. When the switch is off, each sampling capacitor will hold its value until the next revolution. If the RF carrier and the rotating frequency were exactly in phase, the output of each capacitor will be a dc level equal to the average

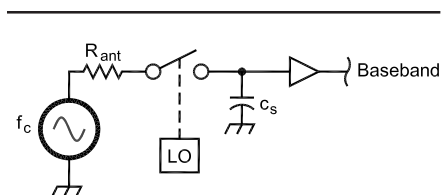


Fig 11—Track and hold sampling circuit: Each of the four sampling capacitors in the Tayloe detector form an RC track-and-hold circuit. When the switch is on, the capacitor will charge to the average value of the carrier during its respective one-quarter cycle. During the remaining three-quarters cycle, it will hold its charge. The local-oscillator frequency is equal to the carrier frequency so that the output will be at baseband.

value of the sample.

If we differentially sum outputs of the 0° and 180° sampling capacitors with an op amp (see Fig 10), the output would be a dc voltage equal to two times the value of the individually sampled values when the switch rotation frequency equals the carrier frequency. Imagine, 6 dB of noise-free gain! The same would be true for the 90° and 270° capacitors as well. The 0°/180° summation forms the *I* channel and the 90°/270° summation forms the *Q* channel of the quadrature down-conversion.

As we shift the frequency of the carrier away from the sampling frequency, the values of the inverting phases will no longer be dc levels. The output frequency will vary according to the “beat” or difference frequency between the carrier and the switch-rotation frequency to provide an accurate representation of all the signal

components converted to baseband.

Fig 12 provides the schematic for a simple, single-balanced Tayloe detector. It consists of a PI5V331, 1:4 FET demultiplexer that switches the signal to each of the four sampling capacitors. The 74AC74 dual flip-flop is connected as a divide-by-four Johnson counter to provide the two-phase clock to the demultiplexer chip. The outputs of the sampling capacitors are differentially summed through the two LT1115 ultra-low-noise op amps to form the *I* and *Q* outputs, respectively. Note that the impedance of the antenna forms the input resistance for the op-amp gain as shown in Eq 7. This impedance may vary significantly with the actual antenna. I use instrumentation amplifiers in my final design to eliminate gain variance with antenna impedance. More information on the hardware design will be provided in a future article.

Since the duty cycle of each switch is 25%, the effective resistance in the RC network is the antenna impedance multiplied by four in the op-amp gain formula, as shown in Eq 7:

$$G = \frac{R_f}{4R_{ant}} \quad (\text{Eq 7})$$

For example, with a feedback resistance, R_f , of 3.3 kΩ and antenna impedance, R_{ant} , of 50 Ω, the resulting gain of the input stage is:

$$G = \frac{3300}{4 \times 50} = 16.5$$

The Tayloe detector may also be analyzed as a *digital commutating filter*.^{12, 13, 14} This means that it operates as a very-high-*Q* tracking filter, where Eq 8 determines the bandwidth and *n* is the number of sampling capacitors,

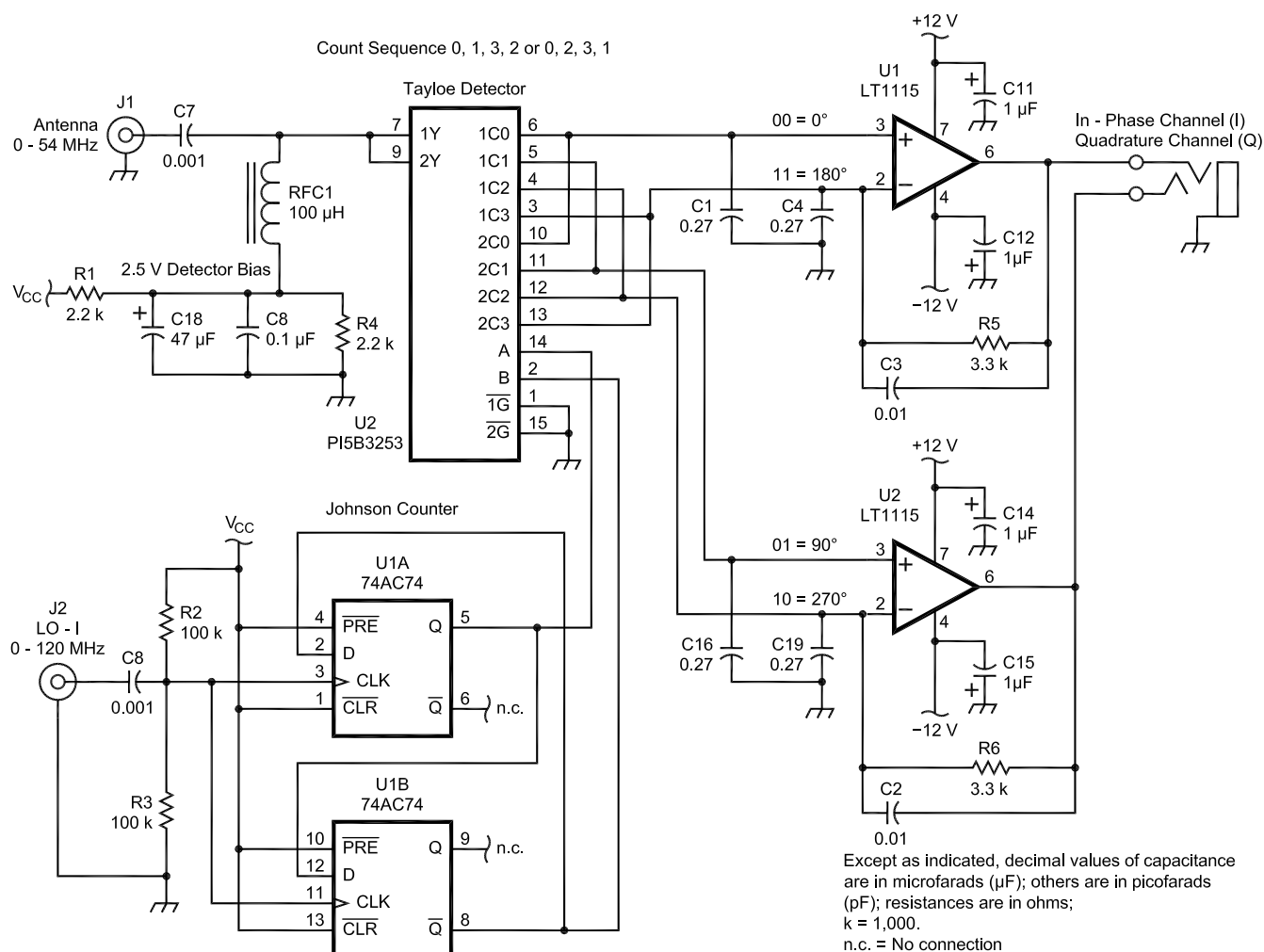


Fig 12—Singly balanced Tayloe detector.

R_{ant} is the antenna impedance and C_s is the value of the individual sampling capacitors. Eq 9 determines the Q_{det} of the filter, where f_c is the center frequency and BW_{det} is the bandwidth of the filter.

$$BW_{\text{det}} = \frac{1}{\pi n R_{\text{ant}} C_s} \quad (\text{Eq 8})$$

$$Q_{\text{det}} = \frac{f_c}{BW_{\text{det}}} \quad (\text{Eq 9})$$

By example, if we assume the sampling capacitor to be 0.27 μF and the antenna impedance to be 50 Ω , then BW and Q are computed as follows:

$$BW_{\text{det}} = \frac{1}{(\pi)(4)(50)(2.7 \times 10^{-7})} = 5895 \text{ Hz}$$

$$Q_{\text{det}} = \frac{14.001 \times 10^6}{5895} = 2375$$

Since the PC SDR uses an offset baseband IF, I have chosen to design the detector's bandwidth to be 40 kHz to allow low-frequency noise elimination as discussed above.

The real payoff in the Tayloe detector is its performance. It has been stated that the *ideal* commutating mixer has a minimum conversion loss (which equates to noise figure) of 3.9 dB.^{15, 16} Typical high-level diode mixers have a conversion loss of 6-7 dB and noise figures 1 dB higher than the loss. The Tayloe detector has less than 1 dB of conversion loss, remarkably. How can this be? The reason is that it is not really a mixer but a sampling detector in the form of a quadrature track and hold. This means that the design adheres to discrete-time sampling theory, which, while similar to mixing, has its own unique characteristics. Because a track and hold actually holds the signal value between samples, the signal output never goes to zero.

This is where aliasing can actually be used to our benefit. Since each switch and capacitor in the Tayloe detector actually samples the RF signal once each cycle, it will respond to alias frequencies as well as those within the Nyquist frequency range. In a traditional direct-conversion receiver, the local-oscillator frequency is set to the carrier frequency so that the difference frequency, or IF, is at 0 Hz and the sum frequency is at two times the carrier frequency per Eq 2. We normally remove the sum frequency through low-pass filtering, resulting in conversion loss and a corresponding

increase in noise figure. In the Tayloe detector, the sum frequency resides at the first alias frequency as shown in Fig 13. Remember that an alias is a real signal and will appear in the output as if it were a baseband signal. Therefore, the alias adds to the baseband signal for a theoretically lossless detector. In real life, there is a slight loss due to the resistance of the switch and aperture loss due to imperfect switching times.

PC SDR Transceiver Hardware

The Tayloe detector therefore provides a low-cost, high-performance method for both quadrature down-conversion as well as up-conversion for transmitting. For a complete system, we would need to provide analog AGC to prevent overload of the ADC inputs and a means of digital frequency control. Fig 14 illustrates the hardware

architecture of the PC SDR receiver as it currently exists. The challenge has been to build a low-noise analog chain that matches the dynamic range of the Tayloe detector to the dynamic range of the PC sound card. This will be covered in a future article.

I am currently prototyping a complete PC SDR transceiver, the SDR-1000, that will provide general-coverage receive from 100 kHz to 54 MHz and will transmit on all ham bands from 160 through 6 meters.

SDR Applications

At the time of this writing, the typical entry-level PC now runs at a clock frequency greater than 1 GHz and costs only a few hundred dollars. We now have exceptional processing power at our disposal to perform DSP tasks that were once only dreams. The transfer of knowledge from the aca-

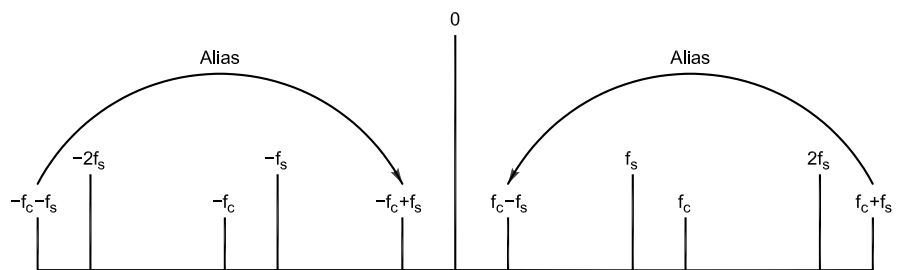


Fig 13—Alias summing on Tayloe detector output: Since the Tayloe detector samples the signal the sum frequency ($f_c + f_s$) and its image ($-f_c - f_s$) are located at the first alias frequency. The alias signals sum with the baseband signals to eliminate the mixing product loss associated with traditional mixers. In a typical mixer, the sum frequency energy is lost through filtering thereby increasing the noise figure of the device.

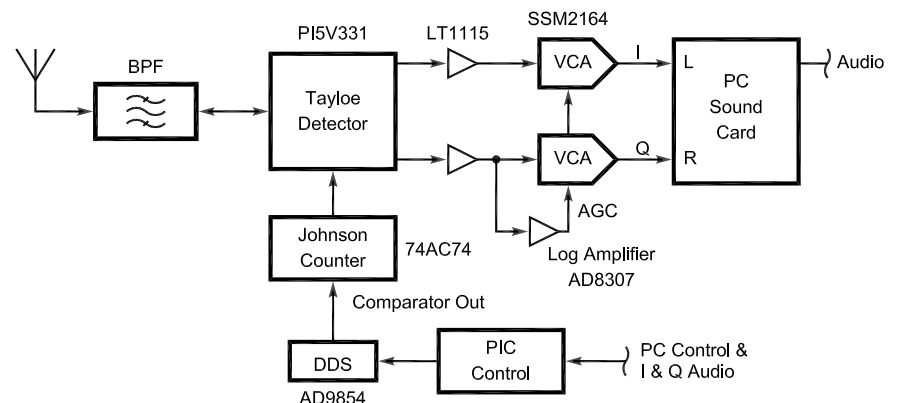


Fig 14—PC SDR receiver hardware architecture: After band-pass filtering the antenna is fed directly to the Tayloe detector, which in turn provides I and Q outputs at baseband. A DDS and a divide-by-four Johnson counter drive the Tayloe detector demultiplexer. The LT1115s offer ultra-low noise-differential summing and amplification prior to the wide-dynamic-range analog AGC circuit formed by the SSM2164 and AD8307 log amplifier.

demio to the practical is the primary limit of the availability of this technology to the Amateur Radio experimenter. This article series attempts to demystify some of the fundamental concepts to encourage experimentation within our community. The ARRL recently formed a SDR Working Group for supporting this effort, as well.

The SDR mimics the analog world in digital data, which can be manipulated much more precisely. Analog radio has always been modeled mathematically and can therefore be processed in a computer. This means that virtually any modulation scheme may be handled digitally with performance levels difficult, or impossible, to attain with analog circuits. Let's consider some of the amateur applications for the SDR:

- Competition-grade HF transceivers
- High-performance IF for microwave bands
- Multimode digital transceiver
- EME and weak-signal work
- Digital-voice modes
- Dream it and code it

For Further Reading

For more in-depth study of DSP techniques, I highly recommend that you purchase the following texts in order of their listing:

Understanding Digital Signal Processing by Richard G. Lyons (see Note 6). This is one of the best-written textbooks about DSP.

Digital Signal Processing Technology by Doug Smith (see Note 4). This new book explains DSP theory and application from an Amateur Radio perspective.

Digital Signal Processing in Communications Systems by Marvin E. Frerking (see Note 3). This book relates DSP theory specifically to modulation and demodulation techniques for radio applications.

Acknowledgements

I would like to thank those who have assisted me in my journey to understanding software radios. Dan Tayloe, N7VE, has always been helpful and responsive in answering questions about the Tayloe detector. Doug Smith, KF6DX, and Leif Åsbrink, SM5BSZ, have been gracious to answer my questions about DSP and receiver design on numerous occasions. Most of all, I want to thank my Saturday-morning breakfast review team: Mike Pendley,

WA5VTV; Ken Simmons, K5UHF; Rick Kirrhof, KD5ABM; and Chuck McLeavy, WB5BMH. These guys put up with my questions every week and have given me tremendous advice and feedback all throughout the project. I also want to thank my wonderful wife, Virginia, who has been incredibly patient with all the hours I have put in on this project.

Where Do We Go From Here?

Three future articles will describe the construction and programming of the PC SDR. The next article in the series will detail the software interface to the PC sound card. Integrating full-duplex sound with *DirectX* was one of the more challenging parts of the project. The third article will describe the *Visual Basic* code and the use of the Intel Signal Processing Library for implementing the key DSP algorithms in radio communications. The final article will describe the completed transceiver hardware for the SDR-1000.

Notes

- ¹D. Smith, KF6DX, "Signals, Samples and Stuff: A DSP Tutorial (Part 1)," *QEX*, Mar/Apr 1998, pp 3-11.
- ²J. Bloom, KE3Z, "Negative Frequencies and Complex Signals," *QEX*, Sep 1994, pp 22-27.
- ³M. E. Frerking, *Digital Signal Processing in Communication Systems* (New York: Van Nostrand Reinhold, 1994, ISBN: 0442016166), pp 272-286.
- ⁴D. Smith, KF6DX, *Digital Signal Processing Technology* (Newington, Connecticut: ARRL, 2001), pp 5-1 through 5-38.
- ⁵The Intel Signal Processing Library is available for download at developer.intel.com/software/products/perflib/spil/.
- ⁶R. G. Lyons, *Understanding Digital Signal Processing*, (Reading, Massachusetts: Addison-Wesley, 1997), pp 49-146.
- ⁷D. Tayloe, N7VE, "Letters to the Editor, Notes on 'Ideal' Commutating Mixers (Nov/Dec 1999)," *QEX*, March/April 2001, p 61.
- ⁸P. Rice, VK3BHR, "SSB by the Fourth Method?" available at ironbark.bendigo.latrobe.edu.au/~rice/ssb/ssb.html.
- ⁹A. A. Abidi, "Direct-Conversion Radio Transceivers for Digital Communications," *IEEE Journal of Solid-State Circuits*, Vol 30, No 12, December 1995, pp 1399-1410. Also on the Web at www.icsl.ucla.edu/aagroup/PDF_files/dir-con.pdf
- ¹⁰P. Y. Chan, A. Rofougaran, K.A. Ahmed, and A. A. Abidi, "A Highly Linear 1-GHz CMOS Downconversion Mixer." Presented at the European Solid State Circuits Conference, Seville, Spain, Sep 22-24, 1993, pp 210-213 of the conference proceedings. Also on the Web at www.icsl.ucla.edu/aagroup/PDF_files/mxr-93.pdf

- ¹¹D. H. van Graas, PA0DEN, "The Fourth Method: Generating and Detecting SSB Signals," *QEX*, Sep 1990, pp 7-11. This circuit is very similar to a Tayloe detector, but it has a lot of unnecessary components.
- ¹²M. Kossor, WA2EBY, "A Digital Commutating Filter," *QEX*, May/June 1999, pp 3-8.
- ¹³C. Ping, BA1HAM, "An Improved Switched Capacitor Filter," *QEX*, Sep/Oct 2000, pp 41-45.
- ¹⁴P. Anderson, KC1HR, "Letters to the Editor, A Digital Commutating Filter," *QEX*, Jul/Aug 1999, pp 62.
- ¹⁵D. Smith, KF6DX, "Notes on 'Ideal' Commutating Mixers," *QEX*, Nov/Dec 1999, pp 52-54.
- ¹⁶P. Chadwick, G3RZP, "Letters to the Editor, Notes on 'Ideal' Commutating Mixers" (Nov/Dec 1999), *QEX*, Mar/Apr 2000, pp 61-62.

Gerald became a ham in 1967 during high school, first as a Novice and then a General class as WA5RXV. He completed his Advanced class license and became KE5OH before finishing high school and received his First Class Radiotelephone license while working in the television broadcast industry during college. After 25 years of inactivity, Gerald returned to the active amateur ranks in 1997 when he completed the requirements for Extra class license and became AC5OG.

Gerald lives in Austin, Texas, and is currently CEO of Sixth Market Inc, a hedge fund that trades equities using artificial-intelligence software. Gerald previously founded and ran five technology companies spanning hardware, software and electronic manufacturing. Gerald holds a Bachelor of Science Degree in Electrical Engineering from Mississippi State University.

Gerald is a member of the ARRL SDR working Group and currently enjoys homebrew software-radio development, 6-meter DX and satellite operations. □□

TOROID CORES



Ferrite and iron powder cores. Free catalog and RFI Tip Sheet. Our RFI kit gets RFI out of TV's, telephones, stereos, etc.
Model RFI-4 \$25.00
 + \$6 S&H U.S./Canada. Tax in Calif.
 Use MASTERCARD or VISA

PALOMAR
 BOX 462222, ESCONDIDO, CA 92046
 TEL: 760-747-3343 FAX: 760-747-3346
 e-mail: Palomar@compuserve.com
 www.Palomar-Engineers.com

Notes on the OWA Yagi

Wouldn't you like a high-performance wide-bandwidth antenna? An Optimized Wideband Antenna (OWA) Yagi may be the answer. Come learn a little about how OWAs work and what potential they hold.

By L. B. Cebik, W4RNL

Perhaps the most-read source of information on the “Optimized Wideband Antenna (OWA) Yagi” comes from a series of Web site entries by Nathan Miller, NW3Z, and Jim Breakall, WA3FET (nw3z.contesting.com). Besides providing a very brief background for the design features of the OWA Yagi, the articles present specific designs for the upper HF bands used in contests.

According to the OWA account, when we place a parasitic element close (less than 0.01 wavelength) ahead of a driven element, we obtain wide-band performance. That is, we get a low SWR relative to 50 Ω , smooth

gain and front-to-back performance over a wide HF amateur band (such as 20, 15 or 10 meters). The authors suggest that the driver and first director perform as if they were a single element having a diameter equal to the spacing between the two elements.

Extensive *NEC-4* modeling studies of the actual OWA designs suggest that we may need an expanded account of how these antennas work. As well, these modeling investigations also suggest some unanticipated benefits of OWA design in antennas larger than the typical six-element HF design. To demonstrate these suggestions, I have transferred the OWA design to two meters, where full coverage of 144-148 MHz is often a challenge. The band exhibits a 2.7% bandwidth relative to its center fre-

quency (146 MHz), which is wider than most of the HF bands from 20 meters on up, with the exception of 10 meters, which has a bandwidth of about 3.5%. We shall look briefly in these proceedings at even wider bandwidths.

As well, modeling the antennas at two meters permits the use of uniform-diameter elements. These elements allow simplified models, from the standpoints of both optimizing a design and reading the results. All of the models that we shall selectively survey will presume elements that are well insulated and isolated from any conductive support boom. Several of the designs have been successfully built, with performance meeting the modeled expectations.

Modeling permits us to view the cur-

1434 High Mesa Dr
Knoxville, TN 37938-4443
cebik@cebik.com

rent magnitude and phase angle on each element (using the element center) relative to the source or feed-point current. The current data provides important clues in our search for an expanded understanding of OWA operation. The downside of the investigation technique is that our presentation will be heavily laden with graphs and tables.

Despite an appearance of extensive investigation, this study is incomplete. It samples only a few of the many OWA designs in my stock, and even if they seem typical, I cannot make a claim of complete coverage. Hence, the conclusions are only suggestive, but not in any way authoritative. If past Yagi developments teach anything, it is that something new lies ahead in the development of parasitic arrays.

Introduction to a Six-Element 2-Meter OWA Yagi

We shall begin with the six-element, two-meter OWA Yagi whose outline appears in Fig 1, with dimensions shown in Table 1. The sketch provides the traditional element designations, which include a single reflector, a single driver and four directors. However, before we are finished with this beam, we shall have occasion to rethink our element designations. The

design is an adaptation of an NW3Z/WA3FET 20-meter design.

The dimensions in Table 1 should arouse our interest. I have given them

in inches and wavelengths for convenience. The first director is 0.052λ from the driver, in accord with the general OWA design precepts.

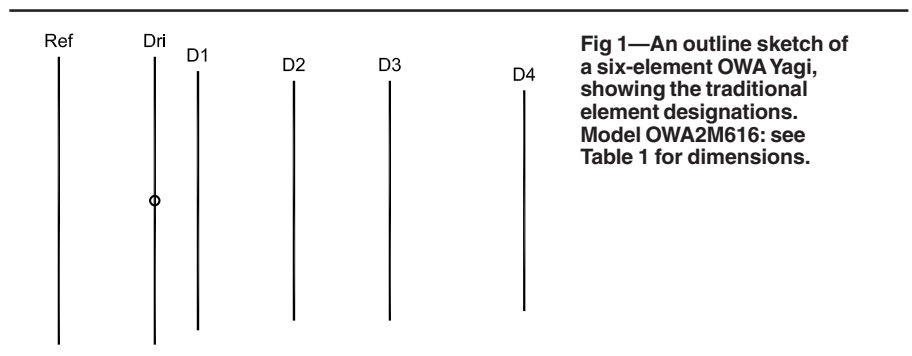


Fig 1—An outline sketch of a six-element OWA Yagi, showing the traditional element designations. Model OWA2M616; see Table 1 for dimensions.

Table 1—Model OWA2M616 Dimensions

Dimensions of a 6-element 2-meter OWA Yagi using 0.1875" ($3/16$ "") diameter elements. Wavelength (λ) measurements are for a design center frequency of 146 MHz.

Element	Length		Cumulative Spacing		Individual Spacing	
	Inches	λ	Inches	λ	Inches	λ
Refl	40.52	0.501	—	—	—	—
Driver	39.96	0.494	10.13	0.125	10.13	0.125
Dir 1	37.38	0.462	14.32	0.177	4.19	0.052
Dir 2	36.31	0.449	25.93	0.321	11.61	0.144
Dir 3	36.31	0.449	37.28	0.461	11.35	0.140
Dir 4	34.96	0.433	54.22	0.671	16.94	0.210

Table 2—6-Element 2-Meter OWA Yagi

NEC-4 reported performance data for model OWA2M616 from 139 to 149 MHz. Current data consist of the relative current magnitude and phase angle on the center segment of each element, where the driver current magnitude is always 1.0 and the driver phase angle is always 0.0° . The "D2 versus D3 currents" consist of the ratio of current magnitude from Director 2 to Director 3 and of the current phase-angle difference between the two directors. (See text for data interpretation.)

Performance

Frequency (MHz)	139	140	141	142	143	144	145	146	147	148	149
Free Space Gain (dBi)	9.38	9.68	9.86	9.97	10.06	10.13	10.19	10.23	10.23	10.16	10.01
180° F/B (dB)	8.34	10.61	12.9	15.35	18.23	22.04	28.2	35.39	26.71	22.17	20
R (Ω)	27.85	32.99	37.33	40.51	42.78	44.79	47.18	49.97	50.82	43.6	27.9
X (Ω)	-8.58	-3.56	-0.1	2.56	5.07	7.61	9.62	9.52	5.18	-1.719	-0.98
SWR (50 Ω)	1.871	1.529	1.34	1.244	1.21	1.215	1.229	1.21	1.109	1.152	1.793

Currents

Ref-Magnitude	0.805	0.764	0.708	0.647	0.588	0.54	0.503	0.472	0.428	0.34	0.208
Ref-Phase ($^\circ$)	147.5	138.36	130.1	123.08	117.28	112.2	106.78	99.29	87.69	71.67	57.19
D1-Magnitude	0.492	0.592	0.686	0.771	0.856	0.952	1.079	1.257	1.481	1.657	1.641
D1-Phase ($^\circ$)	-76.11	-80.96	-86.43	-91.64	-96.19	-100.1	-104.1	-109.5	-118.6	-132.8	-148.4
D2-Magnitude	0.369	0.437	0.5	0.558	0.613	0.67	0.733	0.799	0.845	0.809	0.655
D2-Phase ($^\circ$)	233.1	224.3	214.8	205.1	195.4	185.5	174.69	161.83	145.43	125.6	107.83
D3-Magnitude	0.34	0.403	0.462	0.52	0.58	0.649	0.735	0.844	0.962	1.02	0.949
D3-Phase ($^\circ$)	174.94	164.96	154.44	143.9	133.48	122.87	111.43	97.47	79.44	56.65	33.21
D4-Magnitude	0.301	0.357	0.41	0.459	0.508	0.561	0.623	0.696	0.763	0.769	0.67
D4-Phase ($^\circ$)	92.97	80.21	66.75	53.06	39.26	25.02	9.58	-8.47	-30.94	-58.41	-86.67

D2 versus D3 Currents

Magnitude Ratio	1.085	1.084	1.082	1.073	1.057	1.032	0.997	0.947	0.878	0.793	0.69
Phase Difference ($^\circ$)	58.16	59.34	60.66	61.2	61.92	62.63	63.35	64.36	65.99	68.95	74.62

However, note the lengths of directors D2 and D3: They are identical. (In actuality, OWA designs of this type may use a third director that is slightly shorter or slightly longer—by up to about 1%—than director 2, according to overall design goals.) The lengths of these two directors are no accident, even if their role in the OWA design is often overlooked.

There is often a vast difference between the exceptionally wide 50- Ω SWR curve of an OWA design and the intended operating bandwidth of the antenna. Table 2 presents the modeled characteristics of this six-element Yagi from 139 to 149 MHz, although the performance characteristics focus on the 144-148-MHz span. The design goals use typical Amateur Radio guidelines for the 0.67- λ boom: a free-space gain of at least 10 dBi, a 180° and worst-case front-to-back ratio of at least 20 dB

and as flat a 50- Ω SWR as we may achieve. Fig 2 shows that the antenna easily meets the gain and front-to-back guidelines from 144 to 148 MHz.

Fig 3 presents the 50- Ω SWR curve for the array from 139 to 149 MHz. The curve is typical of optimized OWA designs. Yes, even an optimized broadband antenna may be optimized within its overall design parameters. Most noticeable and telling is the presence of two dips in the SWR, one shallow dip at 143 MHz and one very sharp dip near 147.5 MHz. The rise in SWR above 148 MHz is very steep, while below the operating passband for the antenna, the SWR rises very slowly.

The graph of resistance and reactance across the entire scanned spectrum, Fig 4, shows us why the SWR remains so flat. The feed-point resistance and reactance both vary across an extremely small range, with the

largest incremental changes occurring above the operating passband. The reactance begins as a small capacitive value, changes to a set of inductive values, and returns to capacitive values at the high end of the scanned passband. We might miss these patterns if we look only within the operating passband for the antenna.

Most OWA designs place the operating passband near the upper end of the SWR passband. In this region, we usually find the lowest SWR value in conjunction with the flattest curve at the lower end of the impedance passband. However, the steep rise in SWR above the operating passband requires significant care in array construction to avoid moving the SWR curve into the region of rapid change. In fact, nothing dictates that the operating passband must be in this region. Indeed, with lesser levels of gain and front-to-

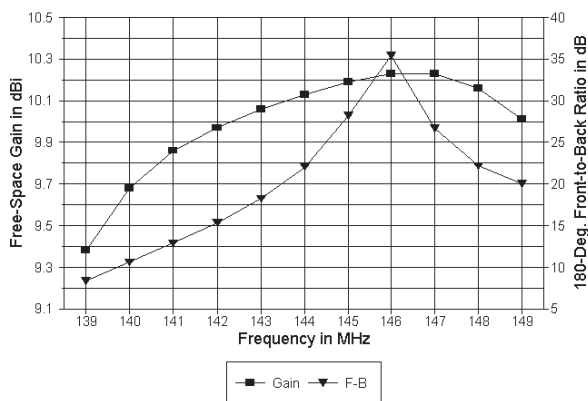


Fig 2—The modeled free-space gain and 180° front-to-back performance of Model OWA2M616 from 139 to 149 MHz. See Table 2 for numeric data.

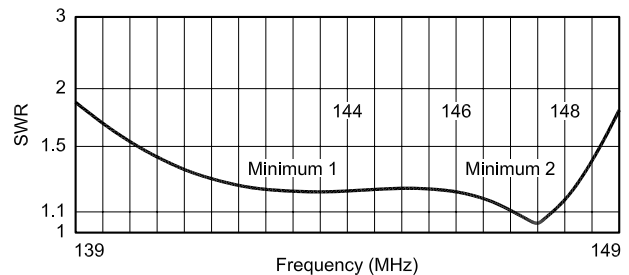


Fig 3—50- Ω SWR curve for model OWA2M616 from 139 to 149 MHz.

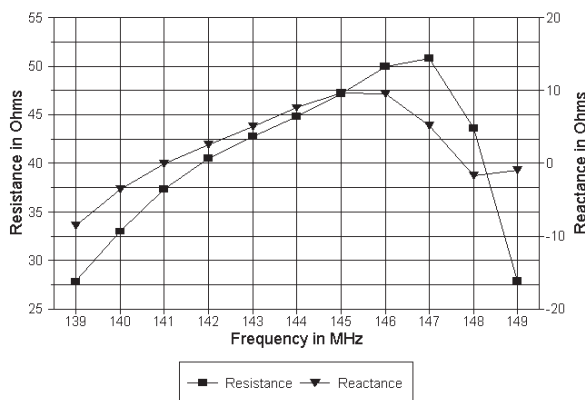


Fig 4—Feed-point resistance and reactance for model OWA2M616 from 139 to 149 MHz.

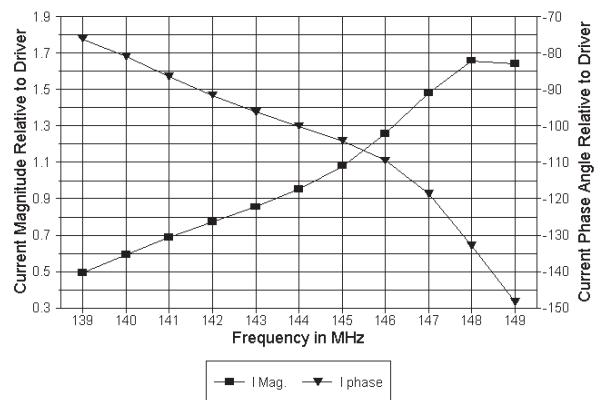


Fig 5—The current magnitude and phase angle on director 1 of model OWA2M616 from 139 to 149 MHz relative to a value of 1.0 and 0.0° on the center segment of the driven element.

back ratio, we may spread the operating region across most of the low SWR region. Moreover, the width of the “low” SWR region is limited mostly by the level to which we are willing to allow the SWR to rise between the minima. Most, but not all, extant OWA designs try to keep the mid-region values as low as feasible.

Designing an OWA Yagi, then, is a balance between the operating specifications (and possibilities for a given boom length) on the one hand and the desired SWR level and curve on the other. Changing one or the other set of specifications will alter the resulting physical design. Hence, there can be no “ultimate” OWA design. However, with a given set of operating and SWR specifications, we can try to see how the OWA achieves its goals.

OWA-1: Understanding the OWA with Reference to the Reflector, Driver and First Director

The initial perspective that we shall take on the OWA follows the received account of its operation. The spacing between the driver and the first director sets the 50-Ω SWR curve for the array. Of course, the length and spacing of the reflector play a significant role in establishing the reference impedance for the SWR curve—in addition to playing a smaller role in setting the operational band-edge performance of the array.

With this perspective applied to our initial six-element OWA Yagi, we find a reflector about $1/8\lambda$ behind the driver, with the first director spaced about 0.052λ ahead. If we set the driver current magnitude to a value of 1.0 and a phase angle of 0.0° for every scanned frequency, we may track the relative current magnitude and phase angle on the first (close-spaced) director. Fig 5 shows the results of this exercise.

As expected, the first director shows a negative current phase angle relative to the driver. However, note that the curve steepens, indicating a greater rate of change above about 146 MHz. At the same time, the current magnitude on the first director continuously increases with rising frequency—until we reach 148 MHz. The current magnitude is actually greater on the first director than on the driver from 145 MHz upward.

In effect, the driver and first director actually form a primary (fed) driver and secondary (parasitic) driver pair. (When applied to different frequency bands, the pair sometimes goes under the names master and slaved driver.

However, for in-band applications, the terms primary and secondary may be more apt.) As the secondary driver becomes dominant, the rate of change of its current phase angle increases.

The question that remains is this: Is the account sufficient to set the OWA design apart as unique? If we limit our investigation only to the reflector/driver/first-director trio of elements, then the concept is not new, but only refined by the use of very close spacing of director 1 to the driver. For example, the DL6WU family of VHF/UHF Yagis uses 0.075λ spacing for director 1 to obtain very wide-band operation for Yagis ranging from 6 to n elements. See Chapter 7 (by Gunter Hoch, DL6WU) of the RSGB publication, *The VHF/UHF DX Book*, edited by Ian White, G3SEK, for perhaps the last iteration of this classic set of Yagis. Experimental Yagi designs using “fat” elements have achieved operating bandwidths (including usable gain and front-to-back ratios) of greater than 23% of the central frequency of the passband.

At a more modest size—in fact, quite comparable in boom length to our six-element OWA Yagi—is an adaptation of a five-element broadband Yagi design that originated from the work of Jack Reeder, W6NGZ (now WW7JR), and that appears in *CQ* magazine of

October, 1996. The design made no pretense about using OWA principles, but simply strove to cover 20 meters within the usual standards for good Amateur Radio performance. I have adapted the design to $3/16$ -inch elements and two meters for comparison with the six-element OWA design.

Fig 6 shows the array outline for comparison with the OWA outline in Fig 1. Table 3 provides the dimensions, which show the boom length to be about $3/4$ -inch shorter than the six-element OWA. However, there are only five elements. The reflector is about 0.123λ behind the driver, with the first director 0.089λ ahead.

Table 4 supplies a complete performance table comparable to the data in Table 2 for the six-element OWA Yagi. We can begin by comparing Fig 7 to Fig 2 to gauge the success of the five-element design in achieving the performance goals. In fact, the performance curves in the two figures have very similar shapes, with the smaller design having lower performance numbers at the scanning limits. From the table, you may determine that over the 144 to 148-MHz operating passband, the five-element Yagi misses the 20-dB front-to-back ratio guideline by an amount too small to make any difference.

The feed-point resistance and reac-

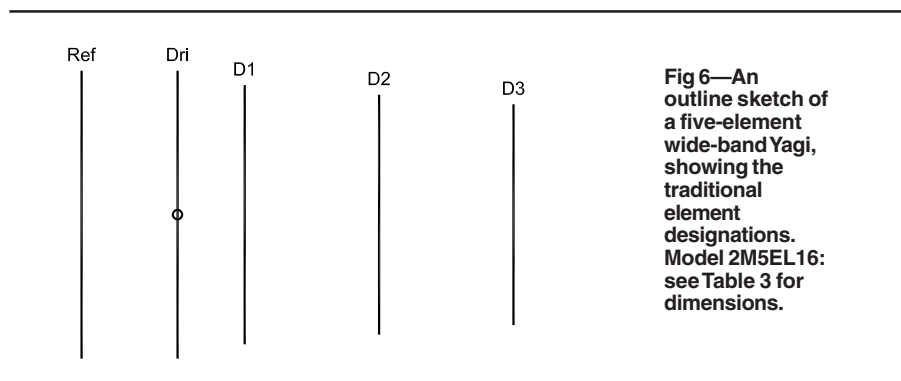


Fig 6—An outline sketch of a five-element wide-band Yagi, showing the traditional element designations. Model 2M5EL16: see Table 3 for dimensions.

Table 3—Model 2M5EL16 Dimensions

Dimensions of a 5-element 2-meter wide-band Yagi using $0.1875"$ ($3/16"$) diameter elements. Wavelength (λ) measurements are for a design center frequency of 146 MHz.

Element	Length		Cumulative Spacing		Individual Spacing	
	Inches	λ	Inches	λ	Inches	λ
Refl	40.46	0.501	—	—	—	—
Driver	39.26	0.486	9.90	0.123	9.90	0.123
Dir 1	37.19	0.460	17.10	0.212	7.20	0.089
Dir 2	36.88	0.456	34.80	0.431	17.70	0.219
Dir 3	35.64	0.441	53.50	0.662	28.70	0.231

Table 4—5-Element 2-Meter Wide-Band Yagi

NEC-4 reported performance data for model 2M5EL16 from 139 to 149 MHz. Current data consist of the relative current magnitude and phase angle on the center segment of each element, where the driver current magnitude is always 1.0 and the driver phase angle is always 0.0°. The “D1 versus D2 currents” consist of the ratio of current magnitude from Director 1 to Director 2 and of the current phase angle difference between the two directors. (See text for data interpretation.)

Performance

Frequency (MHz)	139	140	141	142	143	144	145	146	147	148	149
Free Space Gain (dBi)	9.29	9.62	9.81	9.94	10.05	10.16	10.26	10.33	10.32	10.15	9.69
180° F/B (dB)	7.02	9.18	11.53	13.65	16.37	20.11	26.75	41.94	24.47	19.73	18.23
R (Ω)	25.09	29.83	33.44	35.21	35.43	35.08	35.46	38.1	43.5	39.13	15.36
X (Ω)	-20.77	-15.5	-12.09	-9.41	-6.26	-1.99	3.23	8.02	7.52	-4.93	-1.75
SWR (50 Ω)	2.427	1.911	1.643	1.514	1.454	1.43	1.422	1.387	1.237	1.309	3.26

Currents

Ref-Magnitude	0.818	0.77	0.699	0.618	0.542	0.484	0.45	0.438	0.426	0.319	0.099
REF-Phase (°)	152.42	143.2	135.02	128.74	124.83	123	121.82	118.4	107.48	83.68	80.34
D1-Magnitude	0.507	0.61	0.7	0.77	0.824	0.873	0.942	1.081	1.379	1.759	1.658
D1-Phase (°)	-78.73	-85.44	-93.02	-100.3	-106.3	-110.6	-112.9	-114.3	-119.4	-137.9	-165.8
D2-Magnitude	0.381	0.461	0.539	0.613	0.689	0.779	0.904	1.099	1.399	1.537	1.221
D2-Phase (°)	206.8	197.5	187.3	177.03	167.1	157.41	147.13	134.2	113.77	78.54	40.69
D3-Magnitude	0.316	0.379	0.437	0.487	0.531	0.579	0.641	0.734	0.869	0.91	0.623
D3-Phase (°)	108.7	95.73	81.74	67.54	53.54	39.65	25.09	7.86	-16.82	-56.15	-97.8

D1 versus D2 Current

Magnitude Ratio	1.331	1.323	1.299	1.256	1.196	1.121	1.042	0.984	0.986	1.144	1.358
Phase Difference (°)	285.53	282.94	280.32	277.33	273.4	268.01	260.03	248.5	233.17	216.44	202.29

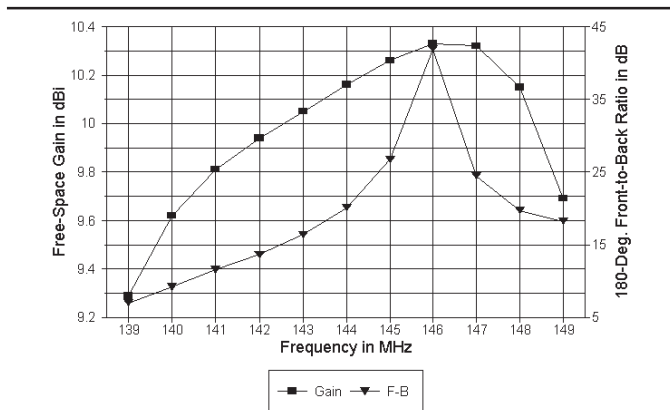


Fig 7—The modeled free-space gain and 180° front-to-back performance of Model 2M5EL16 from 139 to 149 MHz. See Table 2 for numeric data.

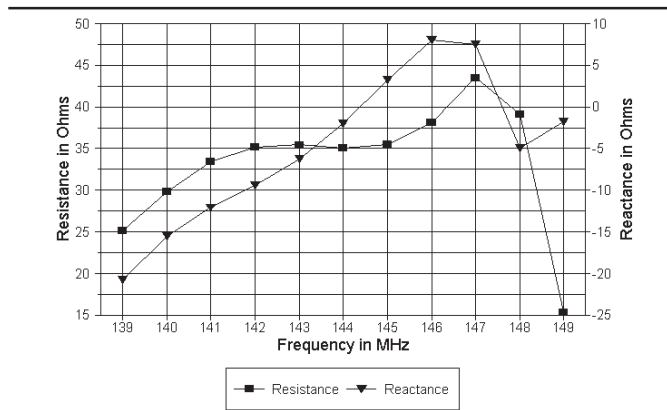


Fig 8—Feed-point resistance and reactance for model 2M5EL16 from 139 to 149 MHz.

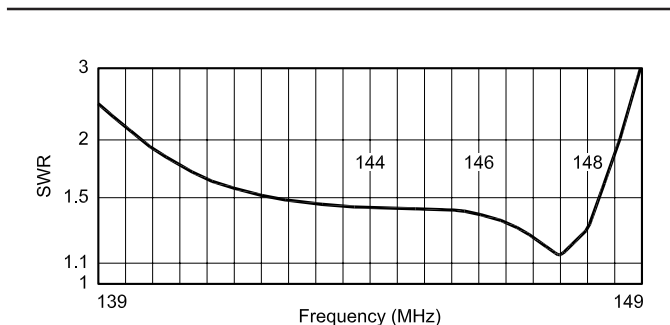


Fig 9—50-Ω SWR curve for model 2M5EL16 from 139 to 149 MHz.

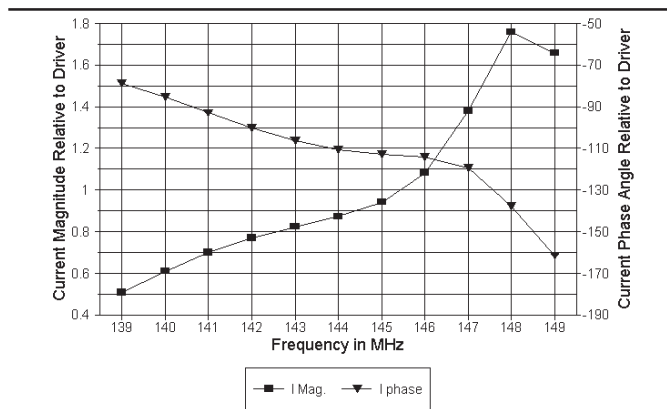


Fig 10—The current magnitude and phase angle on director 1 of model 2M5EL16 from 139 to 149 MHz relative to a value of 1.0 and 0.0° on the center segment of the driven element.

tance curves in Fig 8 also show considerable similarity to those for the OWA Yagi in Fig 4. The median resistance is in the 35 to 40- Ω range because of the spacing of the reflector from the driver. The original array for 20 meters was designed to a certain boom-length limit, so long as the 50- Ω SWR values remained below 2:1 within the operating passband. Fig 9 shows the five-element Yagi 50- Ω SWR curve. It exhibits the same general shape as Fig 3 for the OWA Yagi, but without a definite minimum within the lower frequency region of the span. Had we used a reference impedance of 35 to 40 Ω , the overall curve would have come closer to achieving better than 2:1 values across the scanned passband.

Like the six-element OWA Yagi, the first director functions as a secondary driver. Between 145 and 146 MHz, the current magnitude exceeds a ratio of 1.0:1 relative to the current magnitude on the primary driver, as shown in Fig 10. Indeed, allowing for the difference in curve shapes that is due to changes in the axis increments, the curves for both current magnitude and phase angle are remarkably similar. Only the current phase angle of the smaller array increases at a higher rate at the upper limit of the scanned frequency range.

An interesting facet of the wide-band five-element array appears in Fig 11, a graph of the differentials in current magnitude and phase angle between director 1 (the secondary driver) and director 2. The ratio of director 1 to director 2 current magnitude varies over a quite small range, much smaller than the current magnitude excursions for any other element pair in the array. The current phase-angle difference

also remains relatively constant for nearly the full lower half of the scanned frequency range, decreasing ever more rapidly thereafter. In this upper portion of the frequency range, the secondary driver/first director becomes ever more dominant in driving the array.

In short, there is little in the reflector-driver-director-1 portion of the array to distinguish the six-element OWA Yagi from the five-element wide-band Yagi. Granted, the larger array has a measurably wider impedance bandwidth and slightly narrower boundaries to the range of impedance and current values sampled from 139 to 149 MHz. However, it does not appear that the reflector-driver-director-1 portion of the array is sufficient to account for the smoother performance of the OWA.

OWA-2: Understanding the OWA with Reference Also to the Second and Third Directors

Often overlooked are the second and third directors of the six-element OWA design. These elements are those having almost, if not actually, identical lengths. They show some interesting properties within the overall OWA structure.

A glance at Table 2 shows that the first and second directors of the OWA array do not present the same level of close correlation among the current numbers as the corresponding elements in the five-element Yagi. Indeed, it appears that the first director of the smaller beam does double duty relative to the OWA array with its extra element. The five-element Yagi first director serves both as a secondary driver and as a stabilizing director for wide-band operation. From the

perspective of the six-element OWA Yagi, the second and third directors provide the relatively close correlation of current values independently of the first director, which also serves as the secondary driver.

Fig 12 presents the current magnitudes (relative to a primary driver value of 1.0) for the second and third directors of the OWA array. Using the left axis as a guide, we find the values almost identical until the curves diverge above 145 MHz. In the upper region of the frequency scan, where the secondary driver dominates, the curves diverge in value but have similar shapes.

The figure also shows the current phase angles for the same two elements (relative to a constant primary-driver value of 0.0°). The parallel nature of the curves can hardly escape detection.

In Fig 13, the raw data in Fig 12 becomes a set of differentials. The ratio of current between director 2 and director 3 becomes a smooth curve, with only small changes in value in the lower half of the frequency range. (Compare this smooth curve to the “dipper-shaped” curve for the current magnitude ratio of director 1 to director 2 in Fig 11 for the five-element beam.) The amount of phase-angle difference change is even more startling—less than 16.5° overall from 139 to 149 MHz. Likewise, compare this value to the 72° change in difference in Fig 11 across the same range for the first and second directors of the five-element array. Indeed, we might categorize the second and third directors of the OWA as “stabilizing” directors.

Achieving the greatest impedance bandwidth from the OWA array appears to require the added element

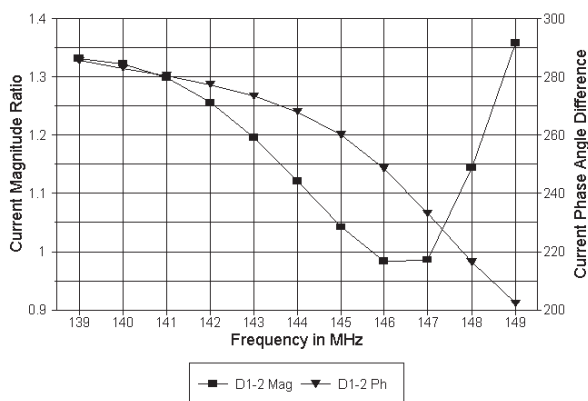


Fig 11—The current-magnitude ratio and the current phase-angle differential between directors 1 and 2 on model 2M5EL16.

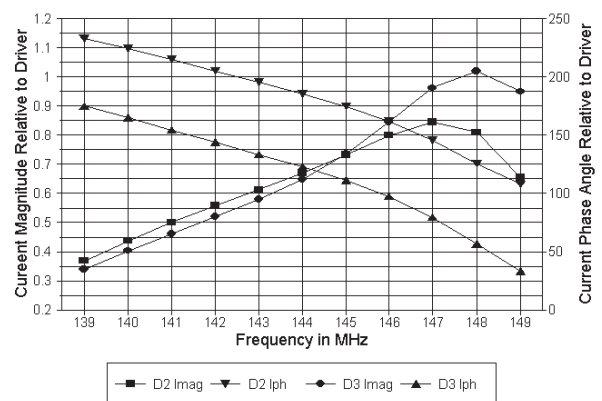


Fig 12—The current magnitudes and phase angles of directors 2 and 3 on model OWA2M616 from 139 to 149 MHz relative to a value of 1.0 and 0.0° on the center segment of the driven element.

within the same boom length in order to arrive at the most stable wide-band operation. Indeed, what sets the OWA design apart from past wide-band parasitic arrays is the combination of a close-spaced secondary driver and the pair of stabilizing directors of equal or very nearly equal length. Closer spacing of the secondary driver permits the achievement of higher median impedance with the same reflector spacing. Since one needs an added director to fill the void in order to reach performance specifications for a given boom length, the new director and the next together—when properly set in length and spacing—complete the broadbanding design operation. Indeed, the impedance bandwidth of the OWA Yagi tends to decrease as the second and third directors diverge in length for a given spacing. In short, it is the entire array design—or at least the first five elements of it—that marks out an OWA Yagi from wide-band Yagis of the past.

The six-element OWA Yagi used as a comparator so far is only one of many possible designs. It is relatively short, and has a narrow operating passband relative to the impedance passband. Therefore, there is still considerable OWA ground to examine.

Some Additional OWA Benefits

The OWA basic platform consists of the reflector through director 3—at least. In a six-element design, only one director remains to control performance at the band edges (in conjunction with small changes to the reflector length). Achieving a wider operating passband—perhaps one that covers most of the impedance passband—becomes considerably easier with the addition of an extra director or two. Ahead of the basic OWA “cell,” we may “stagger” tune the directors to arrive at a very significant operating passband.

For a better test of wide-band performance potential, we may move our discussion to the 420 to 450-MHz band, which has a bandwidth that is nearly 7% of the center frequency. Fig 14 presents the outline of a 12-element OWA Yagi that will cover the entire band with reasonable performance. The dimensions for model OWA432E appear in Table 5. Like many Yagis for this band, the array uses 4-mm-diameter aluminum elements. The remaining dimensions appear in both millimeters and wavelengths. At a boom length (minus any extensions) of 2.93λ , the array is comparable to other 12-element Yagis for this band.

The overall performance of the Yagi

is quite adequate for many purposes. The 50- Ω SWR is only 1.5:1 at the band edges. Free-space gain ranges from 13.35 dBi to 14.70 dBi across the band, with a peak near 445 MHz. The 180° and worst-case front-to-back ratios tend to parallel the gain curve, although with a much sharper peak.

The only assessment that we can reach at this stage is that the array is capable of providing service across the entire band. Further assessment re-

quires some sort of standard against which to measure the OWA Yagi. Perhaps the most notable wide-band Yagis for the 420 to 450-MHz band are those developed by Gunter Hoch, DL6WU. His sequence of arrays evolved over two decades of work, with perhaps the last iteration in the RSGB *VHF/UHF DX Book*. Twelve elements is close to the shortest recommended length for a DL6WU array, but it does provide an interesting comparator against which

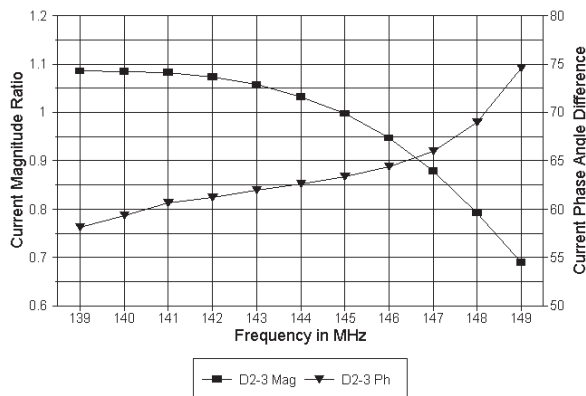


Fig 13—The current-magnitude ratio and the current phase-angle differential between directors 2 and 3 on model OWA2M616.

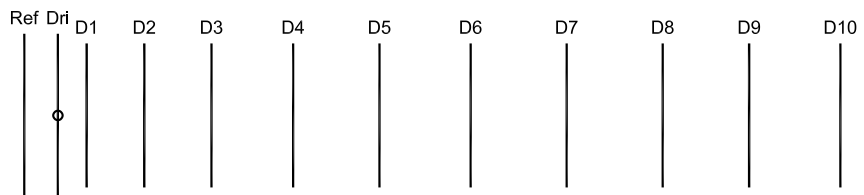


Fig 14—An outline sketch of a 12-element OWA Yagi, showing the traditional element designations. Model OWA432E: see Table 5 for dimensions.

Table 5—Model OWA432E Dimensions

Dimensions of a 12-element 420-450-MHz OWA Yagi, using 0.1575" (4 mm) diameter elements. Wavelength (λ) measurements are for a design center frequency of 435 MHz.

Element	Length		Cumulative Spacing		Individual Spacing	
	mm	λ	mm	λ	mm	λ
Refl	334.4	0.482	—	—	—	—
Driver	331.0	0.477	106.6	0.154	106.6	0.154
Dir 1	302.0	0.435	149.5	0.215	42.9	0.061
Dir 2	297.4	0.429	244.8	0.353	95.3	0.138
Dir 3	297.4	0.429	377.0	0.543	132.2	0.190
Dir 4	296.4	0.427	550.8	0.794	173.8	0.251
Dir 5	288.2	0.415	762.0	1.098	211.2	0.304
Dir 6	281.0	0.405	1010.3	1.456	248.3	0.358
Dir 7	275.2	0.397	1267.8	1.827	257.5	0.371
Dir 8	269.4	0.388	1535.4	2.213	267.6	0.386
Dir 9	263.6	0.380	1770.5	2.551	235.1	0.338
Dir 10	255.6	0.368	2032.5	2.929	262.0	0.378

to set the OWA design just described.

Fig 15 presents an outline of the DL6WU 12-element Yagi, revealing the operative regularity of element spacing and length used throughout the sequence. Table 6 provides the dimensions, once more using 4-mm elements and presented in terms of millimeters and wavelengths. At 2.85λ long, the DL6WU array reasonably approximates the boom-length of the OWA Yagi.

The DL6WU arrays all place the driver 0.2λ ahead of the reflector, with the first director spaced 0.075λ further forward. This combination—suited to the 4-mm elements—warrants the label “wide-band” to a very high degree. Fig 16 overlays the 50- Ω SWR curves for both the OWA and the DL6WU Yagis between 415 and 455 MHz. The extended range illustrates the “reserve” bandwidth provided by the DL6WU array, compared to the relative tightness of the fit between the band limits and the OWA SWR curve. More significant is that the DL6WU SWR curve shows three minima, compared to the standard two for the OWA.

The SWR curves are related to the progression of the relative current magnitude on the first directors of the respective arrays. In Fig 17, the OWA curve hovers just under a relative magnitude (to a driver value of 1.0) of 0.9. Then, at about 442 MHz, the director current magnitude surpasses that of the driver for the remainder of the operating passband. In contrast, the DL6WU curve rises above a value of 1.0 in two places. The rise and fall of the first director’s relative current magnitude correlates also to SWR maximums and minimums.

These and other performance figures for the DL6WU and OWA models appear in Table 7. For the record, Fig 18 compares the free-space gain of the two antenna models. The DL6WU version reaches a peak gain about one-quarter decibel higher than the OWA model, but the OWA gain falls off more slowly at the high end of the band. The gain differential between minimum and maximum is over 1 dB for both arrays.

The OWA array shows a single peak in its 180° front-to-back performance, as indicated clearly by Fig 19. In contrast, the DL6WU array shows two maximums, one slightly below the lower end of the band and the other slightly higher in frequency than the gain peak. The twin front-to-back peaks are related to the number of directors in the array. As one adds direc-

tors according to the DL6WU scheme, the front-to-back peaks move upward in frequency. At a certain point, a new low-end peak emerges and the remain-

ing peaks are closer together in frequency. A 26-element array has three front-to-back peaks. The proximity of peaks in turn limits the amount that

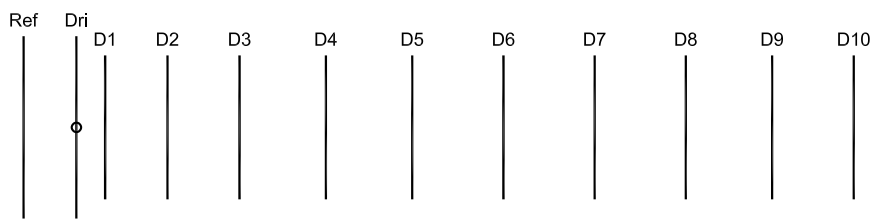


Fig 15—An outline sketch of a 12-element DL6WU Yagi, showing the traditional element designations. Model DL6WU12: see Table 6 for dimensions.

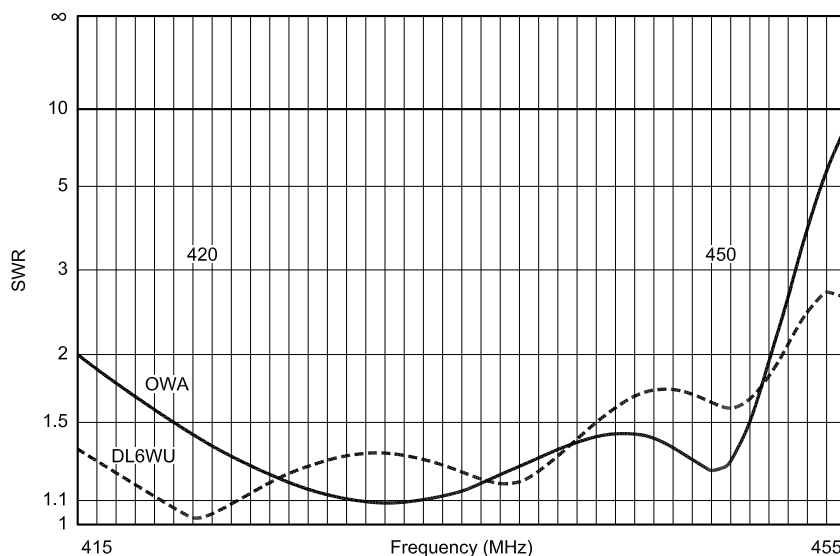


Fig 16—Comparative 50- Ω SWR curves from 415 to 455 MHz for models OWA432E and DL6WU12.

Table 6—Model DL6WU12 Dimensions

Dimensions of a 12-element 420-450-MHz DL6WU Yagi using 0.1575” (4 mm) diameter elements. Wavelength (λ) measurements are for a design center frequency of 432 MHz. Dimensions are adapted from Chapter 10 of *The VHF/UHF DX Book*, from RSGB.

Element	Length		Cumulative Spacing		Individual Spacing	
	mm	λ	mm	λ	mm	λ
Refl	340.6	0.491	—	—	—	—
Driver	330.0	0.476	138.8	0.200	138.8	0.200
Dir 1	301.6	0.435	190.8	0.275	52.0	0.075
Dir 2	299.2	0.431	315.8	0.455	125.0	0.180
Dir 3	295.6	0.426	465.0	0.670	149.2	0.215
Dir 4	292.2	0.421	638.4	0.920	173.4	0.250
Dir 5	289.2	0.417	832.8	1.200	194.4	0.280
Dir 6	286.4	0.413	1040.9	1.500	208.1	0.300
Dir 7	284.2	0.410	1259.5	1.815	218.6	0.315
Dir 8	282.2	0.407	1488.6	2.145	229.1	0.330
Dir 9	280.4	0.404	1728.0	2.490	239.4	0.335
Dir 10	278.8	0.402	1977.8	2.850	249.8	0.360

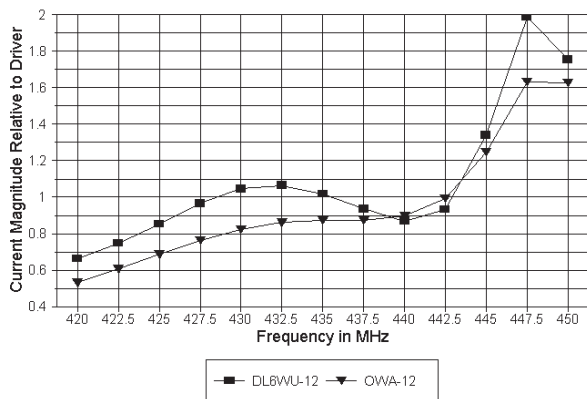


Fig 17—Comparative curves of the relative current magnitude on Director 1 of models OWA432E and DL6WU12, where the primary driver current magnitude is always 1.0.

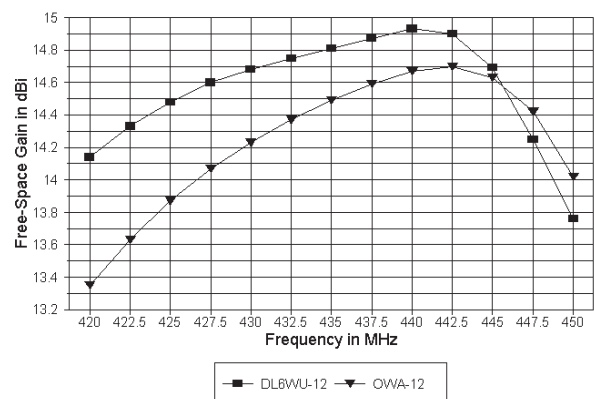


Fig 18—Comparative curves of free-space array gain for models OWA432E and DL6WU12 from 420 to 450 MHz.

the front-to-back value can decrease between peaks. Hence, very long DL6WU Yagis tend to have high minimum front-to-back values.

In terms of SWR bandwidth, gain and possibly front-to-back performance, the DL6WU 12-element array tends to outperform the OWA Yagi. At the present stage of development, it is not clear that the OWA design has reached the limits of its performance. Many folks view the first director in HF OWA Yagis as an added element. Thus, a six-element 20-meter OWA is comparable in length and performance to a standard five-element 20-meter Yagi, both with boom-lengths near 48 feet. However, the OWA design used in the example that we have explored extends the element spacing so that the 12-element boom-length is comparable to that of a standard—or at least a DL6WU—design. Whether element spacing compression to add an 11th director in the same boom length, with appropriate setting of element lengths, can broaden the SWR curve and/or increase the basic gain and front-to-back values across the band remains for further design efforts.

There is one department, little recognized by many Yagi builders, in which the OWA Yagi shows superiority over almost all other Yagi designs of comparable length. Fig 20 illustrates the region of concern with a set of free-space azimuth (E-plane) patterns taken at selected frequencies across the band. Numerical data appear in Table 7. DL6WU himself registers the forward side-lobe strength of his designs as about 17 dB. The 12-element version of his array shows slightly better figures up until the region of high-

Table 7—Comparative Performance Data: OWA2M126A and DL6WU-12

Comparative 420-450-MHz performance data from models OWA432E and DL6WU12. See text for discussion.

OWA12M126A

Frequency (MHz)	420	427.5	435	442.5	450
Free Space Gain (dBi)	13.35	14.07	14.49	14.70	14.02
180° F/B (dB)	16.36	17.58	18.16	25.28	22.47
Worst-Case F/B (dB)	16.36	17.58	18.16	23.48	20.21
Fwd/Fwd Side Lobe (dB)	21.24	23.03	24.82	26.87	22.42
-3 dB Beamwidth (°)	40.2	38.4	35.0	35.0	34.2
Feedpoint R (Ω)	33.41	44.86	44.58	46.38	39.05
Feedpoint X (Ω)	-2.68	3.16	3.23	16.98	-14.23
SWR (50 Ω)	1.504	1.136	1.143	1.431	1.497

DL6WU-12

Frequency (MHz)	420	427.5	435	442.5	450
Free Space Gain (dBi)	14.14	14.60	14.81	14.90	13.76
180° F/B (dB)	24.47	17.26	15.53	21.40	16.11
Worst-Case F/B (dB)	20.83	17.26	15.53	21.40	16.11
Fwd/Fwd Side Lobe (dB)	18.21	18.12	17.36	15.74*	19.78*
-3 dB Beamwidth (°)	37.2	35.0	33.0	31.4	30.8
Feedpoint R (Ω)	48.39	63.76	50.23	46.93	39.87
Feedpoint X (Ω)	-2.75	-1.96	-10.44	21.30	-19.85
SWR (50 Ω)	1.067	1.278	1.231	1.554	1.639

*signals the existence of a main-forward-lobe bulge rather than a true side lobe with an intervening pattern depression.

est gain. From about 440 MHz upward, the first forward side lobe becomes so wide that it merges with the main forward lobe. The result is a “bulge” in the main forward lobe, since the pattern cannot show a depression by which most computer model programs would recognize a new lobe. In Table 7, the bulge for the first forward lobe is almost invisible (in the -12-dB region), leaving one with a value for the forward side lobe that actually applies to the second lobe.

Strong forward side lobes have an interesting consequence beyond radiating power in directions other than the desired one. They also tend to narrow the half-power beam width significantly, perhaps by as much as 3° or nearly 10% of the 30 to 35° beamwidth for these arrays.

In contrast to the strong forward side lobes of the DL6WU array (and many others used in the 420-450-MHz band), the OWA Yagi exhibits a forward side lobe value averaging about

23.7 dB down from the main lobe. The result is a main forward lobe about 3° wider than that of the DL6WU beam. Over narrower operating regions, the OWA Yagi is capable of even better horizontal (E-plane) forward side-lobe suppression. The quest for such suppression does not itself address the equally important question of vertical or H-plane side-lobe suppression.

A second advantage offered by the OWA structure is that it offers a stable basic platform for the development of families of Yagis. The DL6WU Yagi family is perhaps most familiar to builders of VHF and UHF arrays, since the builder can select a boom length and—with reference to a chart provided by DL6WU—the appropriate number, length and spacing of elements to fill the boom. For any boom length above about eight elements, the impedance performance of the ar-

ray will be similar with almost any number of directors.

Table 8 provides the dimensions of a seven-element, two-meter OWA Yagi that is quite capable of forming the

basic unit for a family of two-meter OWA Yagis. The outline appears in Fig 21. The design improves upon the six-element OWA—itself a perfectly good antenna—by optimizing the ele-

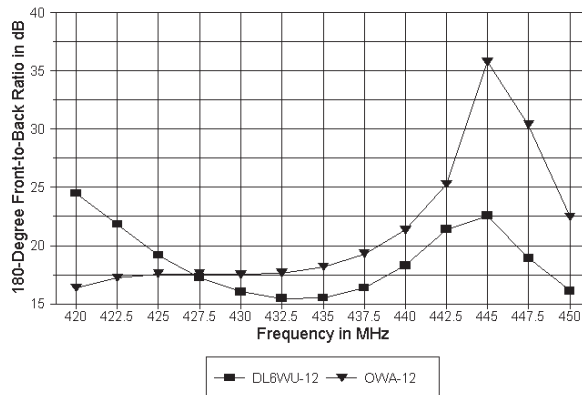
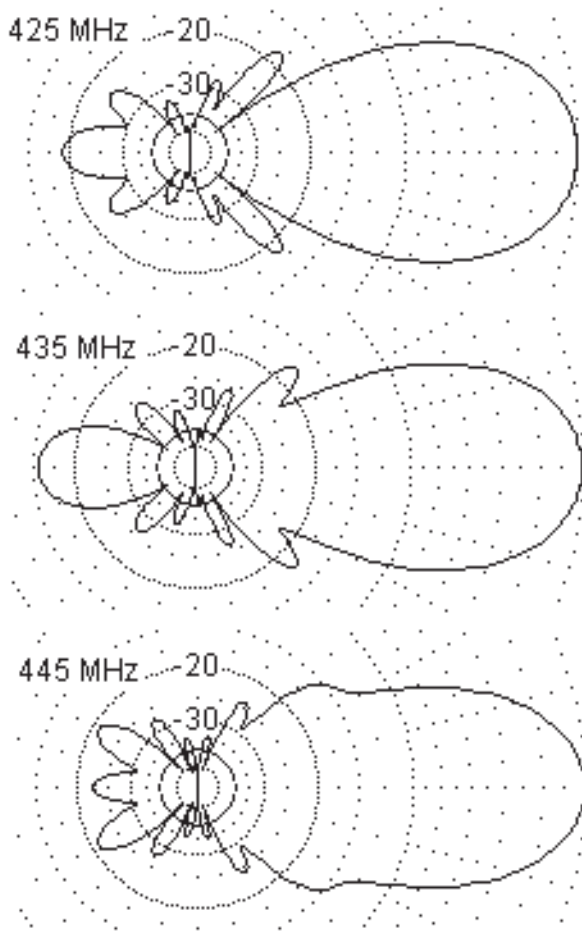


Fig 19—Comparative 180° front-to-back ratio curves for models OWA432E and DL6WU12 from 420 to 450 MHz.

12-Element DL6WU Yagi



12-Element OWA Yagi

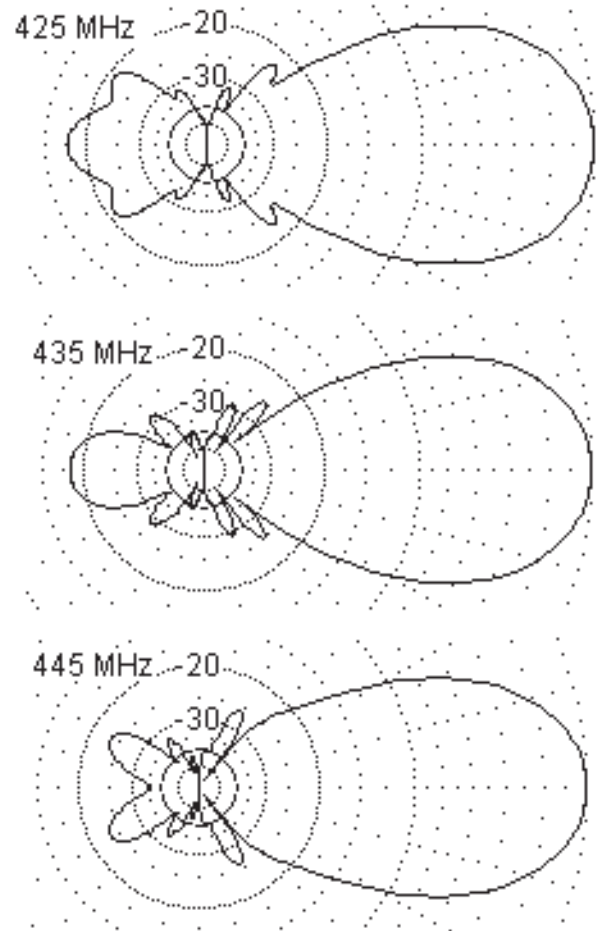


Fig 20—Comparative free-space azimuth (E-plane) patterns of models OWA432E and DL6WU12 at 425, 435 and 445 MHz, with special focus on the forward side-lobe structure and the horizontal -3-dB beamwidth. See Table 7 for numeric data.

ment spacing for the $3/16$ -inch elements. Since these elements are larger in diameter when measured in wavelengths than the HF arrays upon which the VHF designs are based, wider element spacing goes some distance in optimizing the mutual coupling between elements. Compare the dimensions to those in Table 1 for the six-element array.

Table 9 supplies the complete performance and current data for the model, again inviting a comparison with Table 2, the same data for the original six-element OWA Yagi. Fig 22 samples the data by showing the free-space gain and the 180° front-to-back ratio of the larger beam across the scanned frequency range. Across the operating range from 144 to 148 MHz, the gain varies by less than a one-quarter decibel, from a low of 11.37 dBi to a high of 11.6 dBi for a boom length of 1.06λ . The 180° and worst-case front-to-back ratios exceed 20 dB across the same range.

More significant for the moment is that the seven-element OWA Yagi is the basis for a family of OWA Yagis ranging from 7 to 12 elements.

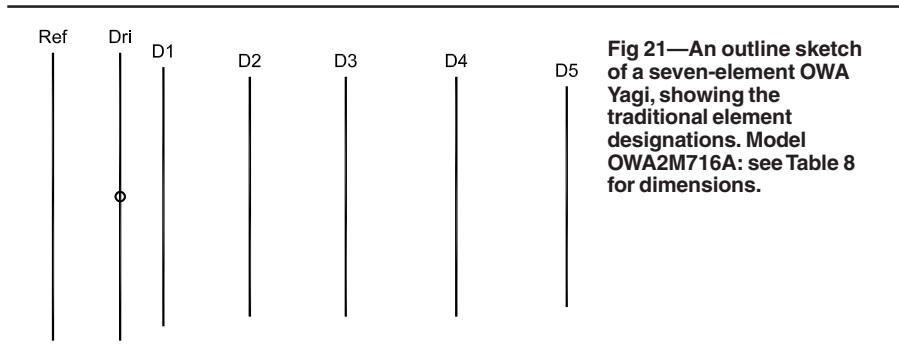


Fig 21—An outline sketch of a seven-element OWA Yagi, showing the traditional element designations. Model OWA2M716A: see Table 8 for dimensions.

Table 8—Model OWA2M716A Dimensions

Dimensions of a 7-element 2-meter OWA Yagi, using 0.1875" ($3/16$ ") diameter elements. Wavelength (λ) measurements are for a design center frequency of 146 MHz.

Element	Length		Cumulative Spacing		Individual Spacing	
	inches	λ	inches	λ	inches	λ
Ref	40.70	0.504	—	—	—	—
Driver	39.66	0.491	10.81	0.134	10.81	0.124
Dir 1	37.00	0.458	15.47	0.191	4.66	0.057
Dir 2	36.32	0.449	27.38	0.339	11.91	0.148
Dir 3	36.32	0.449	42.72	0.529	15.34	0.190
Dir 4	36.20	0.448	63.38	0.784	20.66	0.255
Dir 5	34.50	0.427	85.67	1.060	22.28	0.276

Table 9—7-Element 2-Meter OWA Yagi

NEC-4 reported performance data for model OWA2M716A from 139 to 149 MHz. Current data consist of the relative current magnitude and phase angle on the center segment of each element, where the driver current magnitude is always 1.0 and the driver phase angle is always 0.0° . The "D2 versus D3 Currents" data consist of the ratio of current magnitude from Director 2 to Director 3 and of the current phase angle difference between the two directors. (See text for data interpretation.)

Performance

Frequency (MHz)	139	140	141	142	143	144	145	146	147	148	149
Free Space Gain (dBi)	10.75	11	11.17	11.29	11.4	11.5	11.58	11.61	11.56	11.37	10.99
180° F/B (dB)	11.02	12.86	14.58	16.33	18.35	21.05	25.03	28.73	24.68	20.37	18.11
R (Ω)	30.89	36.35	40.81	43.62	44.94	45.7	47.3	51.01	55.07	46.97	25.4
X (Ω)	-10.72	-6.21	-3.47	-1.62	0.46	3.41	6.92	8.952	4.47	-6.87	-3.62
SWR (50 Ω)	1.734	1.419	1.242	1.151	1.113	1.122	1.165	1.195	1.137	1.167	1.982

Currents

Ref-Magnitude	0.776	0.739	0.685	0.621	0.557	0.505	0.472	0.458	0.438	0.344	0.169
REF-Phase ($^\circ$)	144.28	135.41	127.16	120.13	114.78	110.99	107.63	101.98	89.74	69.2	54.97
D1-Magnitude	0.49	0.582	0.667	0.738	0.798	0.859	0.946	1.098	1.339	1.514	1.359
D1-Phase ($^\circ$)	-76.13	-81.3	-87.23	-93.04	-97.94	-101.5	-103.9	-106.9	-115	-132.2	-150.5
D2-Magnitude	0.396	0.463	0.526	0.585	0.639	0.692	0.752	0.819	0.865	0.783	0.611
D2-Phase ($^\circ$)	231.5	223.6	215	206.1	197.3	188.7	179.79	169.31	155.34	139.86	139.76
D3-Magnitude	0.399	0.464	0.526	0.582	0.637	0.7	0.79	0.934	1.144	1.299	1.234
D3-Phase ($^\circ$)	156.31	145.99	135.17	124.45	114.33	104.9	95.57	84.54	68.13	43.8	20.21
D4-Magnitude	0.365	0.437	0.509	0.58	0.653	0.737	0.847	1.002	1.194	1.271	1.085
D4-Phase ($^\circ$)	65.02	52.36	38.78	24.77	10.62	-3.76	-19.15	-37.43	-62.18	-95.43	-127.8
D5-Magnitude	0.256	0.302	0.346	0.387	0.425	0.467	0.519	0.59	0.671	0.675	0.539
D5-Phase ($^\circ$)	-40.82	-55.52	-71.18	-87.34	-103.7	-120.3	-138	-158.7	174.17	138.53	103.75

D2 versus D3 Currents

Magnitude Ratio	0.992	0.998	1	1.005	1.003	0.989	0.952	0.877	0.756	0.602	0.495
Phase Difference ($^\circ$)	75.19	77.61	80.23	81.65	82.97	83.8	84.22	84.77	87.21	96.06	119.55

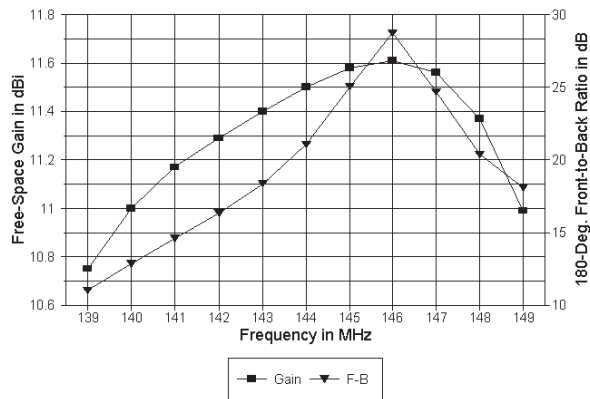


Fig 22—The modeled free-space gain and 180° front-to-back performance of Model OWA2M716A from 139 to 149 MHz. See [Table 9](#) for numeric data.

However, the design requirements for increasing the number of elements vary from those applicable to the simple scheme of a typical DL6WU design. For each additional element, the designer must reset the length and spacing of the former forward-most element to establish it in its new role as next to the most forward element. This step enables the designer to replicate the impedance curve and the shape of the performance curves for the larger array. The final step is setting the length and spacing of the new forward-most element to set the band-edge performance.

Table 10 presents the dimensions of a 12-element OWA Yagi that is the outgrowth of applying the procedure just given. The outline of the array is the same as for the 12-element 420-450-MHz array in [Fig 14](#). The first six elements are identical to those in the seven-element array. The seventh element (fifth director) changed length and spacing, growing in both departments, as it entered the eight-element member of the family.

[Fig 23](#) provides 50-Ω SWR scans for both the 7- and 12-element members of the OWA 20-meter family, using the 139 to 149-MHz sweep with which we started. The scans testify to the stability of the OWA core to support long-boom Yagis while maintaining easily controlled impedance conditions. The performance curves for the 12-element OWA Yagi resemble those for the seven-element cousin, but at a higher gain level. Performance data appears in [Table 11](#). Within the 144 to 148-MHz operating range, the free-space gain averages 14.3 dBi, with a 0.34 dB variation across the band. The lowest worst-case front-to-back ratio is

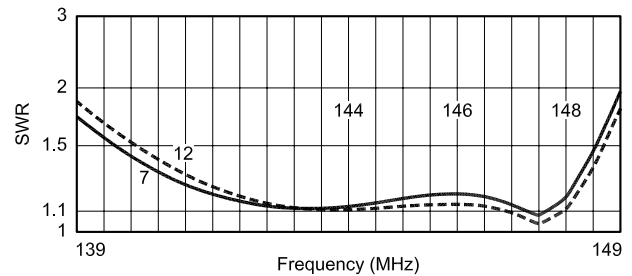


Fig 23—50-Ω SWR curves for model OWA2M716A and OWA2M126A from 139 to 149 MHz.

Table 10—Model OWA2M126A Dimensions

Dimensions of a 12-element 2-meter OWA Yagi, using 0.1875" (³/₁₆") diameter elements. Wavelength (λ) measurements are for a design center frequency of 146 MHz.

Element	Length		Cumulative Spacing		Individual Spacing	
	inches	λ	inches	λ	inches	λ
Refl	40.70	0.504	—	—	—	—
Driver	39.66	0.491	10.81	0.134	10.81	0.124
Dir 1	37.00	0.458	15.47	0.191	4.66	0.057
Dir 2	36.32	0.449	27.38	0.339	11.91	0.148
Dir 3	36.32	0.449	42.72	0.529	15.34	0.190
Dir 4	36.20	0.448	63.38	0.784	20.66	0.255
Dir 5	35.20	0.435	88.85	1.095	25.47	0.311
Dir 6	34.30	0.424	118.0	1.460	29.15	0.365
Dir 7	33.60	0.416	148.6	1.838	30.60	0.378
Dir 8	32.90	0.407	180.4	2.232	31.80	0.394
Dir 9	32.20	0.398	212.0	2.622	31.60	0.390
Dir 10	31.20	0.386	240.0	2.969	28.00	0.347

Table 11—Modeled Performance Data: OWA2M126A

2-meter performance data from model OWA2M126A.

Frequency (MHz)	144	145	146	147	148
Free Space Gain (dBi)	14.10	14.27	14.40	14.44	14.30
180° F/B (dB)	22.90	23.76	24.63	24.65	22.97
Worst-Case F/B (dB)	22.90	23.76	24.60	24.37	22.97
Fwd/Fwd Side Lobe (dB)	25.16	26.69	27.92	26.67	25.06
Feedpoint R (Ω)	48.61	50.22	51.79	53.01	47.49
Feedpoint X (Ω)	4.98	6.07	6.43	3.70	-4.36
SWR (50 Ω)	1.111	1.129	1.140	1.097	1.109

22.9 dB, with the highest front-to-back ratio only 1.7 dB higher. In short, performance is very even across the band.

As significant is the forward side-lobe suppression figure, which averages 26.3 dB across the two-meter

band. Since the worst-case front-to-back ratio is in almost all cases related directly to the main rear lobe, there appears to be a secondary effect, namely, some reduction in the side lobes in the rear quadrants.

Conclusion

If the concept of an optimized broadband antenna (OWA) refers only to the arrangement of the reflector, driver and first director, then there is little to distinguish it from past attempts to achieve wide-band performance. The one possible exception is the closer than usual spacing between the driver and the first director. However, this close spacing does not affect the role of the first director as a secondary or parasitic driver for the array.

In contrast, treating the OWA concept as including all array elements at least through the third director opens the way to appreciating more fully the potentials of this Yagi arrangement. The relative stability of the current ratio and phase-angle difference be-

tween the second and third directors tends to permit increased impedance bandwidth with lower levels of variation. In combination with the reflector-driver-first-director arrangement, the entire assembly offers excellent control over the feed-point impedance throughout at least a 7% overall bandwidth, with greater bandwidths possible.

Although OWA Yagi arrangements often have operational passbands that cover only part of the impedance passband, it is possible to design Yagis for nearly full impedance passband coverage, although present designs have lower average performance than those using only a portion of the impedance passband. As well, the OWA arrangement holds potential to form the basis for families of long-boom Yagis with

only slight reductions in gain relative to gain-oriented designs. However, the OWA designs offer superior front-to-back performance and greater suppression of forward side lobes than most extant Yagi designs.

The OWA Yagi arose from experimental results using computerized optimizing routines. To date, amateur literature has not seen a full analysis of how the OWA acquires its interesting properties relative to other Yagi designs. These notes are but a partial contribution in the direction of more fully understanding the OWA Yagi. As others develop understandings to supplant this one, it is very likely that the proof-of-principle designs used as examples in these notes will also be supplanted by far more capable Yagi arrays. □□

EZNEC 3.0

All New Windows Antenna Software by W7EL

EZNEC 3.0 is an all-new antenna analysis program for Windows 95/98/NT/2000. It incorporates all the features that have made **EZNEC** the standard program for antenna modeling, plus the power and convenience of a full Windows interface.

EZNEC 3.0 can analyze most types of antennas in a realistic operating environment. You describe the antenna to the program, and with the click of a mouse, **EZNEC 3.0** shows you the antenna pattern, front/back ratio, input impedance, SWR, and much more. Use **EZNEC 3.0** to analyze antenna interactions as well as any changes you want to try. **EZNEC 3.0** also includes near field analysis for FCC RF exposure analysis.

See for yourself

The **EZNEC 3.0** demo is the complete program, with on-line manual and all features, just limited in antenna complexity. It's free, and there's no time limit. Download it from the web site below.

Prices - Web site download only: \$89. CD-ROM \$99 (+ \$3 outside U.S./Canada). VISA, MasterCard, and American Express accepted.

Roy Lewallen, W7EL phone 503-646-2885
P.O. Box 6658 fax 503-671-9046
Beaverton, OR 97007 email w7el@eznec.com

<http://eznec.com>

Down East Microwave Inc.

We are your #1 source for 50MHz to 10GHz components, kits and assemblies for all your amateur radio and Satellite projects.

Transverters & Down Converters, Linear power amplifiers, Low Noise preamps, Loop Yagi and other antennas, Power dividers, coaxial components, hybrid power modules, relays, GaAsFET, PHEMT's, & FET's, MMIC's, mixers, chip components, and other hard to find items for small signal and low noise applications.

We can interface our transverters with most radios.

Please call, write or see our web site
www.downeastmicrowave.com
for our Catalog, detailed Product descriptions and interfacing details.

Down East Microwave Inc.
954 Rt. 519
Frenchtown, NJ 08825 USA
Tel. (908) 996-3584
Fax. (908) 996-3702

We Design And Manufacture To Meet Your Requirements

*Prototype or Production Quantities

800-522-2253

This Number May Not Save Your Life...

But it could make it a lot easier! Especially when it comes to ordering non-standard connectors.

RF/MICROWAVE CONNECTORS, CABLES AND ASSEMBLIES

- Specials our specialty. Virtually any SMA, N, TNC, HN, LC, RP, BNC, SMB, or SMC delivered in 2-4 weeks.
- Cross reference library to all major manufacturers.
- Experts in supplying "hard to get" RF connectors.
- Our adapters can satisfy virtually any combination of requirements between series.
- Extensive inventory of passive RF/Microwave components including attenuators, terminations and dividers.
- No minimum order.

NEMAL
Cable & Connectors
for the Electronics Industry

NEMAL ELECTRONICS INTERNATIONAL, INC.
12240 N.E. 14TH AVENUE
NORTH MIAMI, FL 33151
TEL: 305-899-0900 * FAX: 305-895-8178
E-MAIL: INFO@NEMAL.COM
BRASIL: (011) 5535-2368

URL: WWW.NEMAL.COM

A High-Performance Digital-Transceiver Design, Part 1

Data-converter technology has made tremendous strides in the past several years. Let's take a look at how we can achieve high performance in an almost-all-digital radio design.

By James Scarlett, KD7O

There has been much discussion in *QEX* recently on the need for, or the achievement of, high performance in our radios.^{1, 2, 3} This has particularly been the case with receiver strong-signal performance. It has often been shown that amateurs can improve upon existing commercial design by paying proper attention to the analog front end.

The introduction of cost-effective digital signal processing (DSP) has improved performance in some areas.⁴ With respect to strong-signal capability, however, good analog designs are still king. For several years, I have been looking at approaches to an analog front end from a system level. As

the time to build the radio approached, I began to look at applying digital techniques as well. What I learned about the state of digital technology was surprising.

The goal for digital radios has always been to get the converter as close to the antenna as possible, for both receive and transmit; however, data converters have been the limiting factor in getting the necessary performance. They lacked the dynamic range and were noisy. This means we must employ analog circuitry to overcome converter limitations.

The state of the art has changed enough that we can now convert directly between the digital realm and the HF bands.⁵ We still need to amplify the inputs to overcome converter noise. To prevent overload, we need to use band-pass filters instead of a low-

pass filter above 10 meters—which high-performance analog designs do anyway. We cannot yet reach the strong-signal performance of the best analog front-end designs, but it is now possible to exceed the performance of even high-end commercial gear using a direct-to-RF conversion scheme.

This first article in the series will look at the design process for such a transceiver. The emphasis will be on the areas that differ from typical analog designs. In future segments, we'll look at the detailed implementation and performance measurements.

Architectural Overview: The Receiver

By performing conversions directly at RF, receiver and exciter architectures may be greatly simplified. **Fig 1** shows the basic block diagram of a

¹Notes appear on [page 44](#).

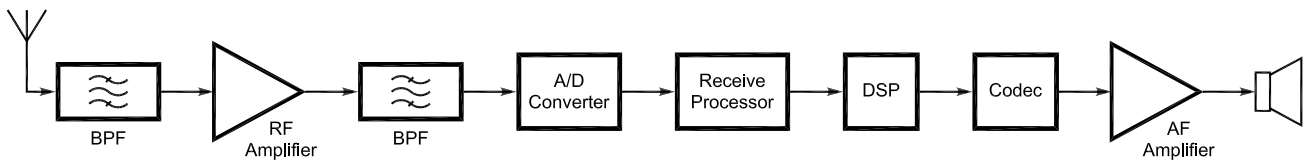


Fig 1—Receiver Block Diagram.

receiver. As you can see, it's missing many stages we're used to seeing!

Since we will be doing all frequency translations digitally, there is no need for an analog mixer. The only analog filters are the band-pass filters for the entire amateur band of interest. All narrow filtering is done digitally. We need a preamplifier to overcome noise in the analog-to-digital converter (ADC).

The weakest link in this architecture is the ADC. A little later, we'll look at these weaknesses and see how we can mostly work around them. The sampling frequency must be high enough to satisfy Nyquist at the widest bandwidth we'll use. There are advantages to getting the sampling rate much higher, though. Therefore, we'll be using a sampling clock on the order of 65 MHz.

The problem is this: DSPs can't accomplish much at that sampling rate! Therefore, we must have some sort of interface between the ADC and the DSP. This is the job of the *receiving signal processor* (RSP), also known as a digital down-converter (DDC). This nifty chip converts the signal to baseband and reduces the sampling rate to a speed that can be handled by the DSP. It also provides extensive filtering and splits the signal into its analytical components for demodulation. The output is then sent to the DSP for further processing.

Architectural Overview: The Exciter

Fig 2 shows the basic exciter block diagram. This is essentially the receiver in reverse order, and conceptually it is just as simple.

The DSP hardware communicates an analytical signal pair representing the baseband information to a *transmitting signal processor* (TSP). This device is essentially an RSP in reverse. It interpolates the signal up to the final sampling rate, while providing the necessary filtering. The analytical pair is then translated to the desired output frequency and combined.

The TSP output is converted to analog at the desired RF frequency by the

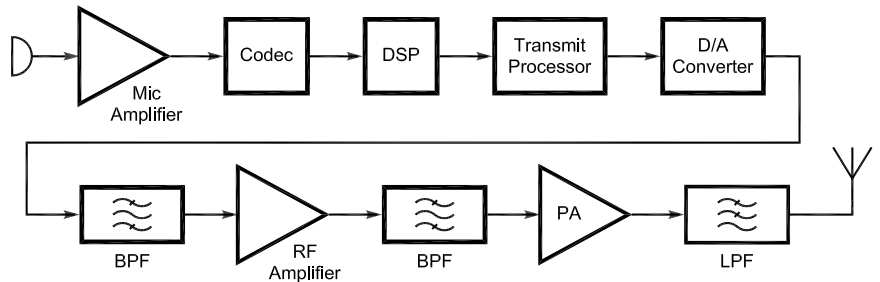


Fig 2—Exciter Block Diagram.

Table 1—Performance Specifications

	RX		TX
20 m <i>IP3</i>	> +30 dBm	Output <i>IMD3</i>	< -30 dBc
10 m <i>IP3</i>	> +20 dBm	Output <i>IMD9-11</i>	< -60 dBc
20 m <i>NF</i>	22 dB	Output Spurs	< -55 dBc
10 m <i>NF</i>	12 dB	Output power	50 W
Image Rejection	> 100 dB	Carrier rejection	< -60 dB
Filter Bandwidth	programmable	Sideband rejection	< -60 dB
Audio Power	4 W, < 10% THD		—
Modes	programmable		programmable

digital-to-analog converter (DAC). Like ADCs, DACs have come a long way in recent years. Again, higher sampling rates help us to meet the Nyquist criterion, avoid aliased signals and improve noise performance.

The output of the DAC must be filtered to eliminate images created by aliasing. As the output frequency lowers with respect to the sampling frequency, this task becomes easier. Given the same sampling rates, any filters that meet spurious requirements for the receiver will be more than adequate for the exciter. Therefore, it's convenient to simply use the same band-pass filters for both.

The filter output is then sent to the amplifier chain to achieve the final output power. This output is also filtered to ensure low spurious levels.

I have avoided much of the theory in the previous discussion. It has been well covered in *QEX*, so this article will concentrate on the actual design process, with emphasis on areas unique to this architecture. We will

revive the theory as needed to make design decisions.

Receiver Design

We will begin the design discussion with the receiver and then move on to the transmit side. Before tackling the actual design, we will review the required performance characteristics. Several of these are outlined in Table 1.

A few notes are in order for some of the specifications. Notice that the two-tone dynamic range is not specified. This can be calculated from the given specifications, using the formulas in Chapter 17 of any recent *ARRL Handbook*.⁶ The problem with this number is that it does not give adequate information about strong-signal capability. A 20-meter receiver can have a 100-dB dynamic range (*DR*) with a noise figure (*NF*) of 5 dB, but 10 dB of that dynamic range is wasted on atmospheric noise. A receiver with 90 dB of *DR* and a *NF* of 20 dB would handle strong signals just as well while retaining adequate

sensitivity for 20 meters. Thus, the third-order intercept point (*IP3*) is a far more useful measure of signal-handling capability.

No number is given for the compression point. That is because of the nature of this architecture. As an ADC is a voltage device, we will not get compression *per se*. The ADC has a maximum input range, outside of which it will clip the incoming signal. Therefore, the total incoming power of signals and noise within the bandwidth of the front-end filter, at the ADC, must not reach this hard limit. Because of the low gain used ahead of the ADC in this architecture,

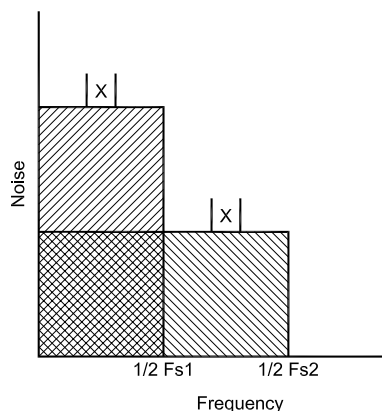


Fig 3—An illustration of processing gain. An ADC creates quantization noise that is spread from dc to half the sampling rate. In this case, sampling rate *F*s2 is twice sampling rate *F*s1. Both examples have the same total noise power, but it is spread over a larger frequency range with the higher sampling rate. Therefore, the noise power in bandwidth 'X' for sampling rate *F*s2 is one half the noise power for *F*s1, for a 3-dB improvement in the SNR.

this can be assured with a high level of confidence.

The noise figure of this receiver in its default state will vary from band to band. As John Stephensen, KD6OZH, showed in his *QEX* article (see [Note 2](#)), external noise varies across the HF spectrum. For this reason, [Table 1](#) reflects the *NF* requirements for both 20 and 10 meters. The receiver is capable of achieving a lower *NF* on the lower bands to take advantage of those occasions when less external noise is present.

Notice the programmable filter bandwidths and modes. Since this receiver is software/DSP based, it can be adapted to whatever characteristics we want!

A Dynamic-Range Spreadsheet

When I was first looking at receiver architectures, I developed a spreadsheet for analyzing noise-figure and dynamic-range tradeoffs. More recently, the spreadsheet was adapted to include ADC calculations. [Table 2](#) shows this spreadsheet with data for the 20-meter band.

The cascade chain in the spreadsheet is calculated based on formulas found in Chapter 17 of recent *Handbooks* (see [Note 6](#)). The input is at the top of the cascade, and the ADC is at the bottom. Therefore, these calculations show that for 20 meters, we have a noise figure of about 22 dB, and an *IP3* of about +35 dBm.

The lower left corner contains user-defined information for the system level, as well as for the ADC. The bandwidth is self-explanatory. The external excess noise ratio (ENR) is the expected level of the atmospheric, cos-

mic and man-made noise. This is discussed in [Note 2](#), which includes a chart that I used to get my numbers. The ADC information will be discussed later, as will the calculated ADC information found in the lower right of the spreadsheet.

The calculated information in the upper right includes the MDS, dynamic range and front-end gain. The external ENR is taken into account with the external-noise dynamic range and with the noise figure shown below it. This allows you to see the dynamic range you get with a given noise level at the antenna, in addition to what you would measure in the lab. Lab measurements will always be better, unless the receiver is not sensitive enough. I did my design for a *NF* of about 6 dB less than the external noise, which causes 1 dB to be added to the noise at the input.

ADC Selection

As I mentioned earlier, this is currently the weakest link in the receiver. Any improvements in the ADC can be translated directly to a better *IP3*. This is why traditional IF-DSP receivers have used low IFs. It allows the use of 16- to 24-bit ADCs that have excellent specifications.

If one samples fast enough, though, 16 bits are not necessary, though they would be nice. It took me a while to appreciate that. By using some easily applied techniques, we can achieve excellent performance using today's high-speed 14-bit converters.

The converter I chose for this application is the Analog Devices AD6645.⁷ This is a 14-bit converter designed for IF-sampling at rates of up to 80

Table 2—Dynamic Range Spreadsheet

Stage	NF	Stage gain	OIP	Total NF	Input IP	MDS (dBm)	DR (dB)	DR including external noise (dB)
LNA / Atten	0	0	180	22.09	34.8	-117.9	101.8	97.2
RF filter #1	0	0	180	22.09	34.8			
Preamplifier #1	0	0	180	22.09	34.8			
RF filter #2	1.5	-1.5	57	22.09	34.8	Total gain		NF
Preamplifier #2	3.5	10	44	20.59	33.3	7		28.99
RF filter #3	1.5	-1.5	57	30.51	51.8			
Input IP	0	0	51.4	29.01	51.4			
input NF	29.01			29.01				
ADC								
BW (Hz)	External ENR (dB)	SNR (dB)	Maximum Signal (dBm)	Sample Frequency (Hz)	Noise Floor (dBm)	NF (dB)	EXT/FE noise at ADC (dBm)	
2400	28	74.5	4.8	6.50E+07	-111.02	29.01	-99.95	

megasamples per second (MSPS). It provides excellent performance with analog inputs up to the lower-VHF range, which allows future expansion to 6 meters without complication.

SNR and Processing Gain

The specified signal-to-noise ratio (SNR) of the AD6645 is approximately 74.5 dB. The maximum input to the ADC in the configuration we'll be using (with the ADC looking back at 200 Ω) is +4.8 dBm. By itself, this doesn't provide an adequate noise floor to operate in a direct-to-digital system. This brings us to our first simple technique, *oversampling*, and its result, *processing gain*.

QEX has already introduced readers to the concept of processing gain (see Notes 4 and 5). This is how we will take advantage of the very high sampling rate. As shown in Fig 3, the total quantization-noise power is the same regardless of the sampling frequency. For higher sampling frequencies, noise power is spread over a greater frequency range. Thus, the noise power in an identical bandwidth is lower when using a greater sampling rate. The SNR will be improved based upon the formula:

$$\text{processing gain} = 10 \log \left(\frac{F_s}{2BW} \right) \text{ dB} \quad (\text{Eq 1})$$

where F_s is the sampling frequency in hertz and BW is the final bandwidth in hertz. For example, with a sampling rate of 65 MHz and a bandwidth of 2400 Hz, the improvement in the SNR would be 41.3 dB.

This information is used in the spreadsheet of Table 2. In the lower left part of the spreadsheet, we enter a nominal SNR of 74.5 dB, a sampling frequency of 65 MHz, and a maximum input level of 4.8 dBm. The data in the lower right gives a noise floor based upon this information and the bandwidth. A value for the noise figure—29 dB in this case—is also calculated from the noise floor. Though noise figure is not normally associated with ADCs, which are voltage (not power) devices, doing so makes the job of the spreadsheet easier. Also included in the lower right of the spreadsheet is the total front-end noise power at the ADC input. I have used this primarily as a sanity check for other calculations. Notice that the front-end noise dominates, not the ADC.

The SNR will also be affected by both aperture jitter within the ADC and clock jitter. This is illustrated by the following formula:

$$\text{SNR} = 20 \log(2\pi F_{\text{in}} t_{\text{RMS}}) \quad (\text{Eq 2})$$

where F_{in} is the analog input frequency in Hertz and t_{RMS} is the RMS jitter in seconds. This formula gives the best possible SNR for a given frequency and level of jitter. Note that jitter performance that would be acceptable for 160 meters could be totally unacceptable for 10 meters. We need to maximize the performance at the highest frequency used.

The aperture jitter of the AD6645 is nominally 0.2 ps. For best SNR performance, we don't want the clock jitter to add appreciably to this. To accomplish this, and to allow for future upgrades to 16 bits, we'll shoot for a clock that has less than 0.1 ps of jitter. This can be translated to SSB phase noise by the formula:

$$L = 10 \log \left(\frac{4\pi^2 \left(\frac{t_{\text{RMS}}}{T_0} \right)^2}{f_2 - f_1} \right) - 3 \quad (\text{Eq 3})$$

where f_1 and f_2 define the frequency range of interest in hertz, and T_0 is the clock period in seconds. In all frequency bands of interest, we will be looking at the phase-noise floor of the oscillator. In the worst case, we'll have a 2-MHz bandwidth. Thus, to achieve less than 0.1 ps of jitter, we need the SSB phase noise to be better than -154 dBc/Hz. This will be no problem to achieve with a good crystal oscillator.

SFDR Performance

Another major concern for the ADC is the *spurious-free dynamic range*

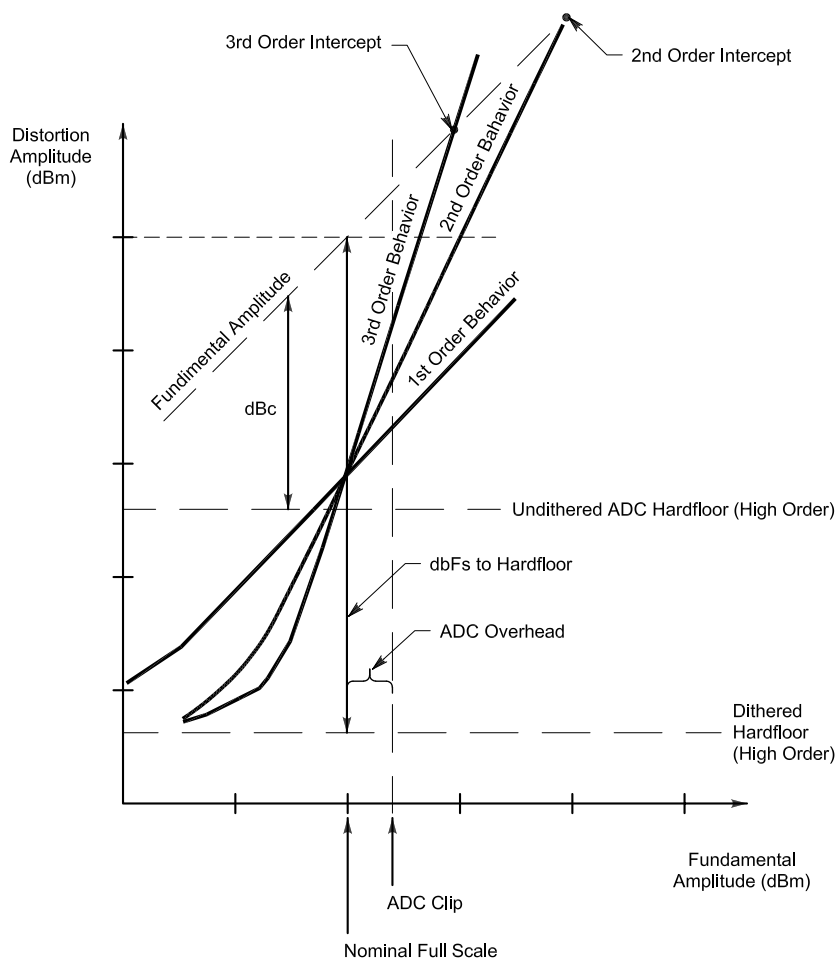


Fig 4—Distortion characteristics and an illustration of the effect of dither in reducing the distortion “hard floor.”

(*SFDR*). For the AD6645, this value is approximately 100 dBFS (relative to full scale) for both single- and two-tone signals. This is very respectable performance, but it can be improved further by using our second simple technique, dither.^{8,9}

Dither is a technique that injects random noise into the ADC to overcome converter nonlinearities. I will not get into all the detailed theory behind dither here, but I will cover some basic concepts as they apply to this design. For a more detailed description, see [Notes 8](#) and [9](#). In short, the *differential nonlinearity (DNL)* within a converter is a major source of spurs. By adding random noise, the *DNL* is “averaged out” and virtually eliminated. This reduces spurious outputs.

[Fig 4](#) illustrates this point. It shows the familiar concept of the intercept point, but also introduces a new concept. A given converter will have a distortion “hard floor” that generally shows up as higher-order spurs. These spurs do not decrease with a reduction of the input level. We lower this hard floor by injecting dither into the ADC. The lower-order terms are also improved somewhat. The amount of improvement depends on how much the *DNL* contributes to the spurious content within a given converter. [Fig 5](#) shows the single-tone improvement for the AD6644, the predecessor to the AD6645.¹⁰

Dither will do nothing to improve the spurs generated within the ADC’s analog front end. These spurs will generally be lower-order terms and will

therefore determine the *IP3* for the ADC. In [Note 9](#), this is referred to as the “soft floor.” Spurs generated in the analog section of the converter will decrease with a reduction of the input. Therefore, if the analog section is good enough (as in the AD6645) the ADC should not be the limiting factor in the receiver’s *IP3*.

For the spreadsheet, I used an *IP3* value for the ADC of approximately +51 dBm. I got this value by assuming a distortion product level of -105 dBm with input tones at approximately -2 dBm (-7 dBFS). This should be achievable, given the assumption that the *DNL* limits the distortion performance, not the analog section. If not, the *IP3* could degrade by a couple of decibels.

The dither level recommended for the AD6645 is -19 dBm. This is the total noise power applied, which we will limit to a bandwidth of less than 500 kHz. Doing this minimizes the *SNR* reduction caused by the addition of dither. It also allows us to accomplish this task using a handful of inexpensive op amps, as we’ll see when we get to the actual implementation.¹¹

ADC Resolution

The bit-resolution requirement for the ADC created the biggest mental block for me, with regard to ADC performance issues. In this architecture, the ADC does *not* require a least-significant bit (LSB) that is smaller than the minimum signal expected. Because of the application of dither, the input signals will be spread over a vast

number of quantization levels—more than 1000 of them. This means that the extra resolution is not necessary until we begin to filter out the dither signal in a later stage. It is interesting that even without injected dither, the analog parts of current 14-bit ADCs generate enough thermal noise to provide self-dither at the LSB level.

ADC Overload

In an analog system, one of the measures of receiver performance is the blocking dynamic range. This is a measure of the level of desensitization created by the presence of large signals. With an ADC, however, we are less worried about “de-sense” than with overload. If the incoming signal exceeds the ADC input range, the result is a clipped signal that can generate massive distortion. In his article (see [Note 4](#)), Doug Smith, KF6DX, used AGC ahead of the converter to prevent clipping. In his implementation, though, there was enough gain in front of the ADC so that there was little sensitivity lost if the gain were reduced in later stages. In this architecture, any gain reduction prior to the ADC results in a corresponding loss of sensitivity.

With a +4.8-dBm maximum input to the ADC and 7 dB of gain in the front end for 20 meters, the ADC will clip with about -2 dBm at the receiver input. We need a little over 17 dB of gain to achieve the desired noise figure at 10 meters, which results in a clipping level of about -13 dBm. I spent quite a bit of time convincing myself that this level would not be reached.

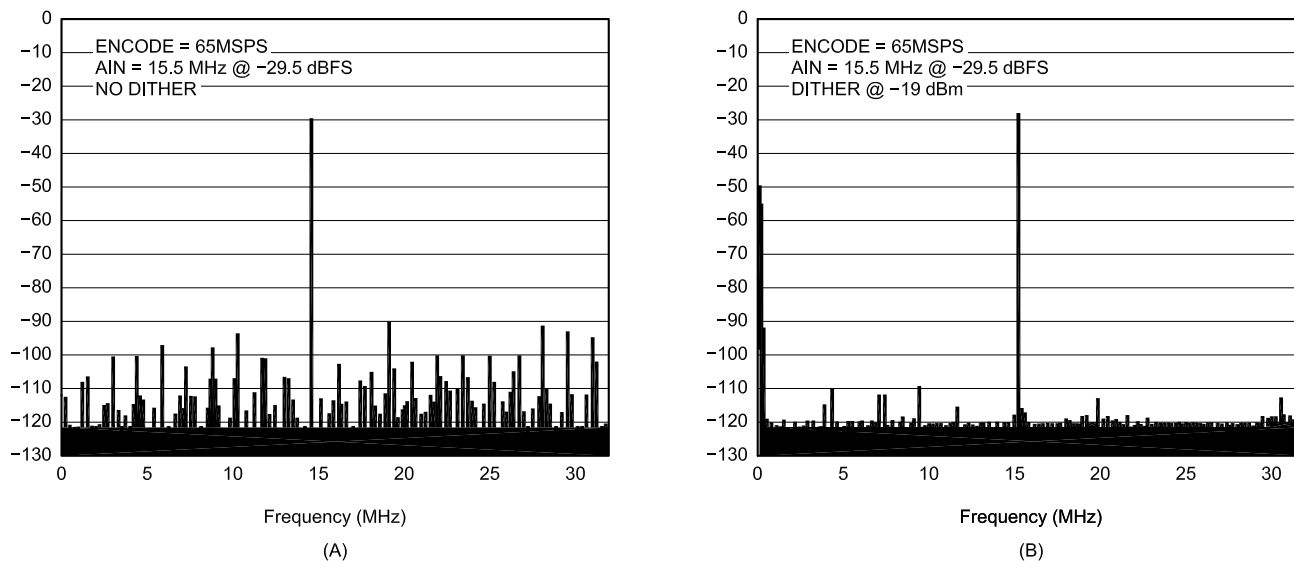


Fig 5—The effect of dither on AD6644 spurious performance.

Early on in the project, I decided that I would make this a ham-bands-only receiver. This allows me to use individual band-pass filters in the front end, which limit the energy that can reach the ADC. It also greatly improves the second-order intercept point for any receiver. To assure myself that the system wouldn't need gain control in the analog section, I did some worst-case calculations of the total power present at the ADC.

Although the probability that the signals present would be correlated is basically zero, I did calculations for both correlated (voltages add) and uncorrelated signals (powers add). I found that even if the band were jammed to the gills with S9+ *correlated* signals (highly unlikely), the clipping point would not be reached. I showed my worst case numbers to Bill Sabin, W0IYH, who termed them "virtually impossible." I then did some rough probability calculations, which indicate that I might clip for a second or so every few years. I'm willing to take that risk in exchange for a simple, clean front-end design. Therefore, all automatic gain-control functions will be performed in DSP.

Digital Down-Conversion

To be able to use the output from the ADC, we need some way to translate the data to a sampling rate that can be handled easily by the DSP. The RSP does this for us. These parts are available from a couple of sources. For my receiver, I chose the Analog Devices AD6620.¹² This part is capable of handling up to a 67 MSPS input data rate and an input path of up to 16 bits. This leaves a future upgrade path when 16-bit ADCs get fast enough.

Fig 6 shows a simplified block diagram of the RSP. We'll use the "real" mode, which takes a single input per sample period. Other modes are available for diversity reception or to allow cascading of RSPs. Take care to ensure that the clock/data setup and hold requirements are met. I'll show a simple way to do this when we discuss the implementation. The input data are split and fed to a quadrature numerically controlled oscillator (NCO). The NCO is followed by two programmable "cascaded integrator comb" (CIC) stages that perform decimation with digital filtering. The CIC stages are followed by a programmable FIR filter, with up to 256 taps, and further decimation. The data are then sent to the DSP via a 16-bit parallel or a 16-, 24- or 32-bit serial link. The incident

and quadrature data words are sent in succession.

The NCO uses a 32-bit frequency tuning word. Phase and amplitude truncation to 18 bits limits the spurious level to better than -100 dBc. The largest spurs occur when the programmed frequency is an integral sub-multiple of half the clock rate, with the larger fractions (that is, $1/2$) generating larger spurs. These spurs should be no problem for this design, as most frequencies fall outside the amateur bands; those that fall in band are higher-order (9th in 80 meters, 17th and 18th in 160 meters). Spurs can be further improved by activating phase or amplitude dither, if necessary. There is a tradeoff here, as the dither will raise the noise floor slightly.

The multiplier output is truncated to 18 bits. Using formulas given by

KF6DX in part 1 of his article (see [Note 4](#)), it was determined that this truncation does not noticeably increase the noise level in the bandwidth of interest.

There are two separate CIC filters. CIC2 is a second-order filter that has a decimation ratio programmable from 2 to 16. The filter itself is fixed, based upon the decimation ratio. This type of filter is optimized to generate a minimum amount of noise, so again the noise level is not noticeably increased, even with the reduced sampling rate. CIC5 is similar to CIC2, except that it is a fifth-order filter with a programmable decimation ratio from 1 to 32. Truncation after each CIC filter is 18 bits.

Signals are then processed in a programmable FIR filter. This filter can have up to 256 taps, depending on the amount of decimation used in the CIC

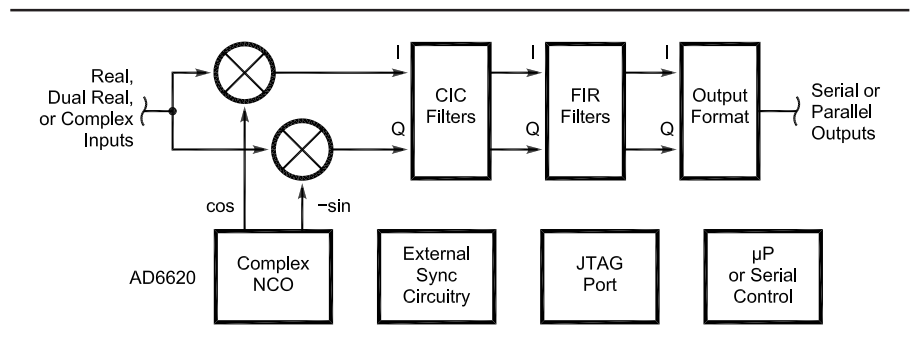


Fig 6—Simplified block diagram of the AD6620 RSP.

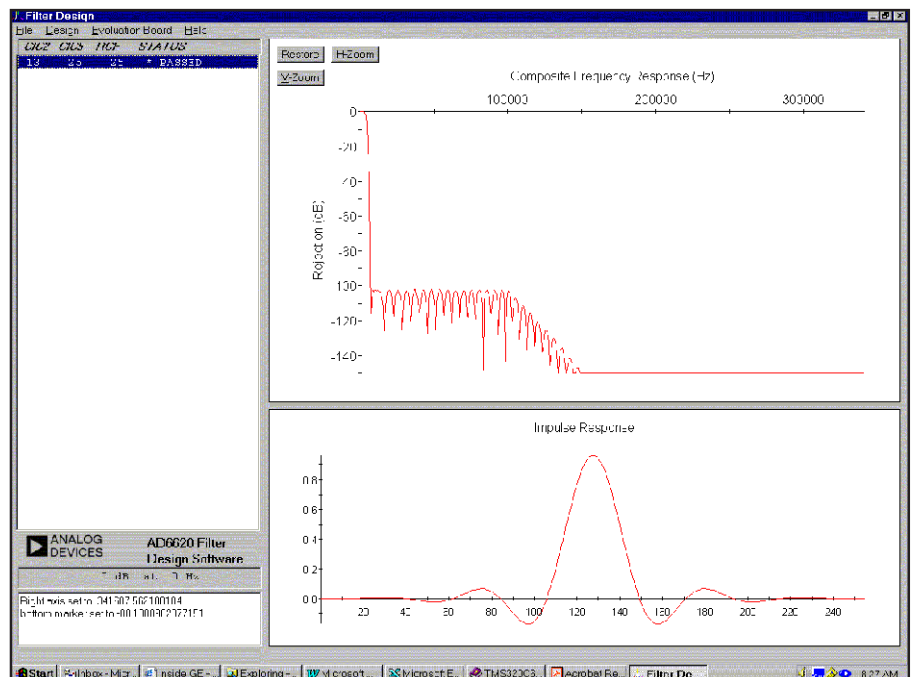


Fig 7—Sample screen from the AD6620 filter-design software.

filters. Although FIR filters generate additional truncation noise in each tap, the noise level remains insignificant by keeping 23 bits of data. Further decimation (programmable from 1 to 32) is performed before the data are formatted and sent to the DSP.

Decimation and FIR filter coefficients can be optimized using software provided by Analog Devices.¹³ This software allows the user to set all necessary requirements, such as decimation ratio, alias rejection and filter response. It then gives possible solutions and allows the user to simulate them. A sample is shown in Fig 7. The upper-left window shows the possible decimation combinations (only one in this case) and whether each combination meets the requirements specified. The two right-hand windows give the frequency and impulse responses for the entire RSP system. A text file contains the FIR filter coefficients the user programs into the part.

The data from the AD6620 can be sent to the DSP in either parallel or serial format. The parallel interface is, however, limited to 16 bits. Since we have now removed the dither from the signal, we need more resolution than that. Therefore, we will use the serial interface. This interface allows data transfer in 16-, 24- and 32-bit words. We'll use the 24-bit mode, which allows all 23 data bits to be sent while maximizing efficiency. The serial port can operate at clock speeds of up to half the input clock rate, so it is no problem to get both the I and Q data words transferred between output samples.

Analog Front End

The analog front end is simplified in this architecture. No mixers are included! Although there are multiple filter copies, the only circuit blocks in the front end are the band-pass filters, a low-pass filter and the preamplifiers.

The combination of these blocks is dependent upon the band in question for two reasons. First, as has already been mentioned, the external noise is different for each band, resulting in different noise-figure requirements. Therefore, at 20 meters and below, there is one preamplifier in line. There are two preamplifiers above 20 meters.

I have also included a pair of resistive attenuators in the front end. One provides 5 dB of attenuation and the other, 10 dB. There are those who might argue that switched attenuators merely mask an inferior design. I would not dispute that argument and it may very well apply to this design.

However, they give a certain amount of flexibility in optimizing noise figures for different bands. For example, the default setting for 40 meters uses the 5-dB attenuator to account for a typically higher external noise level than occurs on 20 meters. This adds 5 dB to the *IP3* on a band that can often use it. The attenuator settings can be changed easily enough, or the first preamplifier can be switched in, to adapt to changing conditions.

The other reason for differences in block use pertains to the band-pass filters. With a sampling rate of 65 MSPS, images begin to occur at 32.5 MHz. Therefore, we must deal with images as if we were using a 32.5-MHz local oscillator. Obviously, this makes image rejection a challenge for the higher bands—10 and 12 meters in particular. To address this, there are three band-pass filters for 10 and 12 meters and two band-pass filters for all other bands. An additional low-pass filter is used on all bands. The resulting analog block diagram appears in Fig 8.

I developed my band-pass filters using the procedures outlined by Mr. Sabin in his *QEX* article.¹⁴ I used a combination of series- and shunt-coupled filters for the lower bands to provide a more symmetrical response. For the higher bands, there is no need for that because of the low-pass filter's contribution to the response.

I adapted the component values to suit my own preferences. For instance, my interests have not taken me to the upper 500 kHz or so of the 10-meter band. Therefore, this portion of the band has a few decibels of additional attenuation (> 3 dB). This buys the extra image rejection I want for the part of the band I do use. I'm always free to change the capacitor values to

include this part of the band later. The inductors for these filters are the same values Bill Sabin used, as they are a known, measured quantity. He also measured the intercept point of these filters to be about +57 dBm, which appears in the dynamic-range spreadsheet.

The block that limits performance in the analog section is the preamplifier. It should have as large an *IP3* as possible. Jacob Makhinson, N6NWP, attained outstanding performance using a push-pull amplifier with "noiseless" feedback.¹⁵ Simulating with Ansoft's *Serenade SV*,¹⁶ I got a +50-dBm output *IP3* value with 40 mA in each of a pair of MRF5811 devices. The noise figure is not critical in this application, but it was around 2 dB.

My simulations with *ARRL Radio Designer (ARD)*, however, showed that the common-base configuration created difficulties when I sandwiched it between the band-pass filters. This is because of the low reverse isolation inherent in the amplifier design. That low reverse isolation would also tend to increase IMD (and decrease the *IP3*) because of reflections from the filters. I therefore adapted the design to a common-emitter configuration. The result is a loss of 5 to 6 dB on the intercept point, but the much greater reverse isolation ensured proper termination for the filters. The result is that I now have an *IP3* for the entire front end that is 4 to 5 dB lower than the original simulation. I considered this a reasonable tradeoff, though I would obviously prefer the higher *IP3*. On the bands using two preamplifiers, the impact is not as great, since the *IP3* of the first preamplifier (that closest to the antenna) does not have as great an effect as the second preamplifier.

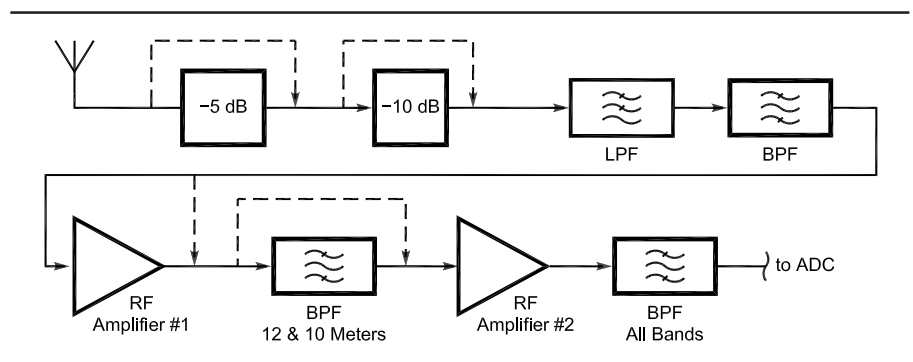


Fig 8—An analog front-end block diagram. Default settings are shown; the attenuators and RF amplifier #1 can be switched in and out as desired. RF amplifier #1 and the second band-pass filter (10 and 12 meters) are switched out during transmit. The switching is not shown for simplicity. The alternate paths are shown as dashed lines. The default settings switch in: -5 dB for 40, 17 and 15 meters, -10 dB for 160 and 80 meters, and RF amplifier #1 in for 17, 15, 12 and 10 meters.

DSP Selection

The first requirement I had for the DSP was that the serial port must accept words of at least 24 bits. As described above, this is the minimum number of bits available from the AD6620 that retains the full resolution. In my case, this led to a bit of overkill. I wanted to use a prefabricated DSP kit, since my strong suit is not designing DSP hardware. In addition, DSPs very often come in ball-grid array (BGA) packages that are not exactly designed for hand soldering.

The popular Analog Devices ADDS-218X-EZLITE kit¹⁷ (inexpensive at \$89) was my first thought, as I had one on hand. However, the serial port on this device allows only 16-bit words. I also had a DSP Starter Kit (DSK) from Texas Instruments for the TMS320C6211 available,¹⁸ which I decided to dedicate to this project. The board includes a 16-bit codec for the audio input/output and a host-interface port to communicate with either a PC or a microcontroller. It also provides far more processing power than

I will ever need for this application, at 1200 million instructions per second (MIPS). The DSP is optimized for use with C code, so we won't need to mess with assembly code—unless you really like it.

This DSK has been replaced with the TMDS32006711DSK, which includes the floating-point equivalent to the '6211. C code written for the 6211 is fully compatible with the 6711. The 6711 DSK is available from TI for \$295. It includes a DSK-only version of their *Code Composer Studio*, which includes the C compiler, simulator and a real-time debugging utility. Analog Devices offers a kit for its 32-bit floating point DSPs (ADDS21065L-EZLITE) for \$299. Analog Devices ADDS-2106X-EZKIT will also do fine and its price is \$179. I am not familiar with the current Motorola kits, but that may be another option.

Exciter Design

Transmit Processing

Sixteen-bit I/Q data is sent from the DSP to the TSP. The TSP in this de-

sign is the Analog Devices AD6622.¹⁹ This part actually has four independent channels that are summed together prior to the output, which is useful in a number of commercial applications. In this case, we'll use only one of the channels.

The part receives the I/Q data over a serial link from the DSP. The design of the AD6622 requires that the TSP be the serial master. As the DSP serial port has independent transmit/receive and can be a serial slave, this is not a problem.

The process of the TSP is very close to the RSP in reverse (see Fig 9). The data pass through a programmable FIR filter, followed by CIC5 and CIC2 filters, which in this case, provide interpolation. An NCO then translates the signal to the desired output frequency. I and Q signals are summed together and summed with any signals from the other channels (disabled in our application). An 18-bit data word is output with a sampling rate of approximately 65 MSPS. By doing the summation at 18 bits in the digital

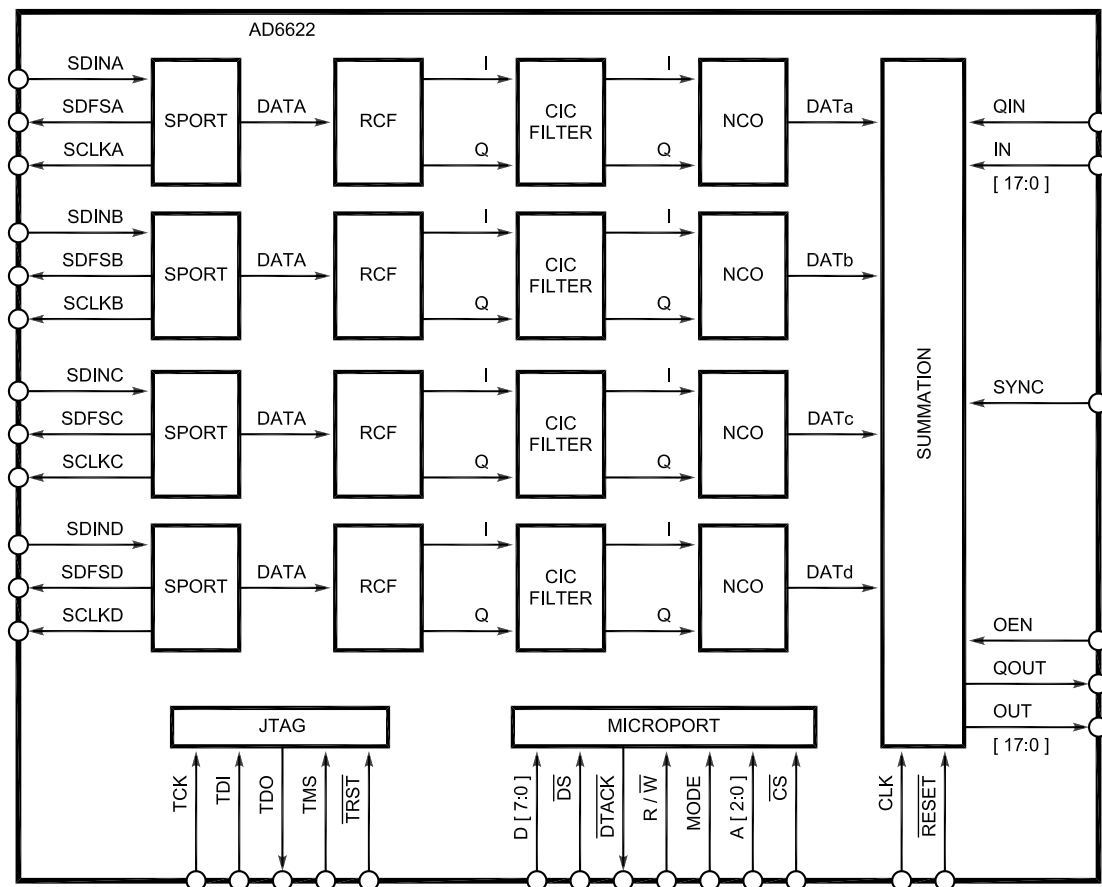


Fig 9—Simplified block diagram of the AD6622 TSP.

realm, we retain the carrier and sideband suppression we need.

Notice that the TSP only provides for summation of the I and Q signals. This requires that we look at SSB generation in a slightly different manner. Normally, the Q signal is shifted by +90° and added to the I signal for LSB, or subtracted from the I signal for USB (see Note 4). Since we cannot subtract in the TSP, we'll take a different approach for USB and shift the Q signal by -90° prior to sending it to the TSP. Try it: The math works out correctly.

Transmit DAC

Like the ADC, the transmit DAC must be able to handle RF signals. This includes the sampling rate, since we must conform to Nyquist and the analog section, which usually consists of differential current sources. The number of converter bits limits the SNR, and therefore we must account for it.

The best high-speed DACs readily available today are 14-bit devices, though there are some 16-bit DACs in the pipeline. These should be perfectly adequate for our design, since we're not trying to do CD-quality work. Also, since we have already summed the I and Q signals digitally, we don't need to worry about truncation effects on carrier or sideband suppression. Since 14 bits are adequate, I chose the AD9772A for this application.²⁰

The AD9772A allows an input data rate of up to 160 MSPS. In addition, it provides for 2× interpolation of the input data, which eases the burden on analog filters. The SNR is on the order of 70 dB throughout the HF band, which is fine for our needs. Spurious performance will easily meet our requirements, especially after analog filtering. The two-tone distortion products will have no impact when compared with the nonlinearity of the power amplifier's output.

Performance will be somewhat dependent upon the quality of the clock, so we will use an oscillator similar to that of the receiver. The oscillator will operate at twice the input data rate, which will minimize noise by not using the on-board PLL. This adds an

additional synthesizer, but I think the tradeoff is worthwhile to get a clean transmit signal with respect to noise.

The output compliance level—the amount of voltage that can safely be generated at the DAC output terminals—is much larger than we use here. The data sheet recommends using only part of the compliance range to minimize distortion. By loading the DAC with 50 Ω, we ensure low distortion levels and allow easy interface to existing analog circuitry.

The output of the DAC is transformed into an unbalanced output, which is buffered and sent to an amplifier with a pair of band-pass filters. The amplifier and filters are actually the ones used in the receiver. This saves space and dollars at the price of a little flexibility and insures low spurious content. The output to the driver and PA is about +15 dBm, which generates very low distortion products.

Audio Section

The audio section of the transceiver interfaces with the DSP via the TI TLC320AD535²¹ codec on board the starter-kit PC board. Some key specifications of the codec are shown in Table 3. The block diagram of the audio section (both transmit and receive) is shown in Fig 10.

The sampling rate of the codec limits our audio bandwidth to a little more than 3 kHz. This is perfectly adequate for our needs. Active audio low-pass filters are used in both transmit and receive paths to prevent aliasing. Both filters have a gain of unity.

The audio from the microphone can have a very wide variation in signal level. To maximize the SNR of the audio input, we will need to amplify the signal until it approaches the maximum level allowed by the codec. Since this will require many different gain settings, we will use a preamplifier

chip designed for use in the computer market. The SSM2166²² provides variable gain dependent upon the input signal level. The designer specifies the desired output level and the input threshold by means of external resistors. We will set the output level to -10 dBu (0 dBu = 0.776 V RMS, 1mW at 600Ω). The additional gain needed to maximize the SNR will come from a second amplifier with a manual gain control.

The codec can provide ±2 V to a 60-Ω load. This output is buffered and then filtered. Volume is controlled using an audio voltage-controlled amplifier (VCA), such as the SSM2018.²³ These devices are designed for professional audio applications and are therefore overkill here, but they are inexpensive and the fidelity is excellent. For the power amplifier, I chose to use a discrete class-B amplifier,^{24, 25} which will provide much more output than needed, with low distortion.

Power Chain

I specified a power output of 50 W for this project. This is adequate for my needs and suitable for driving many different tube or solid-state amplifiers if more power is needed. If you want more power, further information has been presented in QEX.²⁶ (Also see Note 2, Part 3.)

I chose to use the MRF151 FET for the PA. It has excellent gain and bandwidth characteristics, and is operated conservatively at 50 W. The amplifier also operates at a conservative 40 V to maximize component life. The driver operates in class A to provide excellent IMD characteristics. The driver gain required is fairly low, only 10 to 13 dB. The MRF151 provides the rest.

Since the amplifier is single-ended, we will use filters similar to those described by Stephensen (Note 2, Part 3). These filters are optimized for high

Table 3—CODEC Parameters

Sampling Rate	8 kHz
Maximum Input	3 V pk-pk
Input Impedance	50 kΩ
Full Scale Output	±2 V
Output Impedance	60 Ω

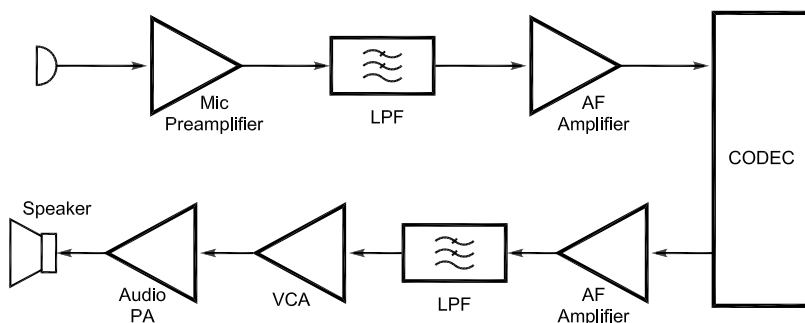


Fig 10—Audio-section block diagram.

attenuation of the second harmonic. They also provide good return-loss characteristics at the harmonic frequencies to reduce IMD.

Summary

This article has described the thought processes behind a high-performance transceiver design that interfaces directly between the digital domain and the desired operating frequency. Signal-handling issues were addressed and tradeoffs explained. The expected receive performance of the transceiver has been modeled to be better than that of commercially available radios. Later articles will cover the detailed design of the transceiver.

I would like to thank Brad Brannon, N4RGI; Bill Sabin, W0IYH; and Doug Smith, KF6DX, for their assistance during various definition stages of this project.

Notes

- ¹U. Graf, DK4SX, "Performance Specifications for Amateur Receivers of the Future," *QEX*, May/June 1999, pp 43-49.
- ²J. Stephensen, KD6OZH, "The ATR-2000: A Homemade, High-Performance HF Transceiver," *QEX*, Part 1 Mar/Apr 2000, pp 3-15; Part 2 May/June 2000, pp 39-51; Part 3 Mar/Apr 2001, pp 3-8.
- ³M. Mandelkern, K5AM, "A High-Performance Homebrew Transceiver," *QEX*, Part 1 Mar/Apr 1999, pp 16-24; Part 2 Sep/Oct 1999, pp 3-8; Part 3 Nov/Dec 1999, pp 41-51; Part 4 Jan/Feb 2000, pp 47-56; Part 5 Mar/Apr 2000, pp 23-37.
- ⁴D. Smith, KF6DX, "Signals, Samples, and Stuff—A DSP Tutorial," *QEX*, Part 1 Mar/Apr 1998, pp 3-16; Part 2 May/June 1998, pp 22-37; Part 3 Jul/Aug 1998, pp 13-27; Part 4 Sep/Oct 1998, pp 19-29.
- ⁵B. Brannon, N4RGI, "Basics of Digital Receiver Design," *QEX*, Sep/Oct 1999, pp 36-44.
- ⁶P. Danzer, N1II, Editor, *The ARRL Handbook for Radio Amateurs*, (Newington, Connecticut: ARRL, 1997), pp 17.5-17.11.
- ⁷Analog Devices, AD6645 datasheet, Rev PrC, 12/01. At the time of writing, this part was not yet released. Samples are available. See www.analog.com for the datasheet and further information.
- ⁸B. Brannon, "Overcoming Converter Nonlinearities with Dither," AN-410, Analog Devices. This application note can be found at www.analog.com.
- ⁹Agilent Technologies, "The Dynamic Range Benefits of Large-Scale Dithered Analog to Digital Conversion in the HP89400 Series VSAs," Product Note 89400-7, 1994. Available at www.agilent.com.

¹⁰Analog Devices, AD6644 datasheet, Rev 0, 5/00.

¹¹Analog Devices, *High Speed Design Techniques* (Norwood, Massachusetts: Analog Devices, 1996), pp 5.41-5.48.

¹²Analog Devices, AD6620 datasheet, Rev A, 6/01.

¹³Further information on the AD6620 filter design software can be found at www.analog.com/techSupport/designTools/evaluationBoards/Ad6620sw1.html.

The software is a free download.

¹⁴W. Sabin, W0IYH, "Narrow Band-Pass Filters for HF," *QEX*, Sep/Oct 2000, pp 13-17.

¹⁵J. Makhinson, N6NWP, "A High Dynamic Range MF/HF Receiver Front End," *QST*, Feb 1993, pp 23-28.

¹⁶D. Newkirk, W9VES, "Simulating Circuits and Systems with *Serenade SV*," *QST*, Jan 2001, pp 37-43.

¹⁷Further information about the EZ-Kit Lite for various DSP products is available at www.analog.com.

¹⁸Information for the compatible TMS320C6711 DSK is available at www.ti.com.

¹⁹Analog Devices, AD6622 datasheet, Rev 0, 5/00.

²⁰Analog Devices, AD9772A datasheet, Rev 0, 3/01.

²¹Texas Instruments, TLC320AD535 datasheet, Rev B, 2000.

²²Analog Devices, SSM2166 datasheet, Rev A, 6/99.

²³Analog Devices, SSM2018 datasheet, Rev A, 7/94.

²⁴P. Cope, W2GOM/7, "A Class-B Audio Amplifier," *QEX*, Mar/Apr 2000, pp 45-47.

²⁵D. DeMaw, W1FB, and W. Hayward, W7ZOI, *Solid State Design for the Radio Amateur*, (Newington, Connecticut: ARRL, 1977), pp 79, 137-138.

²⁶W. Sabin, W0IYH, "A 100-W MOSFET HF Amplifier," *QEX*, Nov/Dec 1999, pp 31-40. □

Denver is the Digital Epicenter



September
13-15!

If you have an interest in digital communications, you can't afford to miss the **21st annual ARRL/TAPR Digital Communications Conference**. This is an international forum for radio amateurs to meet, publish their work and present new ideas and techniques.

This conference is for all amateurs—experienced or otherwise! Presenters and attendees will have the opportunity to exchange ideas and learn about recent hardware and software advances, theories, experimental results and practical applications.

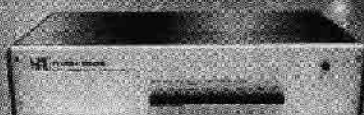
The host hotel is the **Denver Marriott Southeast**,
6363 E Hampden Ave, Denver, CO 80222; tel **303-758-7000**.

Register today! Call Tucson Amateur Packet Radio at **972-671-8277**.
www.tapr.org

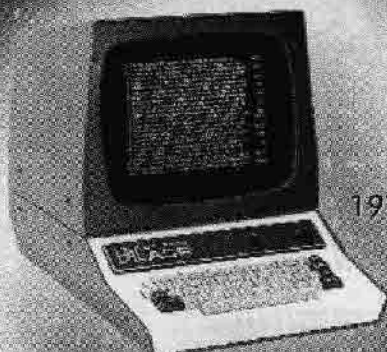
A TRADITION OF INNOVATION



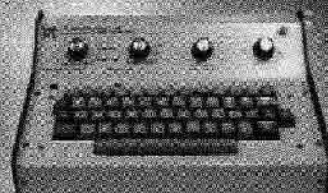
1970: Mainline ST-6



1972: RVD-1002



1978: DS-3100 ASP



1974: DKB-2010



1975: ST-6000



1981: CT-2100

New Software Features
for PCs with Soundcards!
• Waterfall Tuning Display
• PSK31 Support



1985: ST-8000



1998: DXP38

1972 • Thirty Years of Innovation and Excellence • 2002



From the legendary ST-6 to the DSP-based DXP38, HAL continues to provide the amateur with innovative digital communications products.

P.O. Box 365, Urbana, IL 61801-0365 • Phone: 217-367-7373 • FAX 217-367-1701 • www.halcomm.com

Improved Dynamic-Range Testing

Dynamic range is an important measure of transceiver performance. Learn to avoid the pitfalls of measuring it and reap a reward in accuracy.

By Doug Smith, KF6DX

Dynamic-range testing of transmitters and receivers is increasingly important in view of today's crowded bands. That is evidently true for commercial services, the military and Amateur Radio alike. Recently, I became more aware of certain factors in play during such testing that tend to significantly degrade the accuracy of the results. Let me explain what I discovered and put forth some suggestions for improvement.

What is Dynamic Range?

Dynamic range may be broadly defined as the ratio of the smallest us-

able signal to the largest tolerable signal. That definition applies as well to transmitters as it does to receivers, but I shall begin my discussion with receivers, since they usually must exhibit larger dynamic ranges than must transmitters.

Noise should determine the lower limit of a receiver's dynamic range. That lower limit may be defined by the signal-to-noise ratio (SNR) of a desired signal at its output. By the accepted standard, the lower limit occurs when a desired signal, modulated by a single sinusoid or tone, has SNR = 0 dB. Then, signal power equals noise power. That power level is called the *noise floor*. It has also been called minimum discernable signal (MDS),¹ but we are trying

to get away from that term because it implies something about individual perception. Many operators and automated systems can discern signals below the noise floor (SNR < 0 dB).

Either noise or distortion may determine the upper limit of receiver dynamic range. When upper-limit measurements are noise-limited, it is often because of so-called *reciprocal mixing*, wherein noise sidebands on a local oscillator mix with out-of-band interference to produce in-band noise. When upper-limit measurements are distortion-limited, several interrelated mechanisms may be to blame. I leave out any discussion of strong in-band signals here and focus on interference outside the receiver's passband.

Second-order intermodulation distortion (IMD2) occurs when two un-

¹Notes appear on [page 52](#).

desired signals combine nonlinearly to produce their sum and difference frequencies. IMD2 happens when receiver components behave according to a *square law*. When the level of the two undesired signals is increased simultaneously by 1 dB, IMD2 increases by 2 dB. Third-order IMD (IMD3) occurs when receiver components behave according to a *cube law*. For every 1 dB of increase in the two offending signals, IMD3 increases by 3 dB. It might seem funny, but receivers can exhibit both square-law and cube-law behavior at the same time.

One quantification of IMD is called *intercept point* (IP): the power level at which IMD product strengths allegedly rise to match those of each interfering signal. See Fig 1. In modern receivers, IPs may be quite high. It is not unusual to see receivers with third-order intercept points (IP3s) of +30 dBm (1 W) and second-order intercept points (IP2s) of +80 dBm (100 kW). IPs form an excellent basis for comparison of receiver distortion performance. They usually cannot be measured directly at those power levels but must be extrapolated from lower-level measurements.

To do that, one makes the assumption that IMD products behave according to either a square law or a cube law. One injects interfering signals of sufficient amplitudes to produce mea-

surable in-band IMD products and compares power levels. *IMD dynamic range* (IMD DR) is the ratio of the level of one of two equal-power, off-channel signals producing some in-band power, P , equal to the noise floor, to that of a single, in-band signal producing that same power, P .

Sometimes, receiver IMD responses deviate significantly from the straight lines that square-law or cube-law behavior predict. Nonetheless, one generally accepted way to calculate intercept points is to take the noise floor plus twice the IMD2 dynamic range for IP2 and noise floor plus 1.5 times the IMD3 dynamic range for IP3. In a receiver with a classic response, this yields IPs precisely. A more generic formula can be used for *any* two points along the two lines in Fig 1, without knowing where on the lines the points actually fall. For IP2, the equation is:

$$IP2 = 2P_{QRM} - P_{OC} \quad (\text{Eq 1})$$

where P_{QRM} is the level of one of the two off-channel signals causing the IMD and P_{OC} is the level of an on-channel signal producing an identical output power from the receiver. For IP3, the equation is:

$$IP3 = \frac{(3P_{QRM} - P_{OC})}{2} \quad (\text{Eq 2})$$

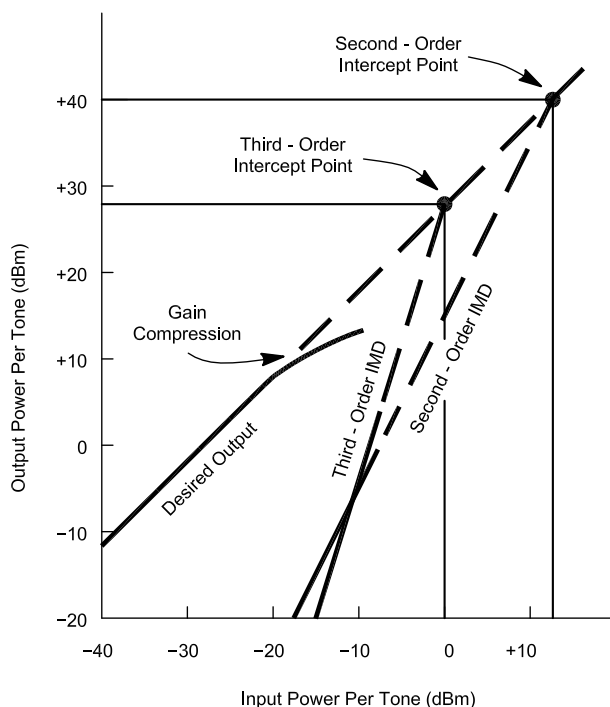


Fig 1—Showing where fundamental receiver response and IMD intercept.

On Small-Signal Measurements and the Nature of Noise

The chief enemy of small signals is noise. Noise is generated in receivers by the random motion of atomic particles inside circuit elements. A famous paper published in 1905 quantifies it.² Physical law states that available noise power is directly proportional to the temperature (in kelvins) of the thing generating the noise. Noise from a signal source (a test generator) is also delivered to a receiver and it may be significant. That is likely when receiver noise figures are low—less than 6 dB or so. Such noise must be distinguished from receiver-added noise during testing.

A signal delivered from a source to a receiver has a certain SNR in the bandwidth of interest. A receiver's job is to preserve that SNR as best it can. All physical circuits add some noise, though. Under controlled conditions, the ratio of a receiver's output SNR to its input SNR is called its *noise factor*. When expressed in decibels, the ratio is called the *noise figure*. To make noise-figure specifications complete, a temperature must be included. Usually, "room temperature" (290 kelvins) is assumed.

I mentioned that noise in signal sources propagates directly to a receiver output. Since noise powers add, noise from signal generators may skew measurements when the noise figure of the thing being measured is low. So the effective source impedance of the noise source must be known during noise-floor measurements. In actual operation, though, low receiver noise figures are not always necessary. A strong, noisy signal on 80 meters, say, would not have its SNR degraded much by a receiver having a noise figure as high as even 20 dB.

Noise may be defined as the output of a randomly driven process. It can be understood by taking a large-scale view of the world. Given the large number of very small particles in the universe and the variety of forces at work on them, it is perhaps no surprise that seemingly random events occur. Some say that given the starting conditions and the laws of basic forces, the state of the universe at any time may be determined from its past state. Others have shown that presumption to break down at very small scales. Such small-scale breakdowns have a way of making themselves evident at much larger scales.

In many ways, we find now that the universe tends to go from a more-or-

derly state to a less-orderly state.³ That situation seems inextricably linked to the passage of time.⁴ So many pseudo-random events have occurred since the start of time that the electrical noise we experience may be characterized as truly random.

In a receiver circuit, a noise voltage may take on almost any value. Over relatively short time frames, though, it has some peak amplitude, A , and a peak-to-peak amplitude of $2A$. The average value of that noise voltage is zero because it is just as likely to be positive as negative. It is also equally likely to be small as large. One may use these facts to compute the average and RMS power of noise.

Over short time frames, a small leap reveals that the average *absolute* value of noise having peak amplitude A is $A/2$. We can prove that by integrating the noise voltage over the range of possible values and dividing by the range:

$$\begin{aligned} E_{\text{AVG}} &= \frac{1}{2A} \int_{-A}^A e \, de \\ &= \frac{1}{2A} \left[\frac{e^2}{2} \right]_{-A}^A \\ &= \frac{1}{2A} \left[\frac{A^2}{2} + \frac{A^2}{2} \right] \\ &= \frac{A}{2} \end{aligned} \quad (\text{Eq 3})$$

The average power is therefore proportional to the square of that, or $A^2/4$. The peak-to-average ratio of noise is thus about 6 dB over the short haul.

To find the RMS value of noise—or any function—take the average (mean) of the square of the function (its mean square), then take the square root of that. For noise, this yields:

$$\begin{aligned} E_{\text{MS}} &= \frac{1}{2A} \int_{-A}^A e^2 \, de \\ &= \frac{1}{2A} \left[\frac{e^3}{3} + \frac{e^3}{3} \right]_{-A}^A \\ &= \frac{A^2}{3} \\ E_{\text{RMS}} &= \frac{A}{\sqrt{3}} \end{aligned} \quad (\text{Eq 4})$$

RMS noise power is one-third of its peak power. Compare this with a sine wave, whose RMS power is one-half of its peak power, or with a square wave, whose RMS power is equal to its peak power.

The exercise above is important be-

cause it reveals a pitfall that often arises when measuring sensitivities of receivers. A common procedure is to connect an ac voltmeter to a receiver loudspeaker and, in the absence of input signals, set the volume control so that the meter reads 0 dB. A desired signal, usually a single tone, is then injected into the receiver until the meter rises by some amount, often 3 dB or 10 dB, depending on the type of measurement. Normally, 3 dB would be used for a noise-floor measurement.

If the ac voltmeter were a peak-reading type calibrated as RMS, it would indicate $A/\sqrt{2}$ when the noise alone were present. The real RMS value of the noise is $A/\sqrt{3}$, so the error would be:

$$\varepsilon = 20 \log \left(\frac{\frac{A}{\sqrt{2}}}{\frac{A}{\sqrt{3}}} \right) = 20 \log \left(\frac{\sqrt{3}}{\sqrt{2}} \right) \approx 1.76 \text{ dB} \quad (\text{Eq 5})$$

If the ac voltmeter were an average-reading type, the error would be:

$$\varepsilon = 20 \log \left(\frac{\sqrt{3}}{2} \right) \approx -1.25 \text{ dB} \quad (\text{Eq 6})$$

In the first case, the SNR looks worse than it should, while in the second case, it looks better than it should.

A true RMS-reading voltmeter must be used to get accurate results using the voltmeter method. The presence of noise in a 10- or 12-dB SNR sine-wave signal is not enough to produce a significant error in the reading when the voltmeter is calibrated as RMS.

To compute a receiver's noise figure from its noise floor, bandwidth must be precisely known. Noise-floor measurements made with filters having undefined bandwidths and responses do not constitute a good basis for comparison. One receiver's 500-Hz filter might be closer to 350 Hz and another closer to 700 Hz, producing up to a 3-dB difference in noise-floor power even if their noise figures were the same. Passband ripple and stop-band response (shape factor) may throw results off by several more decibels. My first suggestion, therefore, is that noise figures form a more useful basis for comparison of receiver sensitivities than measurements of noise-floor power.

To find a particular receiver's noise figure, its effective bandwidth must be determined. Effective bandwidth is easy to find for filters having flat passbands and low shape factors. It may be

computed for any filter by integrating its normalized response over frequency:

$$BW_{\text{eff}} = \int_0^{f_{\text{max}}} A(f) df \quad (\text{Eq 7})$$

where $A(f)$ is the filter's amplitude response at frequency f . For this computation, the largest value of $A(f)$ found is defined as unity and all other values are normalized to that passband peak.

Tones used to measure noise-floor power must be at or near the passband peak. Noise figure may then be computed by finding the difference between the theoretical noise floor of a perfect receiver ($NF = 0$ dB) and the measured noise floor. In a 500-Hz bandwidth, the theoretical limit is about -147 dBm at room temperature. Noise figure is the true measure of a receiver's noise performance as it provides bandwidth-independent information.

Alternatively, a calibrated broadband noise source may be considered instead of a single tone during noise-floor testing. Theoretically, a receiver's frequency response is then irrelevant because the test signal has energy at all frequencies, but this method has its own pitfalls. It does not account for the effects of poor opposite-sideband rejection and spurious responses of a receiver. A unit with poor opposite-sideband rejection, for example, might yield erroneous noise figures because additional energy would appear in the passband that was caused by energy outside that passband.

On the other hand, one can readily measure a receiver having good levels of spurious rejection and opposite-sideband suppression with this method. When the effective source resistance of the noise source is accurately known, a receiver noise figure may be found by comparing its output power with and without the external noise source. Because of its bandwidth independence, many RF designers consider this method the best way to go.

IMD Measurements

Receiver IMD measurements involving large, off-channel signals are difficult to perform accurately. One reason for that involves trouble in generating a clean two-tone signal for application to the receiver under test.

A typical test setup for receiver IMD is shown in Fig 2. Two signal generators are combined in a hybrid combiner. The output of the combiner is fed into the receiver via an attenuator.

Some isolation between the generators is achieved exclusive of the com-

biner because typical laboratory generators use internal attenuators to set their output levels. The external attenuator is strictly necessary because the combiner must be operated into its designed load impedance to get additional isolation. The hybrid combiner achieves a certain isolation level between generators' outputs when its load impedance is right. In typical combiners, that is no better than about 35 dB. Some energy from each generator appears at the other and nonlinearity in generator output stages generates IMD in the test signal.

When the combiner output is not correctly terminated, some energy from the combined output signal is reflected back toward both generators. The attenuator in Fig 2 must therefore provide a good termination, equal to the characteristic impedance of the system—usually 50 Ω. For example, were the termination impedance at the combiner output $60 + j0 \Omega$, the SWR would be 1.2:1 and the reflection coefficient, ρ , would be about 0.10. The isolation between signal generators would be degraded to a value equal to twice the combiner 3-dB insertion loss minus $20 \log(0.10)$ or roughly $6 + 20 = 26$ dB.

Sometimes, 35 or even 50 dB of isolation is insufficient to prevent IMD in generator output stages. Some laboratory generators do fine at lesser isolations, but any doubt may be easily overcome during IMD2 testing because the frequencies of the two generators are so far apart. For example, two signals at 6 and 8 MHz may be combined to test for IMD2 at the sum frequency of 14 MHz. It is reasonably simple to employ a low-pass filter at the 6-MHz generator and a high-pass at the 8-MHz generator to increase isolation. Such filtering is generally impractical, though, when two signals 20 or even 5 kHz apart must be used to

test IMD3 in receivers. Crystal filters have been used, but even crystal manufacturers have a tough time characterizing the IMD response of quartz, especially at signal powers near 0 dBm. In addition, crystal filters are good for only one set of frequencies. It is better to start with a combiner having very high port isolation.

I have recently discovered how to build broadband combiners exhibiting isolation several orders of magnitude greater than that of ordinary combiners. That is, isolation is typically 65 dB instead of 35 dB. I have measured isolation as high as 90 dB at 200 MHz. Insertion loss is about 6 dB instead of the normal 3 dB, but the net gain in isolation is still quite worthwhile. The ARRL Lab is currently evaluating one of my prototypes.

During receiver IMD testing, a reference power level is chosen. That may be at the noise floor or it may be much higher than that. It should not matter: The idea is to find a point on the line representing the square- or cube-law response of the receiver in the presence of two, equal-level interfering tones. A reference power level much higher than the noise floor is good because it avoids difficulties in measuring noise powers. Noise is constantly changing and as the *ARRL Handbook* rightly points out,⁵ picking a reference level well above the noise floor makes life easier.

Having selected a reference power level, a single, on-channel signal is applied and some measure of receiver response is noted. That can be an indication on the S meter, such as S-5, or an another absolute measure of the receiver's output power. (A measurement that distinguishes the level of the IMD product from the noise is preferred over a broadband measurement. More on this below.) Then the on-channel signal is removed and a

clean, off-channel two-tone interfering signal is applied. The levels of the two tones are simultaneously increased until the same S-5 indication is attained. IP and IMD DR are then computed and recorded. This procedure applies equally well to second-order and third-order tests.⁶

The results of tests must produce noise-floor, IMD DR and IP numbers that agree. In other words, $IP2$ must equal twice the $IMD2$ DR plus *noise floor*, and $IP3$ must equal 1.5 times the $IMD3$ DR plus *noise floor*. Published numbers should be accompanied by an estimated margin of error. When the numbers do not correlate within the margin of error, something is wrong.

Take that with a grain of salt, because quite often receivers that are supposed to behave according to perfect square or cube laws act differently in the presence of signals at various levels. Were one to inject signals equal to the calculated $IP3$ of a receiver, for example, one might find that the real $IP3$ is much different—or one might “toast” the receiver!

My second suggestion is that as many reference power levels be used in IMD DR testing as are necessary to determine the slope of the IMD line. ARRL Lab Supervisor Ed Hare, W1RF1, demonstrates the need for that nicely in his sidebar “[What is the ‘Real’ Intercept Point?](#)” From the receivers he has measured, note that the calculated IPs strongly depend on the reference levels used. Errors of 10 dB or more are easy to get when taking only one set of points on the response curves. That has unfortunately engendered considerable doubt about accuracy in many instances. While receivers don't always follow square or cube laws exactly, the assumption must be made that they do when finding IPs and some fit to a straight-line response must be sought.

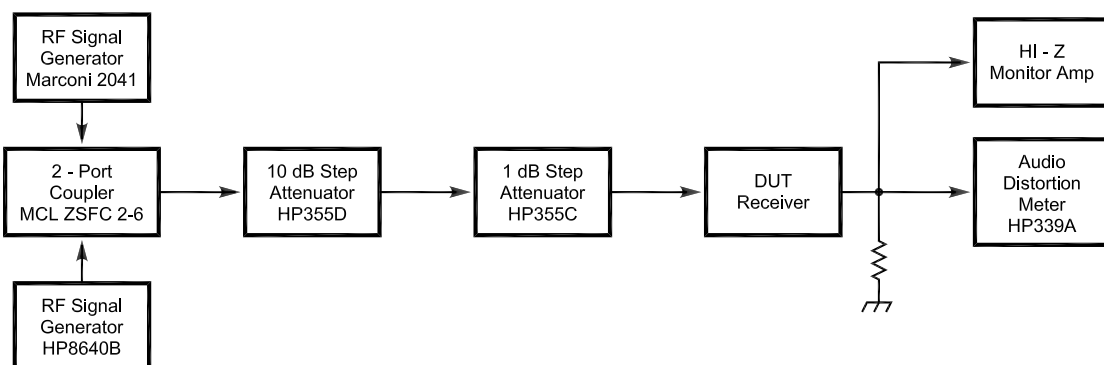


Fig 2—A typical receiver IMD test setup.

What is the “Real” Intercept Point?

Fig 1 shows how the relationship between a receiver’s on-channel response and third-order intermodulation response can be summarized into a single number—the third-order intercept point (IP3). As seen on the graph, this is the point where the first-order and third-order response lines intersect. The intercept point can be a good way to easily compare one receiver with another. If the response of a receiver perfectly matches the curves shown, the intercept point can be calculated using any

two points at the same receiver output level. One would get the same IP3 using measurements made at S9 as one would with measurements made at the noise floor.

Unfortunately, for test and design engineers, real-world receivers do not know that they must follow this theoretical response. In many cases, receivers perform just a little bit differently than expected. This can make the real intercept point of a receiver subject to the judgement of the person looking at the real response curves and trying

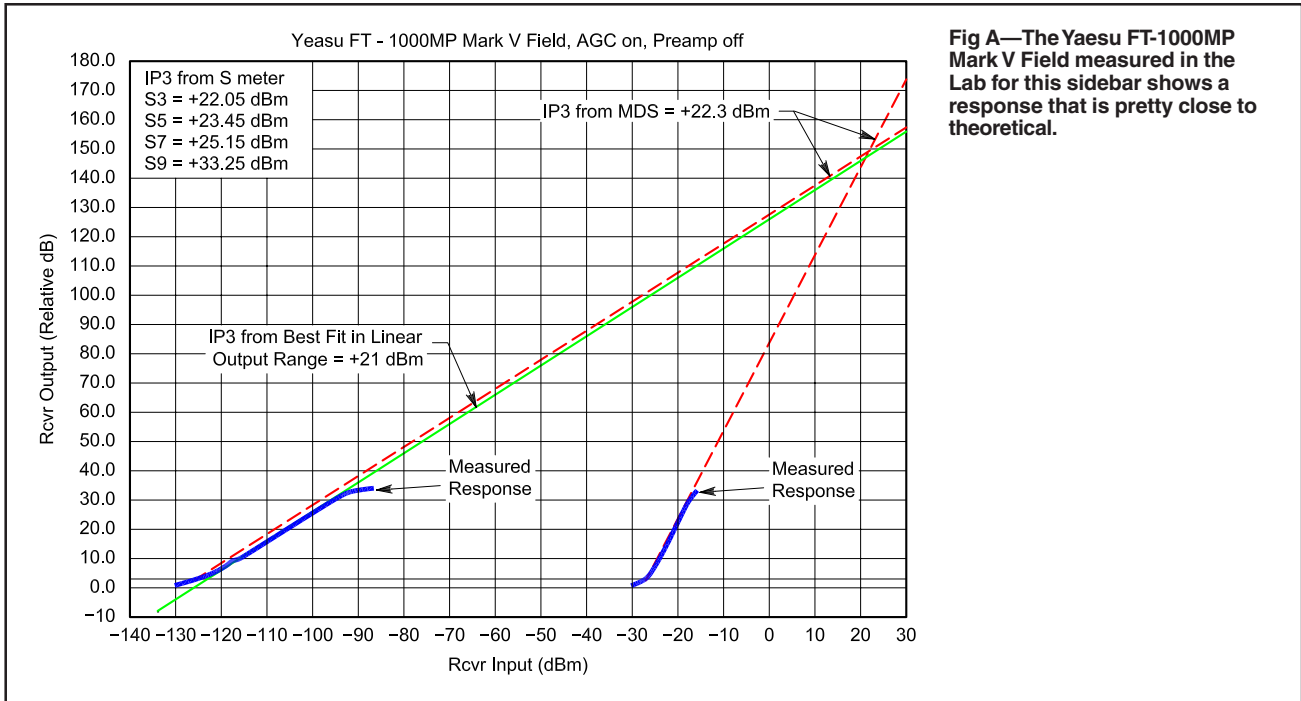


Fig A—The Yaesu FT-1000MP Mark V Field measured in the Lab for this sidebar shows a response that is pretty close to theoretical.

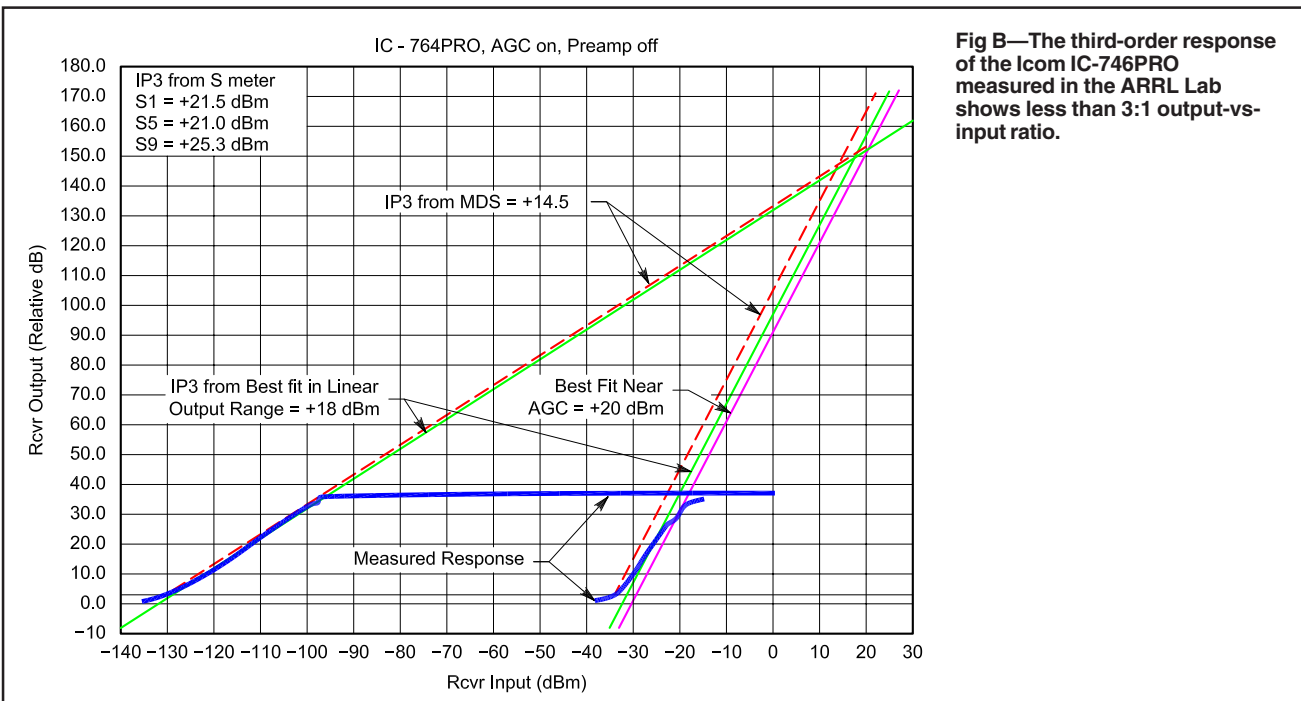


Fig B—The third-order response of the Icom IC-764PRO measured in the ARRL Lab shows less than 3:1 output-vs.-input ratio.

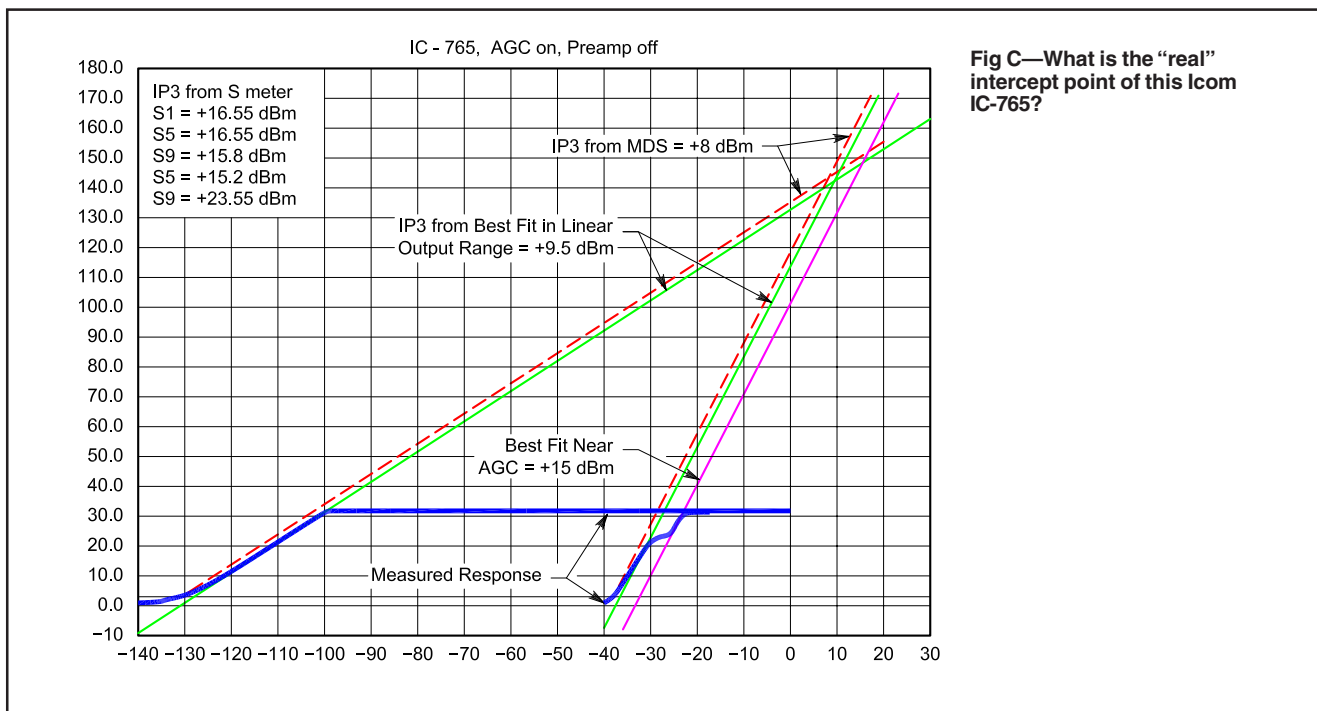


Fig C—What is the “real” intercept point of this Icom IC-765?

to decide just what the IP3 of a receiver really is.

The ARRL Lab grabbed a few radios from W1AW and did some IP3 testing. (How many hams would love to be able to do that?) The results are shown in Figs A, B and C. One of the radios behaved pretty close to the theoretical response, but the other two don't really seem to know that their responses are supposed to be straight lines.

Fig A shows the measured response of a Yaesu FT-1000MP Mark V Field. In this case, the receiver response is pretty close to what theory predicts. The first-order response (on-channel) increases by 1 dB for every 1 dB of increase in signal, at least up until receiver AGC levels the receiver output. The third-order intermodulation response appears at much higher levels of off-channel signals, and once it appears, the receiver output increases 3 dB for every 1 dB of input level. If one makes measurements of the input levels at any point, one gets approximately the same IP3. Because these are all relative measurements, the receiver S-meter can be used as an indicator of relative receiver output. The inset box in the graph shows the IP3 calculated using various S-meter readings. At S9, the deviation from theoretical has pushed the IP3 up quite a bit. The receiver AGC may be responding to the very strong off-channel signals 20 kHz away.

Fig B shows a less-classic receiver response—that of the IC-746PRO. In this case, the on-channel response is classic, but the third-order response increases by less than 3 dB for every 1 dB of receiver input. In this case, if one calculates IP3 using measurements made at the noise floor, one will get a lower number than that obtained by using IMD measurements made at stronger signal levels. I speculate that the two signals, spaced at 20 kHz and 40 kHz from the desired signal, may not be at the same level inside the receiver at the point where the intermodulation is occurring.

The differences in receiver responses have little to do with today's technology. Fig C shows the measured re-

sponse of the IC-765 we borrowed from W1INF, the ARRL HQ club station. Its third-order response shows a little “burble” within a few decibels of where receiver AGC would become active. In this case, the calculated IP3 is much higher for stronger input levels than it is for measurements made at the noise floor.

As an important aside, none of these deviations from theoretical indicates a receiver problem. They are just artifacts of how very strong signals sometimes behave inside of complex receivers.

In the case of the receivers shown above, what is the “true” intercept point of each receiver? There really is no true number, but one could rightfully argue that one made by using a “best fit” of the theoretical lines against the actual curves best represents the receiver's true IP3. That sounds good in principle, but in practice, doing the tests for these sidebars took considerable time. *QST* readers want to see Product Reviews as soon as possible, and the ARRL Lab can't take the time to do much extra testing for radios being reviewed. Measurements made at the noise floor are difficult to make, and the influence of the measured noise on an IP3 calculation made from receiver responses at the noise floor is not a very accurate way to make measurements. Even more important, in almost all “real-world” use, the ambient noise level when an antenna is connected to receiver is probably 10 or 20 dB higher than the receiver input noise. In addition, if an intermodulation product is only a few decibels above the noise, it is not going to have as much impact on listening as would one at a higher level. For that reason, the ARRL Lab has used an S5 receiver output level as the point at which IP3 calculations are made since the mid 1990s. This probably represents a reasonable strong signal that is apt to be encountered in the real world. Although this is not quite as accurate as a best-fit calculation, as can be seen from the graphs, an S5 calculated IP3 is reasonably close to the “real” IP3 of the radios tested.—Ed Hare, W1RFI, ARRL Lab Supervisor

Effects of Phase Noise

In the *May/June 2002 QEX*,⁷ Peter Chadwick, G3RZP, took on the task of deciding how much dynamic range HF receivers need. He made some measurements of actual received signal strengths and based his conclusions on those. He found that quite often, phase noise causes reciprocal mixing that masks the IMD performance of receivers.

Phase noise is the unwanted phase modulation of frequency-control elements in a receiver. Especially during IMD3 testing, phase noise may limit one's ability to measure dynamic range. That is because the interfering signals are close enough to one's passband to cause significant reciprocal mixing. In fact, the effect may prevent one from actually measuring the IMD DR of the receiver under test in the usual way. It is an undesirable situation, but it is what led Peter to define phase-noise dynamic range.

Phase noise also comes into play prominently during measurement of so-called *blocking dynamic range*. That measurement is designed to indicate the ability of a receiver to accommodate a single strong, off-channel signal while receiving a weak, on-channel signal. In older rigs, a strong adjacent-channel signal often reduced the output level of the on-channel signal. There could have been several reasons for that, including saturation of some stage or actuation of analog AGC. Modern rigs typically run into the reciprocal-mixing problem before other blocking effects rear their heads, though. Reciprocal mixing generally causes receiver output power to increase, rather than decrease, because of noise mixed into the passband.

Getting back to the case of noise-limited IMD measurements, we are stuck with having to decide how to pick IMD products out of reciprocal-mixing noise. It is not okay to just guess at the IP. I have found an audio spectrum analyzer very useful in digging IMD products out of the noise. The resolution bandwidth of the analyzer may be reduced until a discrete IMD product stands out. So, rather than using a voltmeter to measure receiver output power, a spectrum analyzer is a good tool for measuring the power of a single IMD product alone. When performance is limited by phase noise in every test of interest, though, IMD DR loses much of its relevance.

Transmitters have Dynamic Range, Too

The concept of intercept point applies equally well to transmitters. The chief difference from receivers is that for transmitters, output IP is specified instead of input IP. If an SSB transmitter had IMD3 levels 30 dB below one of two tones at 100 W each, then its output IP3 would be $30 / 2 = 15$ dB greater than 100 W, or $15 + 50 = 65$ dBm. Such a figure may be used to compare transmitters much as it is to compare receivers, although that is not often done. It is more sensible to talk about a transmitter's maximum output power at some level of IMD.

Tim Pettis, KL7WE, discovered a unique way of combining (with good isolation) the outputs of two transmitters to produce an IMD-free test signal for driving high-power amplifiers during IMD testing.⁸ It uses six $1/4$ lengths of coax in two rings. It is a narrow-band solution, so a separate fixture must be constructed for each frequency range tested. Like other combiners, it is sensitive to termination impedance, but it includes a way to adjust isolation for various loads.

Hum and noise measurements are normal parts of transmitter testing. The dynamic range of a transmitter may also be defined in terms of the maximum signal-to-noise-and-distortion (SINAD) ratio it produces.

Conclusion

I hope my suggestions help you

perform improved dynamic-range testing. Careful methods, good instrumentation and a little persistence lead to accurate and repeatable results.

Many heartfelt thanks to Leif Åsbrink, SM5BSZ, for getting me going on this topic and for discussing it with me in such a rational manner. He deserves most of the credit for the ideas I present. Thanks also to Ed Hare, W1RFI; Mike Tracy, KC1SX; and Zack Lau, W1VT, for their valuable input and kind assistance.

Notes

¹M. Tracy, KC1SX, *ARRL Test Procedures Manual*, ARRL, Rev G, Jan 2002. ARRL members may download the manual at www.arrl.org/members-only/prodrev/testproc.pdf.

²1905 was a good year for Albert Einstein. Along with his papers explaining the photoelectric effect and special relativity came "On the Motion Required by the Molecular Kinetic Theory of Heat of Small Particles Suspended in a Stationary Liquid," *Annalen der Physik*, 1905.

³T. Ferris, Ed., *The World Treasury of Physics, Astronomy and Mathematics* (New York: Little, Brown and Co, 1991).

⁴R. Feynman, *Six Not-So-Easy Pieces* (Reading, Massachusetts: Addison-Wesley, 1997).

⁵D. Reed, KD1CW, Ed., *The 2001 ARRL Handbook* (Newington, Connecticut: ARRL, 2001), p 15.20.

⁶*ARRL Handbook*, pp 17.5-17.6.

⁷P. Chadwick, G3RZP, "HF Receiver Dynamic Range: How Much Do We Need?" *QEX*, May/June 2002, pp 36-41.

⁸T. Pettis, "Hy-Brid Hi-Power," *Proceedings of the 1998 Central States VHF Conference*, ARRL Order #6915. □□

Quality communications
equipment since 1942.

WWW.RFfun.com

universal radio inc.

Universal Radio
6830 Americana Pkwy.
Reynoldsburg, OH 43068
◆ Orders: 800 431-3939
◆ Info: 614 866-4267
◆ Fax: 614 866-2339

Tech Notes

[When it comes to pileup-busting DX antennas, big is beautiful. However, big may not be in the cards for suburban hams living under the shadow of restrictive zoning laws. When the only choice is “small or none-at-all,” inductive loading often provides the best strategy for achieving useful performance. This Tech Note looks at a method for predicting how loading-inductor Q affects an antenna’s performance overall—Peter Bertini, K1ZJH, QEX Contributing Editor, k1zjh@arrl.org]

Predicting the Impact of Loading Coil Q on Antenna Performance

By Rick Littlefield, K1BQT

Inductor Q is the figure of merit we use to express the relative quality of a coil. Q is defined as the ratio of reactance to resistance ($Q = X/R$). If a coil exhibits a reactive component of $400\ \Omega$ and a resistive component of $2\ \Omega$, its Q is 200 ($400/2 = 200$).

Coils used for lumped loading typically exhibit Q s ranging from less than 100 to more than 500. The Q for any given coil is influenced by many factors, including its length-to-diameter ratio (L/D), wire loss, spacing between turns and losses in the supporting coil

form. Once installed on an antenna, the Q of an otherwise superior coil may be degraded by factors such as weather sealant or encapsulation materials, abutting element tubes and attachment hardware.

High- Q loading coils are more efficient, and this fact alone often motivates builders to use the highest Q possible to minimize losses. However, selecting a coil solely based on efficiency may not always yield the best design outcome. For many applications, factors such as fabrication cost, bandwidth, physical size, weight, wind loading and feed impedance may require consideration. In the end, the optimal value of Q is often determined by a confluence of many variables.

Procedure

This experiment describes a simple method for applying *EZNEC* to predict the impact of coil Q on three key antenna parameters:

- Antenna Gain
- Feed-point Impedance
- Bandwidth

Gain change is important because it equates to changes in inductor loss. It is useful to know about changes in feed-point impedance to make matching decisions. Bandwidth, which is always compromised by inductive loading, monitors the antenna’s useful span of frequency coverage.

To test the concept of using *EZNEC*

to monitor these three parameters, I began by modeling a generic OCFD vertical. I chose the configuration in Fig 1, primarily because it allows me to run identical Q trials on two different bands by changing only the loading coil.

Before starting trials for a specific band, I determined the amount of inductive reactance needed to resonate the antenna near my frequency of interest. Once this (preferably rounded) figure was established, I applied the formula $X/Q = R$ to determine the corresponding coil resistance needed to yield each value of Q . For example, if $700\ \Omega$ of reactance was used to resonate the antenna and the desired inductor Q was 200, I entered $3.5\ \Omega$ of coil resistance in the *EZNEC* Loads window to satisfy the equation ($700/200 = 3.5$).

To complete each Q run, I began by recording the antenna’s feed-point resistance at resonance (defined as $R + j0$). I then found the antenna’s relative bandwidth by entering its feed-point resistance into the SWR plot’s Alternate Impedance box and normalizing the SWR curve for that value. Finally, I ran an E-plane radiation plot to predict antenna gain. With all other variables remaining equal, changes in gain equate to changes in coil loss.

The plot shown in Fig 2 shows the outcome of my 20-meter trials. The most obvious data feature is the sharp

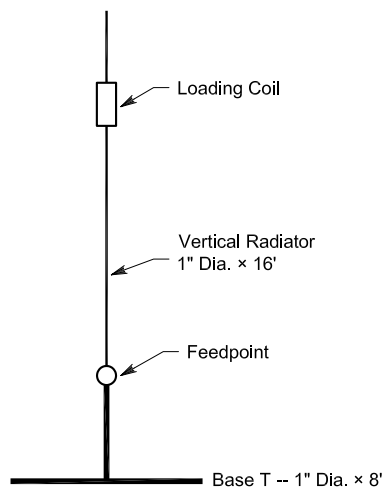


Fig 1—A trial antenna configured as a simple OCFD represents a typical loaded portable antenna.

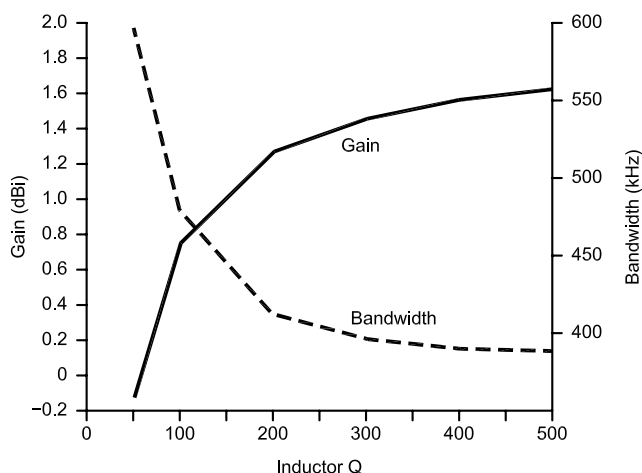


Figure 2—A plot of gain versus bandwidth illustrates the relationship between coil losses and frequency coverage for operation on 20 meters.

crossover relationship between bandwidth and gain. While dramatic, the significance of this data has meaning only when weighed against the antenna's intended application. For example, if Q is degraded from 500 to 100 on 20 meters, the projected gain loss is less than 1 dB—an imperceptible change in on-air signal level. If the intended application is to offer a lightweight portable antenna for low-power use, any losses resulting from the lower- Q coil might easily be offset by benefits such as smaller inductor size, reduced weight, lower cost, and 100 kHz of added band coverage. However, if the objective is to provide a permanent station antenna for a 1500-W RTTY installation, the extra bandwidth and small size would offer no benefit, while the increase in coil losses might cause the inductor to go up in smoke!

The key to interpreting this data is to first identify which changes matter. For example, while degrading Q below 200 may yield a rapid decline in efficiency, increasing it above 200 will yield a comparatively small improvement. Thus, it may not pay to install a costly silver-plated air-wound coil with a Q of 500 if a Q of 200 will do the job.

It is important to note that the numbers presented in Fig 2 are very specific, applying *only* to this antenna when it is operated on 20 meters. If the radiator was smaller and the inductor was called upon to contribute greater loading, the impact of inductor Q would become magnified (and vice versa). By way of example, consider what happens when the same radiator is reloaded for 40 meters (Fig 3). Under these circumstances, when Q is reduced from 500 to 100, the resulting signal loss increases by 2 dB with a correspondingly larger amount of the applied RF power being converted into heat. So, while a Q of 100 may represent a viable compromise at 14 MHz, a substantially higher-quality coil may be needed at 7 MHz to limit losses to an acceptable level.

Conclusion

By modeling values of Q on EZNEC, it is relatively easy to make informed loading-coil selections for specific antennas based upon predicted gain, feed-point resistance and bandwidth data. Using this approach, much of the guesswork is eliminated. □□

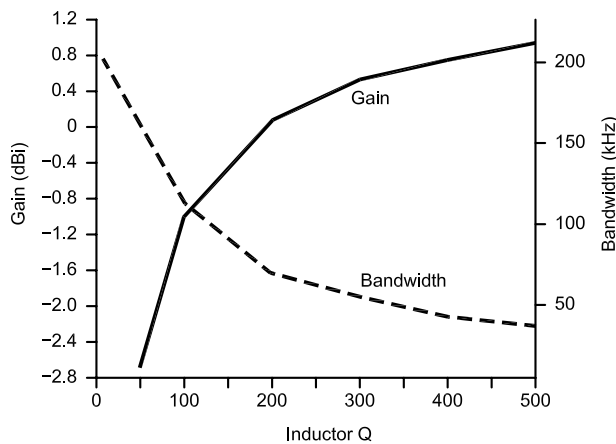


Fig 3—Inductor Q becomes more critical to the antenna's performance on 40 meters, where more loading is required to achieve resonance.

Table 1—Data Predicts the Relationship between Inductor Q and Antenna Performance

Antenna #1, $f_0 = 14.2$ MHz

Q	50	100	200	300	400	500
Gain (dBi)	-0.15	0.74	1.27	1.46	1.56	1.62
Z (Ω)	71.5	58.2	51.4	49.2	47.8	47.1
BW (kHz)	600	490	420	400	395	395

Antenna #2, $f_0 = 7.15$ MHz

Q	50	100	200	300	400	500
Gain (dBi)	-2.7	-1.07	0.06	0.52	0.76	0.92
Z (Ω)	147	81.5	48.6	37.9	32.2	29.1
BW (kHz)	205	110	65	55	45	40



SALE
Atomic Watch
hard mineral lens,
hi-tech polymer case
black leather band
\$109.95

ATOMIC TIME™

...self setting
...correct time
...atomic clock

World's most exact time...
atomic clocks, atomic watches
and weather stations

- for any time zone
- synchronized to the u.s. atomic clock in colorado
- accurate to 1sec. in 1 mil. years
- engineered in germany

complete line of atomic clocks
JUNGHANS MEGA CERAMIC Watch
JUNGHANS MEGA CARBON Watch
JUNGHANS MEGA CLOCKS
JUNGHANS SOLAR WATCHES
ATOMIC SPORTS WATCHES
ATOMIC SCHOOL/OFFICE CLOCKS
ATOMIC INDUSTRIAL CLOCKS
Oregon Scientific Weather Stations,
Weather Forecast, World Time, NOAA
Radios, Radio Controlled Clocks...
call for our FREE Brochure
or go to www.atomictime.com
credit card orders call toll free
1-800-985-8463
30 Day Money Back Guarantee
send checks incl. s&h \$6.95 to
ATOMIC TIME, INC.
1010 JORIE BLVD.
OAK BROOK, IL 60523



atomic dual alarm
clock w. temperature
day and date, black
3.5x4.5x2
\$29.95



atomic radio with
2 alarms and
temperature,
day, date, LCD
\$39.95



jumbo digit atomic
clock w. temperature
& day and date, wall
or desk 3.5 x 8.5 x 1
• \$49.95



NEW
Junghans atomic
carbon, stainless bezel,
sapphire lens LCD day,
date - carbon/leather
band • \$279.00



black arabic 12" wall
clock for home or
office • \$59.95
(wood \$69.95)

By Zack Lau, W1VT

A Simple 24 GHz Transceiver

Many people attempt to use 10-GHz circuits for 24 GHz, often with mixed results. The difficulty is that 24-GHz Gunn oscillators typically drift more than 10-GHz oscillators, so narrow bandwidth demodulation circuits that are difficult to use on 10 GHz become nearly impossible on 24 GHz using cheap equipment. Typically, a bandwidth of 200 kHz is used on 10 GHz, to allow the use of surplus WBFM (wide-band frequency modulation) receivers intended for FM-broadcast use. However, this rarely works well in practice, since many good sites for microwave work have strong FM signals that render broadcast receivers unusable for IF work. Thus, it is essential that the intermediate frequency be chosen to minimize interference. Typically, 30 MHz works well, though one contest group, the Mount Greylock Expeditionary Force, W2SZ, has done well with a 10.7-MHz IF.

225 Main St
Newington, CT 06111-1494
zlau@arrl.org

Designing a WBFM IF Receiver for 24 GHz

I decided to design a simple IF receiver optimized for 24 GHz. To compensate for the worse stability of 24-GHz oscillators, I elected to widen the bandwidth to 2 MHz. The bandwidth increase results in a 10-dB decrease in threshold sensitivity compared to the typical 200 kHz wide receiver, but it makes WBFM much more practical over short distances. The wider bandwidth is also useful for mechanically tuned systems that do not have the benefit of varactor tuning to compensate for frequency drift. Thus, you might consider using this receiver with cheap 10-GHz Gunn transceivers. The sensitivity is -95 dBm for 10% distortion, with a MAR-6 MMIC preamplifier.

If you need a 200-kHz-bandwidth design, I'd suggest the one in my November 1994 *QEX* column.¹ I've also found that the Icom Q7A has a sensitive 30-MHz WBFM receiver designed for 75-kHz deviation. It is tunable, so there is no difficulty covering

¹Notes appear on [page 60](#).

the typical 30 and 33 MHz intermediate frequencies. I measured a 12-dB SINAD sensitivity of -106 dBm at 30.000 MHz. The sensitivity was better at 29.972 MHz, -109 dBm. If you want to use headphones with the Q7A, remember that it uses a four-conductor connector for the audio and PTT connections.

The wide bandwidth greatly simplifies receiver design. No heterodyning is necessary to achieve a sufficiently narrow receiver bandwidth, so mixer, oscillator and filter circuits can be eliminated. Fig 1 shows the different block diagrams. The oscillator can be particularly problematic for beginners, as proper operation may be difficult to verify without test equipment. Listening to 40.7 MHz may be difficult—it is not a popular frequency. In contrast, the no-tune transverter designs by Jim Davey, K8RZ, and Rick Campbell, KK7B, used frequencies easily tuned by an FM broadcast receiver. Thus, it was easy to verify oscillator operation with equipment found in nearly every home.

Alignment is also greatly simplified. The filter is designed around the nomi-

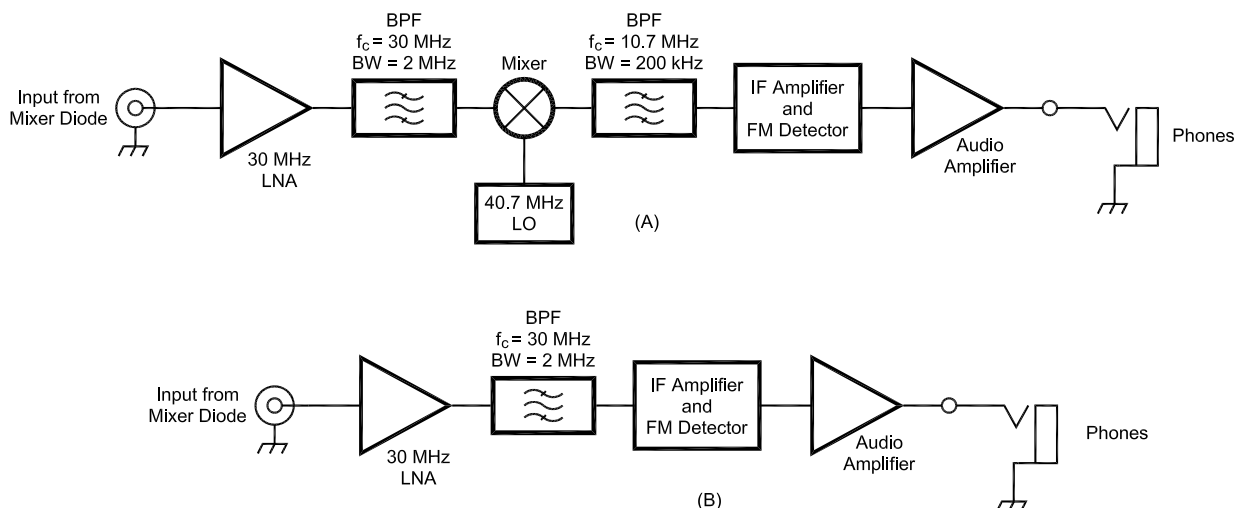


Fig 1—Block diagrams: At A, a traditional 30-MHz WBFM receiver; at B, a simple WBFM receiver.

nal values of the tunable inductors—it is quite possible to get a useful receiver using the inductors just as they come from the Toko factory. Tuning is only needed to optimize the sensitivity. That's quite a change from a superheterodyne receiver, which won't receive 30-MHz signals unless the local oscillator and mixer are functioning. Optimizing receiver sensitivity is just a matter of decreasing the signal level while tuning the receiver for maximum quieting. At the sensitivity threshold of a WBFM detector, it is quite easy to hear minor differences in tuning. Contrast that to a superheterodyne receiver, where you need to worry about the oscillator starting properly to hear anything at all and need to make sure that you aren't tuned to the image frequency.

It is difficult to build a 30-MHz filter with 200-kHz bandwidth, as it represents a loaded Q of 150. It is not impossible; my Nov '94 RF column features a 40-meter band-pass filter with the astounding loaded Q of 243. However, the extensive metalwork and large

physical size may discourage all but the most serious homebrewers. By contrast, a 30-MHz filter with a Q of 15 is rather simple to design and build.

A minor challenge was designing the filter using commonly available parts. In addition, I wanted to minimize the parts count, as long as it did not make it tougher to duplicate. Saving a dollar on parts is no bargain if you need expensive test equipment to make it work. The smallest readily available value for leaded capacitors is 10 pF—small values down to 1 or 2 pF do exist,

but finding them can be a challenge for novices. A T network, using three capacitors, as shown in Fig 2 is a possible solution, but not if the goal is to minimize parts count. I elected to put capacitors at both ends of the variable inductor, so that the coupling taps could be placed at a relatively low-impedance point. Increasing the value of C2 and C4 lowers the impedance presented to the coupling capacitor C3. This is shown in Fig 3A. This reduced the coupling between resonators, as compared with the typical top

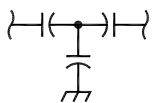


Fig 2—A T network used to obtain more practical capacitor values.

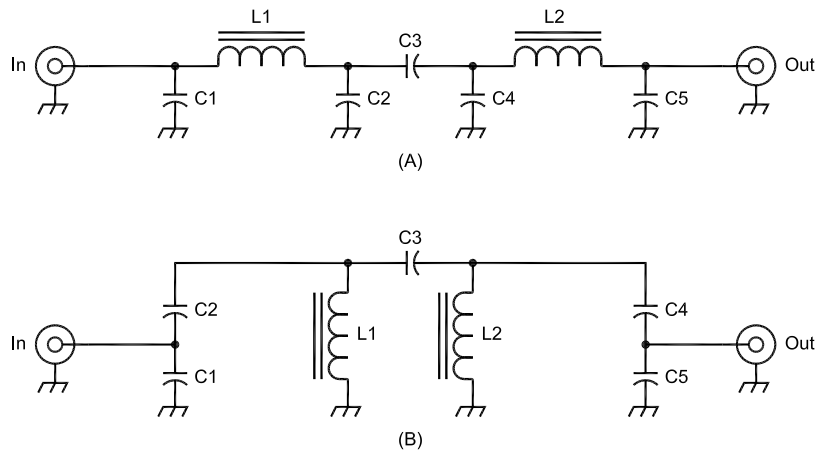


Fig 3—At A, a band-pass filter with coupling between two high-value shunt capacitors, C2 and C4. At B, a top coupled band-pass filter.

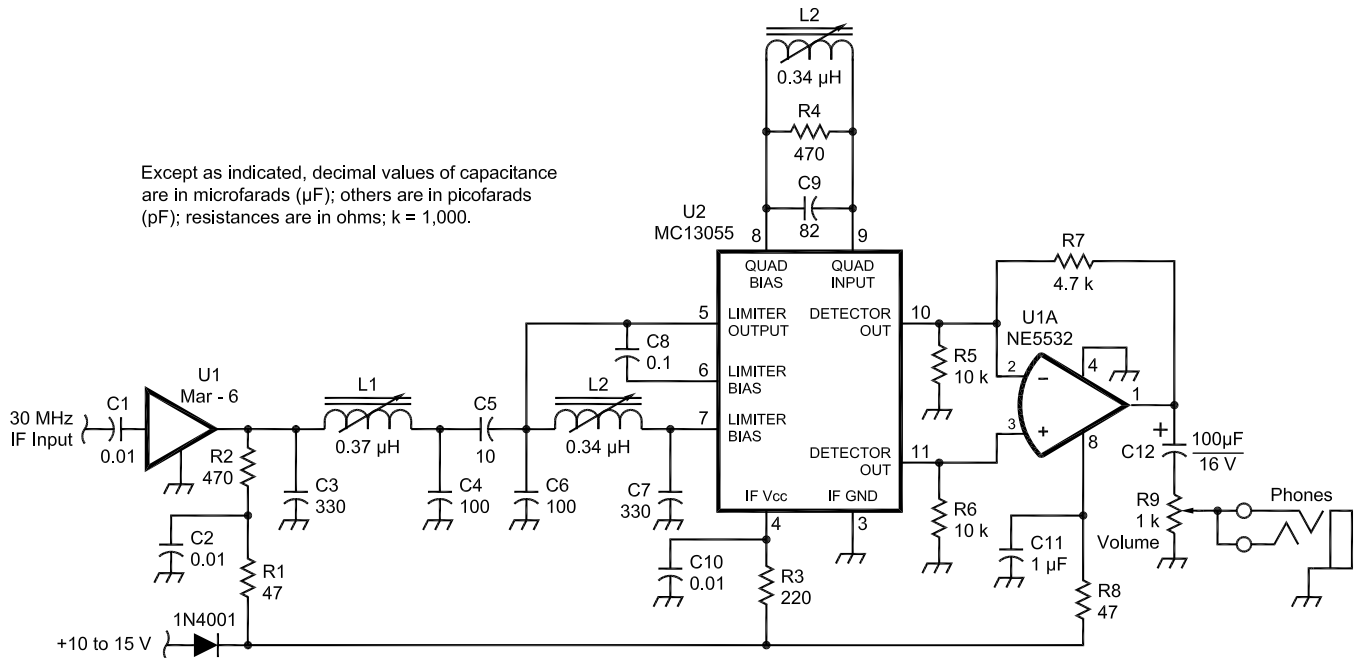


Fig 4—Schematic of the complete 30-MHz WBFM receiver.

L1, L2, L3—0.34 μH tunable inductors (Digi-Key TK-2907 or Toko E526HNA-100079)

U1—Mini-Circuits MAR-6 or Agilent MSA-0685 MMIC

U2—Motorola MC13055 wideband FSK receiver IC

coupled network shown in Fig 3B.

It was a bit trickier to accommodate the mismatch between the filter and the MC13055 input circuit. Like many low-noise circuits, matching the input circuit for maximum power transfer yields inferior performance. An analysis of Motorola's test circuit suggests that while the chip has an impedance of 4.2 k Ω with shunt capacitance of 4.5 pF at 40 MHz, optimum performance is obtained with a source impedance of 700 Ω , with enough parallel inductance to tune out the shunt capacitance. Thus, I designed two circuits simultaneously. One circuit has a 700- Ω load to model the desired impedance transformation, which is what the chip sees. The second has a 4.2-k- Ω load to model the actual filter shape and bandwidth, because the filter is actually terminated in a 4200- Ω load by the chip. I assumed that the impedance at 30-MHz is similar to the 40-MHz data provided by Motorola. Since the receiver worked as expected, I did not attempt to characterize the chip more accurately.

The resulting circuit is shown in Fig 4. Notice that I placed the input of the MC13055 across the inductor. This is a simple way of stepping up the impedance, while keeping the circuit as simple as possible. Thus, the band-pass filter transforms the roughly 50- Ω source impedance of U1, the 30-MHz preamplifier, to 700 Ω . However, the filter is actually terminated in a 4.2 k Ω load, so its band-pass is sharper than if it were terminated in a 700 Ω load.

The low loaded Q of the filter permits the use of shielded slug tuned coils. While several times more lossy than toroidal inductors, they are much easier for a beginner to assemble. There is no tedious coil winding or confusion over counting turns properly. There is one serious drawback to slug tuned coils. The slugs are often broken by the ill-advised use of metal screwdrivers. Not only that, but the broken bits can literally glue the remaining slug to the coil form, making it impossible to remove. It is very important to use the proper tuning tools. Fortunately, Jerry, K0CQ, posted a great idea to the Microwave Reflector run by Tom Williams, WA1MBA—you can make your own tools out of fiberglass circuit-board material. I found it quite easy to sand the circuit board to shape. More importantly, it is often easier to make another tool than to find one you misplaced!

I originally considered the CA3089 FM IF system—it does work at 30 MHz

with about 12 dB less sensitivity than at 10.7 MHz, even though it isn't specified to work there. This was accomplished by using a 0.375- μ H inductor and an 82-pF capacitor for the quadrature network. This moved the center frequency up to 30 MHz. I did the testing with 75-kHz deviation, but it should be easy to widen the bandwidth by reducing the resistor across the quadrature network to 1 k Ω or 470 Ω . The adventurous might consider experimenting with 3089s—selected samples ought to work just fine.

However, I ended up using the Motorola MC13055 wide-band FSK receiver chip, as it requires fewer parts. It is also designed to work at 40 MHz, so even chips that barely meet specifications should work well. Its more

modern design lends itself nicely for use in data applications.

Testing the 2-MHz wide receiver can be problematic, as most signal generators will not generate such a wide signal at 30 MHz. I generated the signal by starting with a 500-MHz signal and heterodyning down to 30 MHz. This was accomplished with a second signal generator operating at 470 MHz, an SBL-1 mixer with 7 dB loss and a 40-MHz low-pass filter. The low-pass filter eliminates the image at 970 MHz. This test setup is shown in Fig 5. Fortunately, I have access to a pair of HP 8640B signal generators.

I recommend Toko inductors if you don't have the test equipment to measure inductance. I did some tests and found the tolerances to be good—the

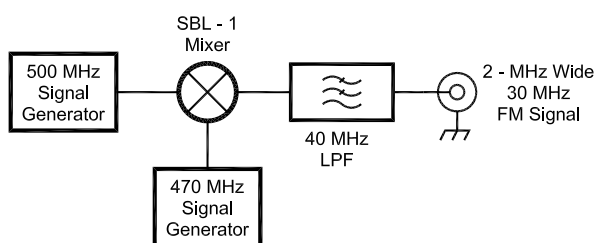
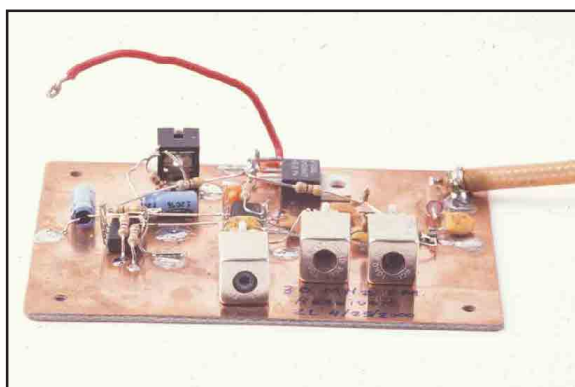
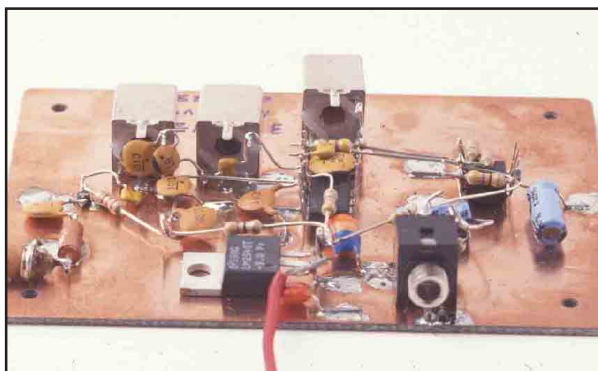


Fig 5—Block diagram of a method to generate a 2-MHz wide 30-MHz FM signal.



(A)



(B)

Fig 6—Photographs of the WBFM receiver prototype from the front: (A) front and (B) rear.

project almost becomes “no-tune.” It can be frustrating to use cheap inductors that won’t even tune to the right value, being too far from their specifications to tune properly.

I decided against using pre-emphasis/de-emphasis with this simple transceiver. It can be an effective technique to improve the signal-to-noise ratio (SNR) of the recovered signal, but such techniques typically involve rolling off the gain response; so more front-end gain is needed to compensate for the reduced gain. This is fine for complex systems, but tough when the goal is to minimize parts count while maintaining reliability. It makes more sense to keep the gain down to enhance reliability. Too much gain can result in unwanted oscillations that seriously degrade SNR.

Unlike SSB/CW receivers, the volume of a recovered FM signal is well defined. There is little chance of an unexpected signal blasting through the detector. Thus, there is no need for limiting circuits to protect a listener’s hearing, as is sometimes required with simple CW QRP rigs. I used a single stage of a dual op-amp for the audio circuitry. The extra stage could be used for audio filtering, if desired. The NE5532 is a good chip for driving headphones, having low distortion and reasonably good output. The single op-amp version, the NE5534 could be used instead, but this chip is typically more scarce than the dual version.

I don’t recommend using the other half of the chip as a microphone amplifier for the transmitter, as it may be difficult to stop unwanted oscillations. The audio from the transmitter also shows up in the receiver once a signal is properly acquired. A Gunn trans-

ceiver demodulates modulation on either the transmitted or the received signal. Thus, you need to minimize the feedback path between the microphone amplifier and the receiver audio amplifier.

R9 is used as an audio-gain control. It should work well if high-sensitivity headphones are used. Placing the gain control at the output should reduce the susceptibility to RFI, a concern if this is to be used near high-power transmitters. A capacitor at the output helps to prevent RF picked up by the headphone wires from entering the receiver circuitry. I specified inexpensive leaded capacitors to bypass RF—in severe cases, it may be worthwhile to use a more costly feedthrough capacitor, along with a shielded metal box to enclose the circuitry.

I decided that it was important for

this receiver to operate well over a wide supply-voltage range. Thus, I optimized the resistors on the MAR-6 to provide about 12 mA with a 10.5-V supply and 20 mA with a 15-V supply. Similarly, R3 is chosen to keep U2 happy with a supply voltage between 10 and 15 V. This technique is cheaper than using a low dropout regulator, such as an LM2940T-9.0, that was used with the initial prototype. You can see it in Fig 6, photographs of the prototype. D1, a 1N4001, provides essential reverse-polarity protection. The prototype also has a 220-Ω ¼-W resistor instead of the 1 kΩ audio potentiometer used in the final version.

To minimize the parts count, the MC13055 is used to establish the dc reference for the audio stages. This is possible with the relatively low gain of the audio system. I would not suggest

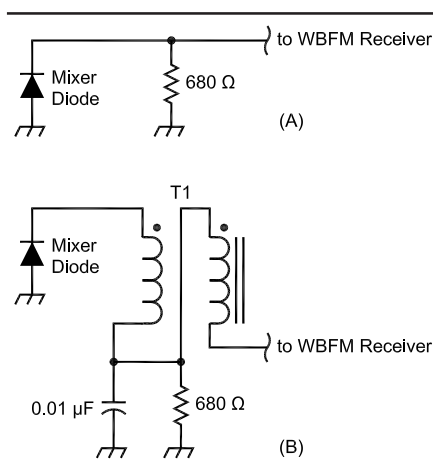


Fig 8—(A) Simplest IF connection to the mixer diode. (B) IF matching to the mixer diode with a transformer.

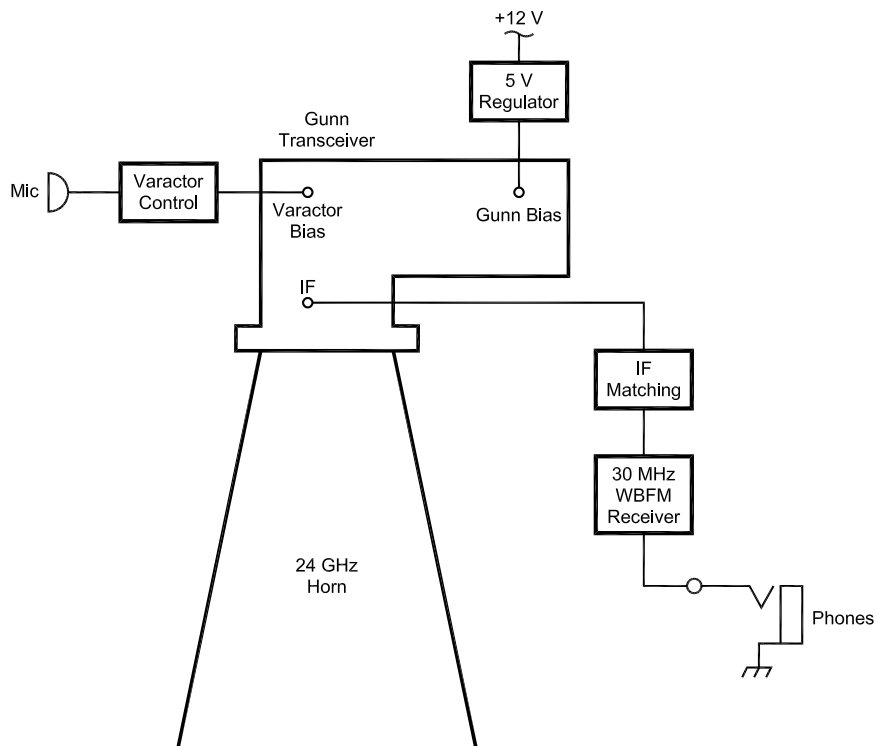


Fig 7—Diagram of one-half of a Gunn transceiver system. Two of these are required to make a communications system.

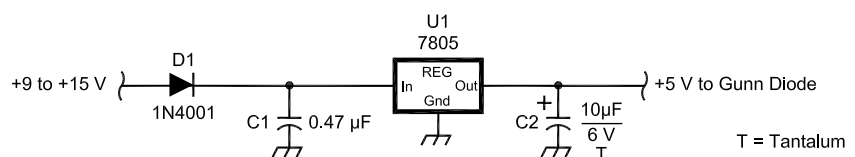


Fig 9—A 5-V regulated supply.

using this technique with the high-gain systems commonly used for SSB/CW work. DC decoupling is often necessary to prevent the quiescent voltage from hitting either supply rail.

A Basic Gunnplexer System

Obviously, this FM receiver is just one part of a 24-GHz communications system. A typical communications system is shown in Fig 7. A 24-GHz Gunn transceiver needs a power supply, an antenna, a varactor-voltage generator circuit, IF matching and a WBFM receiver.

The IF matching circuit is sometimes overlooked. Not only must it efficiently transfer power from the mixer diode to the receiver, but it must also provide dc bias to the diode. Extremely poor performance will result if there is no dc path for the diode. Fig 8 shows two possible circuits. The simplest is just a bias resistor to ground. However, better performance is usually obtained by stepping up the impedance to the diode—M/A-Com recommends 200 Ω for the MA87729-MO1.² It would also help performance if the bias resistor did not waste any receive signal. Fig 8B shows just such a circuit. The bypass capacitor shunts the signal around the bias resistor. Ten turns of #28 AWG enameled wire, bifilar wound on an FT-37-43

core, works very well from 10 to 30 MHz, typically with 0.15 dB of loss. To maximize performance, it may be worthwhile to experiment with different bias-resistor values.

The power supply is typically 5 V for 24-GHz Gunn diodes. The proper voltage is often marked on the case of the oscillator. While it is possible to modulate this voltage, such oscillators may be finicky to use. A simple 7805 regulator, as shown in Fig 9 works well, as long as you properly heat sink it. With a 12.5-V supply, the regulator dissipates over 50% more heat than the Gunn diode. Thus, a diode that draws 200 mA will require that the regulator dissipate (200 mA \times 7.5 V) or 1.5 W. The added expense of a low drop-out regulator is not required for 12-V operation. I do recommend adding a series diode for reverse polarity protection. C2, a tantalum capacitor mounted directly at the Gunnplexer pins, is necessary to prevent unwanted bias oscillations.

The antenna is typically a horn, though dishes are often used for long distance work. I strongly recommend first using a horn, as they are tolerant of construction errors. About the only serious design error that I've seen is someone making the horn too short for its size. Unless you make a horn sufficiently long, you won't get the ex-

pected gain for its aperture. It is less critical that the corners of the horn match up nicely. If you want accurate horn dimensions, I recommend Jeff Miller's article in the Eastern VHF Proceedings.³ He gives dimensions for 24-GHz horns. Fig 10 shows a simple horn antenna for 24 GHz. I like to make mine out of very thin unetched double-sided circuit board. I wrap copper tape around the edges at the mouth of the horn, to insure that the inside surfaces of the horn make good contact with the waveguide flange. It is lighter than brass, copper or tin. As a bonus, 20-mil-thick circuit board is often quite cheap at flea markets, since few hams have a use for it.

Fig 11 shows the key dimensions of a standard WR-42 waveguide flange.⁴ I make cheap flanges out of 25 mil or thicker brass sheet. It isn't tough to file the rectangular hole if you start with a couple of drilled holes. A miniature milling machine works much faster, if you intend to make lots of flanges and take the time to set up a fixture to hold the squares of metal. If you make your own, it is a good idea to match up your homebrew flange against a standard, such as a Gunnplexer output. One of the few ways to make a horn antenna work poorly is to cross polarize it to the waveguide.

An example of a relatively sophisticated varactor-voltage control circuit appears in the Nov 1994 QEX, where I described improved 10-GHz designs in my RF column. Such sophistication isn't necessary—people have obtained excellent results from a potentiometer voltage divider and a single-transistor microphone amplifier. Fig 12 shows a simple varactor control system.

The microphone amplifier increases the output of a low-impedance microphone, typically 600 Ω , to a signal

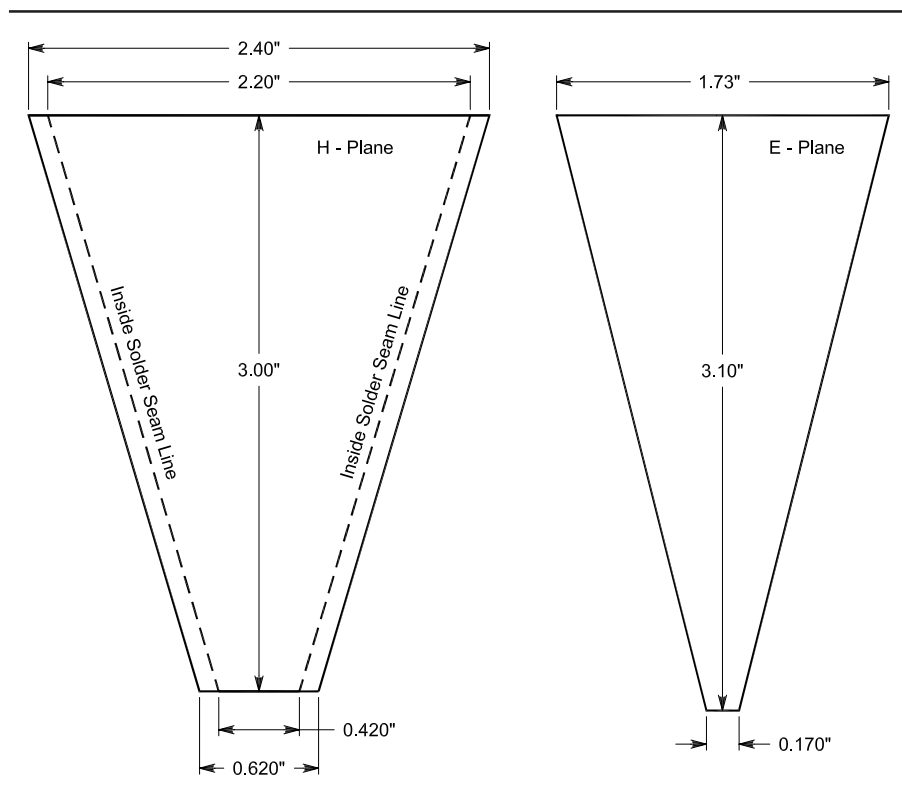


Fig 10—20-dBi-gain 24-GHz horn dimensions.

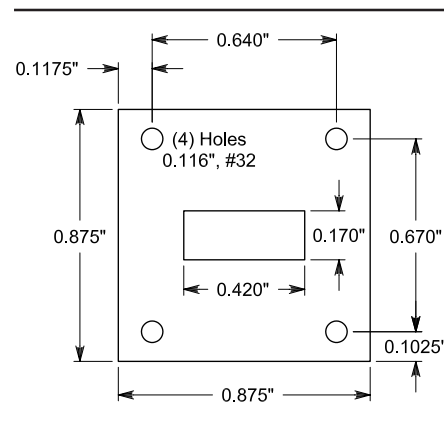


Fig 11—WR-42 flange dimensions.

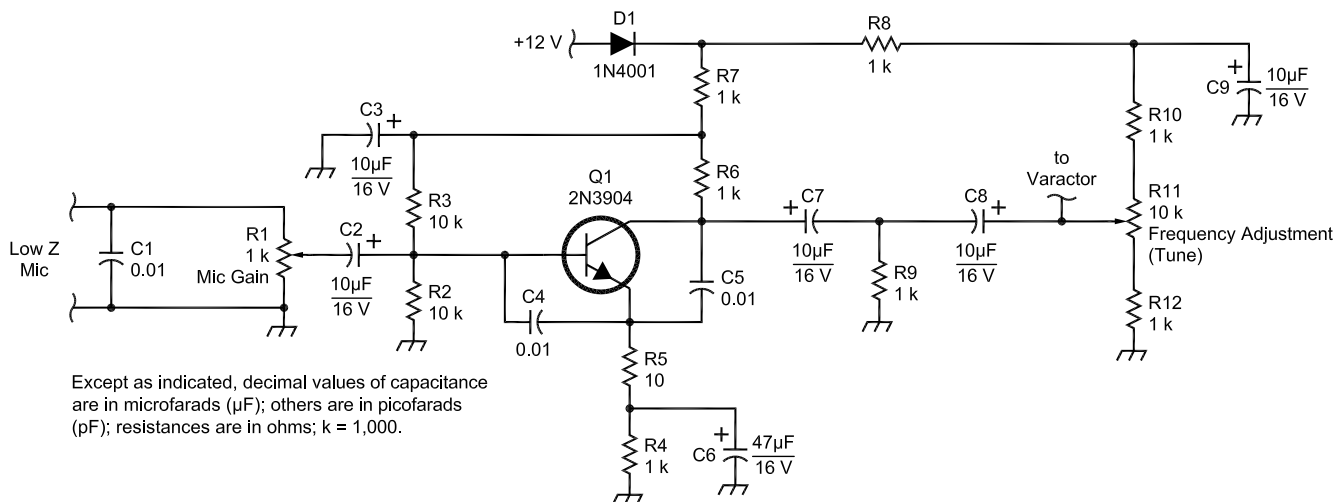


Fig 12—Microphone amplifier and frequency adjustment for varactor-tuned Gunn oscillators.

strong enough to frequency modulate the Gunn-diode oscillator. The output of a microphone is roughly 10 mV; while the sensitivity of a varactor tuned 24-GHz Gunn oscillator is 10 MHz/V. Thus, a gain of roughly 20 dB is necessary to produce a 2-MHz-bandwidth signal. The sensitivity of a varactor modulator is greater at lower voltages; it is useful to have a gain control to compensate for this.

The microphone amplifier uses a few more bypass capacitors than the typical simple design. I think the extra cost is worthwhile in eliminating potential interference problems. C4 and C5 provide RF bypasses, so transistor Q1 is much less likely to rectify RF. Nevertheless, it has a very wide bandwidth, with -3 dB points of 160 Hz and 60 kHz, far more than needed. A good choice for RF bypassing is 0.01- μF stacked metallized film capacitors. Not only are they small and inexpensive, but metal film isn't piezoelectric like ceramics. (Piezoelectric effects can cause problems in audio circuitry used in portable applications.) Similarly, R7 and C3 form a 16-Hz low-pass filter, to remove noise coming in on the 12-V power line. C7, C8 and R9 could be replaced by a single bipolar capacitor. The high-pass network prevents reverse polarity from appearing across the output coupling capacitor.

The varactor tuning circuit is also a little different: I added three 1-k Ω resistors. While they do restrict the

tuning range, they offer some useful benefits. R10 and R12 are the most useful. They prevent the power supply or ground from shorting the microphone audio: Why can't I hear my voice? Otherwise, when the tuning control is set to either end of its range, the microphone amplifier will see a very low impedance, which prevents the varactor from seeing much audio. R8 and C9 form a 16-Hz low-pass filter for decoupling the power supply from the varactor tuning circuit. This should result in cleaner audio when

operating from noisy power supplies.

Notes

- ¹Z. Lau, W1VT, "RF: 10-GHz WBFM—Improved Designs," *QEX*, Nov 1994, pp 25-31.
- ²Available from SHF Microwave Parts Company, www.shfmicro.com. They also sell the MC13055 and MAR-6.
- ³J. Miller, WA1HCO, "Accurate Dimensions for Horn Antenna Design," *Proceedings of the 20th Eastern VHF/UHF Conference of the Eastern VHF/UHF Society*, pp 59-69.
- ⁴J. Anderson, WD4MUO/O, "Waveguides for Millimeter Waves," *Proceedings of the Microwave Update '98*, pp 210-219. \square

American Radio Relay League
225 Main Street
Newington, CT 06111-1494 USA
For one year (6 bi-monthly issues) of QEX.
In the US:

ARRL Member \$22.00
 Non-Member \$34.00

In Canada, Mexico and US by First Class mail:

ARRL Member \$35.00
 Non-Member \$47.00

Elsewhere by Surface Mail (1-2 week delivery):

ARRL Member \$27.00
 Non-Member \$39.00

Elsewhere by Airmail:

ARRL Member \$55.00
 Non-Member \$67.00

QEX Subscription Order Card

QEX, the Forum for Communications Experimenters is available at the rates shown at left. Maximum term is 6 issues, and because of the uncertainty of postal rates, prices are subject to change without notice.

Subscribe toll-free with your credit card 1-888-277-5289

Renewal New Subscription

Name _____ Call _____

Address _____

City _____ State or Province _____ Postal Code _____

Payment Enclosed

Change

Account # _____ Good thru _____

Signature _____ Date _____

Remittance must be in US funds and checks must be drawn on a bank in the US. Prices subject to change without notice.

11/88

Letters to the Editor

Wave Mechanics of Transmission Lines, Part 3: Power Delivery and Impedance Matching (Nov/Dec 2001)

Stephen Best, VE9SRB's, article is an excellent presentation of forward and reflected power in transmission lines. I enjoy [such] stimulating articles and I hope to contribute an article on VHF rhombic antennas.

I am particularly interested in the quarter-wave transformer discussed on p 47. I was surprised to find that Eq 16 can be derived from Eqs 17 and 20.

The derivation is based upon making the reflections from the first and second discontinuities equal. A forward wave will reflect a portion of its power at the first discontinuity, and then travel one-quarter wavelength to the second discontinuity. A second reflected wave would originate at that second discontinuity and return toward the transmitter. The second reflection would have traveled one-half wavelength during the round trip when it reaches the first discontinuity and would be 180° out of phase with the newly arriving wave. If the amplitude of the second reflection were equal to that of the first, total annihilation of reflected waves occurs. Thus, a properly designed quarter-wave transformer should have no reflection at its design frequency. That implies an SWR of 1:1.

Eq 17 gives the reflection coefficient ρ_T at the first discontinuity:

$$\rho_T = \frac{\frac{Z_T}{Z_0} - 1}{\frac{Z_T}{Z_0} + 1} \quad (\text{Eq 1})$$

Eq 20 gives the reflection coefficient ρ_S at the second discontinuity:

$$\rho_S = \frac{\frac{Z_A}{Z_T} - 1}{\frac{Z_A}{Z_T} + 1} \quad (\text{Eq 2})$$

where Z_0 is the characteristic impedance of the transmission line, Z_T is the characteristic impedance of the quarter-wave line and Z_A is the impedance of the antenna.

Equate the two reflections:

$$\frac{\frac{Z_T}{Z_0} - 1}{\frac{Z_T}{Z_0} + 1} = \frac{\frac{Z_A}{Z_T} - 1}{\frac{Z_A}{Z_T} + 1} \quad (\text{Eq 3})$$

Simplifying:

$$\frac{Z_T - Z_0}{Z_T + Z_0} = \frac{Z_A - Z_T}{Z_A + Z_T} \quad (\text{Eq 4})$$

$$(Z_T - Z_0)(Z_A + Z_T) = (Z_A - Z_T)(Z_T + Z_0)$$

and expanding both sides:

$$Z_T^2 + Z_T Z_A - Z_A Z_0 - Z_0 Z_T = Z_A Z_T + Z_A Z_0 - Z_T^2 - Z_0 Z_T \quad (\text{Eq 5})$$

Subtracting like values from both sides and further manipulation yields:

$$\begin{aligned} 2Z_T^2 &= 2Z_A Z_0 \\ Z_T^2 &= Z_A Z_0 \\ Z_T &= \sqrt{Z_A Z_0} \end{aligned} \quad (\text{Eq 6})$$

Be careful! The above derivation does not consider the complex nature of impedance. Ted Moreno warns against this in his monograph, "Microwave Transmission Design Data" (Norwood, Massachusetts: Artech House, 1989, ISBN 089006346X).

A Smith chart will clarify T. Moreno's position. First, normalize the impedance of the transformer section. Starting at the resistance axis at the normalized impedance of the antenna, draw an SWR with center at 1.0 on the axis and proceed 0.25 λ toward the generator. The resulting semicircle will reach the resistive axis at the normalized value of the transmitter's transmission line. This plot represents a quarter-wave transformer driving a purely resistive load.

If the antenna had a reactance (all antennas do, except at resonance), the starting point on the Smith chart would not be on the resistive axis. The 0.25- λ rotation would not return the SWR semicircle to the resistive axis and the reflected wave, which has a reactive component, would not annihilate the reflections from the first discontinuity. Nevertheless, quarter-wave transformers are great inventions.—*Lincoln Kraeuter, KB1EYQ, 92 Whippoorwill Circle, Mashpee, MA, 02649*

Some Notes on Turnstile Antenna Properties (Mar/Apr 2002)

The antenna configurations described in this excellent article will work as simulated only if the individual dipoles have balanced feeds. When fed with a single coax, there is a path from one side of each dipole to ground over the outside of the coax shield. Even if the coax were run straight down from the feed point, the outside shield current would seriously distort the individual dipole's radiation pattern and couple the two dipoles together.

Walt Maxwell, W2DU, explains the problem in *Reflections* (ARRL, 1990, Chapter 21). In *Antennas* (2nd edition; McGraw-Hill, 1988), Kraus mentions using lines of "dual coaxial type" to drive each dipole. By that, he means two coax lines with their shields connected together. "Twinax" or twin-lead should also work well, but not a single coax. L. B. Cebik is by no means alone in overlooking this point. The *ARRL Antenna Book* describes a turnstile with unbalanced, single coaxial feed.

Use of a balun can also solve the problem. A current balun would probably be okay, but some simulation would be required to see how good the balun's performance would need to be. The most elegant balun solution I have seen is the "infinite" or "inherent" balun that Maxwell describes for his quadrifilar helix antenna. It is often used with commercial VHF/UHF folded dipoles.

The example of Mr. Cebik's Fig 10, showing how to obtain quadrature currents by detuning one dipole downward and the other upward in frequency does show balanced feed, but I don't believe the half-wave lines are necessary. It would be interesting to see the simulation results with the effect of the coax shield included; also, with imperfect baluns.—*Byron Blanchard, N1EKV, 16 Round Hill Rd., Lexington, MA 02420*

The author responds:

The problem of antenna currents on the outside of coax braids is perennial and applicable to all forms of coax-fed antennas. Perhaps I should have made clear at the outset that all turnstile antennas portrayed in the article presumed that appropriate means had been taken to ensure that effects from this phenomenon were not present in sufficient magnitude to disturb the results of the other analytical tests made on “turnstiling.” This condition is inherent to the use of antenna models as the basis of analysis, and the point of the article was precisely these other tests, focused on current magnitude and phase. So, no point has been missed, since the universality of the potential for such currents dictates the use of appropriate means to attenuate such currents in all antenna work involving coaxial cables.

There are several methods of overcoming such currents, including the use of either bead or coiled-coax chokes and the use of balanced lines, either shielded or unshielded, according to circumstances. None of the current magnitude and phase phenomena noted in the article arise from coax-braid currents.

Since you reference Fig 10 specifically, let me note that the lines in the top portion of the figure for the more successful quadrature-feed demonstration model are indeed necessary—or is some equivalent means of isolating the feed points. With direct parallel feed as in the lower portion of the figure, the current will not divide equally between paralleled legs of the antenna. Indeed, in W1VT’s original short-leg model, the differential of the loading coils used to achieve the impedance part of the quadrature condition results in very different current magnitudes and phase angles on the paralleled legs, relative to the ideal condition. Simplicity had been the aim of the original suggestion under discussion. Some demonstration models may be available from ARRL, should you care to explore the situation further.

Your last suggestion of modeling the coax braid in addi-

tion to the antenna elements and phasing line may be partially feasible. However, the results would be highly dependent upon the line length, and it remains somewhat an open question as to whether coax braid can be modeled effectively as an added wire on one side of the feed-point terminals for all possible circumstances. Exploring the modeling adequacy of introducing the line as a physical wire as well as a non-radiating mathematical construct within such modeling cores as NEC-2 would amount to a very useful and major study, if one sought comprehensiveness. Thanks for your interest in the article and the subject matter.—*L. B. Cebik, W4RNL, cebik@cebik.com*

On IMD Testing

I’ve been thinking a bit more about this IMD-measurement business. Having a flight delayed so that you’re 17 hours late gives time for thinking!

Let’s assume we have two generators, connected by equal-length cables to a combiner, which is connected to an attenuator and then to a receiver. Let’s assume there’s a mismatch loss of 0.1 dB at each interface, except at the receiver, which has a 0.5 dB mismatch loss. Now we have an uncertainty in the signal levels at the receiver caused by eight interfaces of (RMS addition) 0.57 dB. Let’s assume our signal generators are accurate to 0.5 dB, and we have an RMS uncertainty of 0.9 dB in level. Because of the “3-for-1” law, that’s a 2.7 dB uncertainty in third-order intercept.

Now I believe that the figures quoted on mismatch losses and the generator accuracies are at the tighter end of what is obtainable in the average professional lab; an amateur’s lab is likely to be quite a bit worse. I haven’t included in the above any consideration of the loss in the cables or the combiner.

Conclusion? I think there’s a potential uncertainty in measurements of intercept point of around 3 dB, even when measured in a professional lab.—*Peter Chadwick, G3RZP; Peter.Chadwick@zarlink.com*

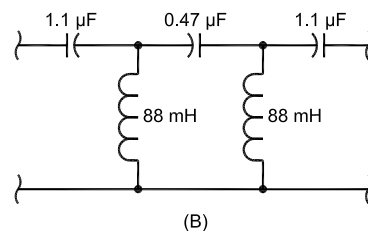
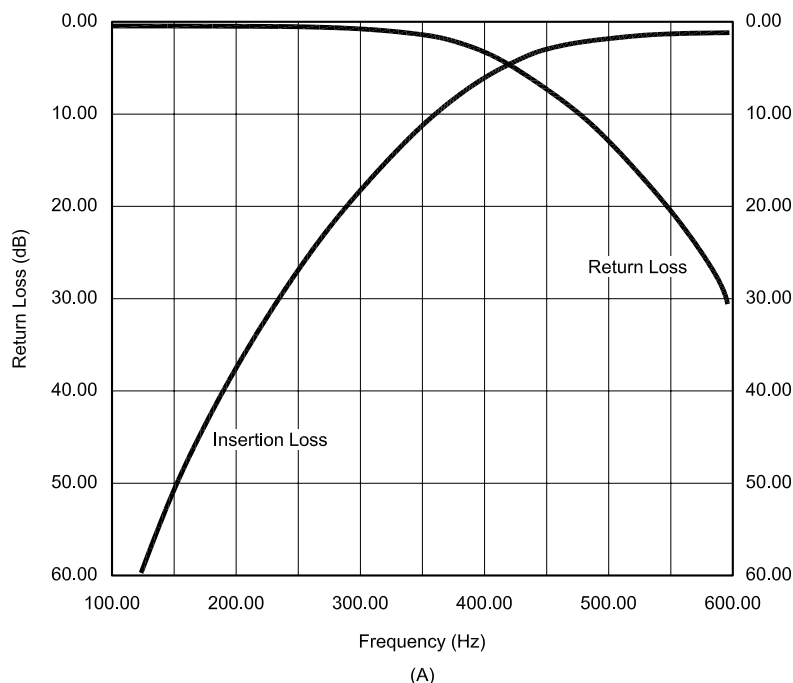


Fig 1—Filter response (A) and schematic diagram (B).

Peter,

Apparently, the potential for error is even greater than what you have described. With help, I uncovered data in which IP3 disagrees with reported IMD3DR and MDS numbers by more than 15 dB! I have made big mistakes myself in the past by not paying close attention to such factors as you mention.

For me, the upshot of the whole thing is that a margin of error must be estimated and included with measured dynamic-range data. If the idea is to provide a basis for comparison of rigs, we must know all the circumstances of the test—*Doug Smith, KF6DX, QEX Editor, kf6dx@arrl.org.*

Filters in “A Homebrew Regenerative Superheterodyne Receiver” (May/June 2002)

Because I am the ARRL Technical Advisor on passive LC filters, I’m always interested in all passive LC filters that are published in ARRL publications.

The constant-k high-pass (490-Hz cutoff) filter design that appeared on p 32 Fig 10 of the May/June 2002 *QEX* immediately caught my eye because of an apparent error in the filter schematic diagram. It appears that there is a capacitor missing between the two 80- μ F capacitors, otherwise the two shunt 330- μ H inductors are simply in parallel and can be replaced by one inductor. Please check with the author, Bill Young, WD5HOH, to determine if there is a capacitor missing from the diagram. The Fig 10 caption states the design is from L. Metzger’s *Electronics Pocket Handbook* (second edition, Prentice Hall, p 42). I do not have this book so I cannot check the original diagram.

Further examination of this design indicates that it is inappropriate for the application discussed in the article. For example, a 330- μ H inductor has impedance of only 1.04 Ω at the 490-Hz cutoff frequency, and the impedance of the 80- μ F capacitors is only 3.98 Ω . These reactances are much too low for this application, in my opinion.

I cannot use filter design software to evaluate the filter performance until I find out the value of the missing capacitor. Based on my experience, however, an impedance level of 4 Ω (as used in this design) is much too low to obtain an effective audio filter with a cutoff frequency of 490 Hz.

I suggest the following design for better performance. My proposed design is based on a 5th-order Chebyshev high-pass filter, design #64, SWR MAX = 1.041, listed on page 30.21 of the 2002 *ARRL Handbook*. After the *Handbook* design is scaled to an impedance of 400 Ω and a

3-dB cutoff frequency of 425 Hz, the series-C and shunt-L values are 1.1 μ F, 0.47 μ F, 1.1 μ F, 88 and 88 mH, respectively. The computer-calculated insertion and return-loss responses (plotted with *ELSIE* filter design software, see Reference 1) are shown in Fig 1 with the schematic diagram and component values. The C1 and C5 capacitors of 1.1 μ F are easily realized with standard 1.0- μ F, 100-V metallized Mylar capacitors with another 0.1- μ F capacitor in parallel. The 0.47- μ F value can be realized with one standard capacitor of this value. The 88-mH inductors (with a *Q* estimated at about 20, see Reference 2) can be realized with two surplus 88-mH inductors. The component values and impedances are reasonable because the filter design impedance is 400 Ω . The filter input and output can be matched to 4 or 8 Ω with a Mouser 42TM118 8/400- Ω transformer. I expect the performance of my proposed design to be significantly better than that shown in Fig 10 of the *QEX* article. Those wishing to obtain two 88-mH inductors to build the proposed design can get them from me postpaid for \$2, to cover postage.

In addition, the caption of the constant-k low-pass filter, Fig 5, states that $f_c = 3100$ Hz, but the actual f_c is 3100 kHz. Why the obsolete constant-k design is used instead of a modern Chebyshev design is not explained. For example, a low-pass Chebyshev with a similar cutoff frequency, termination impedance and return loss needs only two single inductors of 270 μ H, instead of the four 150- μ H inductors required by the constant-k design. The Chebyshev capacitors needed are two 22 pF and one 41 pF.—*Ed Wetherhold, W3NQN, ARRL TA, Passive LC Filters, 1426 Catlyn Pl, Annapolis, MD 21401-4208*

References

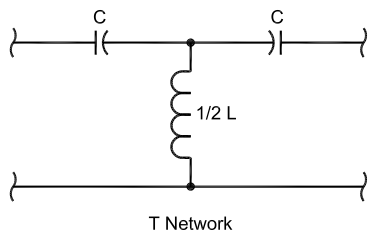
¹*ELSIE* Filter design software. See 2002 *ARRL Handbook*, p 16.38, footnote 1 and p 30.11 listing for Trinity Software.

²E. Wetherhold, W3NQN, “Inductance and *Q* of Modified Surplus Toroidal Inductors,” *QST*, Sep 1968, pp 36-39.

Ed Wetherhold:

Thanks for your letter of May 8, 2002, inquiring about two of the filters in the regenerative superheterodyne receiver published in the *May/June QEX*. A capacitor is *not* missing from Fig 10 of the article. The filter is correct exactly as printed in the *May/June* article. Fig 2 is a sketch of the high-pass filter information from page 42 of the Metzger handbook cited in my article.

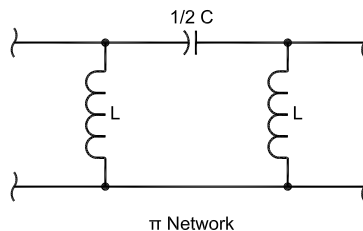
I recalculated the cutoff frequency from the values given in Fig 10 using the analysis equation for f_c and got 490 Hz.



Analysis

$$Z_0 = \sqrt{\frac{L}{C}}$$

$$f_c = \frac{1}{2\pi\sqrt{LC}}$$



Design

$$L = \frac{Z_0}{2\pi f_c}$$

$$C = \frac{1}{2\pi f_c Z_0}$$

Fig 2—Design information for the constant-k filter used by WD5HOH for his article in the *May/June 2002 QEX* (see text).

Keep in mind that the load for this filter is about 4 Ω (two 8 Ω headphones in parallel). Yes it could be designed for a 400 Ω load, but then a transformer is needed as you say. To me, the component values I used are reasonable because they were available from Mouser at low cost. Performance of the filter I built was good to my ears because it improved intelligibility of speech. That's a subjective evaluation. I don't have the means to measure and plot filter response.

I have not used the filter from Fig 10 of the article lately because I found that the box it is in interferes with the phone plug for the tape recorder I have plugged into the receiver. I am now driving a pair of LM380 audio amplifiers through a surplus step-up transformer. This arrangement enables me to use speakers and headphones. I have accomplished the desired attenuation of low audio frequencies for improved intelligibility by inserting a capacitor between the LM386 output and the step-up transformer primary. The capacitance value was determined with a capacitance decade box. I reduced the coupling capacitance until the received speech sounded about right.

You're right about the cutoff frequency for the filter in Fig 5. It should be 3100 kHz. The "k" was left out. I missed that. If you look at the upper right hand corner of page 31, you will see that the cutoff frequency was stated to be "about 3 MHz."

I used the constant-k design because the equations are easy for me to use. This is not a mass-production receiver. I was not attempting to minimize the number of components. If one section did not have quite enough roll-off, two sections would do the job. The receiver is, I think a "proof of

concept" exercise. I would be very interested to see the receiver redesigned with better filters (and a better mixer while you're at it). By the way, you didn't mention the low-pass filter in Fig 8. It came from the same handbook.

Feel free to redesign this receiver as your knowledge, experience and imagination lead. That's what I had in mind.—*Bill Young, WD5HOH, 343 Forest Lake Dr, Seabrook, TX 77586; blyoung@hal-pc.org*

Corrections to May/June 2002 Letter

I just read my letter in the last issue. My e-mail address is n0xeu@arrl.net. The other one (mk2331@sbc.com) is no longer good (I changed jobs). My call sign is now W0XEU, (was N0XEU), not N0EU. I do not believe the errors to be yours; I must have mistyped and I apologize.—*Matt Kastigar, W0XEU* □□

Next Issue in QEX/Communications Quarterly

What would discussions of software-defined radios be without the software? [Next time](#), we have two pieces on just that. One concentrates on a PC-based user interface for a popular computer-controlled rig. The other focuses on object-oriented programming environments and getting started writing your own applications. □□



Join the effort in developing Spread Spectrum Communications for the amateur radio service. Join TAPR and become part of the largest packet radio group in the world. TAPR is a non-profit amateur radio organization that develops new communications technology, provides useful/affordable kits, and promotes the advancement of the amateur art through publications, meetings, and standards. Membership includes a subscription to the *TAPR Packet Status Register* quarterly newsletter, which provides up-to-date news and user/technical information. Annual membership US/Canada/Mexico \$20, and outside North America \$25.



TAPR CD-ROM

Over 600 Megs of Data in ISO 9660 format. TAPR Software Library: 40 megs of software on BBSs, Satellites, Switches, TNCs, Terminals, TCP/IP, and more!

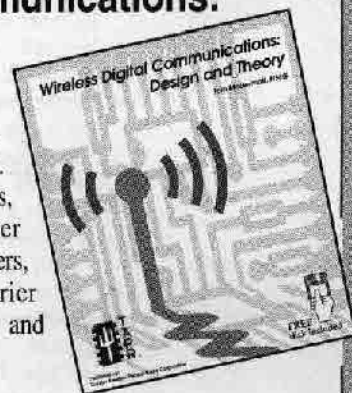
150Megs of APRS Software and Maps. RealAudio Files.

Quicktime Movies. Mail Archives

from TAPR's SIGs, and much, much more!

Wireless Digital Communications: Design and Theory

Finally a book covering a broad spectrum of wireless digital subjects in one place, written by Tom McDermott, N5EG. Topics include: DSP-based modem filters, forward-error-correcting codes, carrier transmission types, data codes, data slicers, clock recovery, matched filters, carrier recovery, propagation channel models, and much more! Includes a disk!



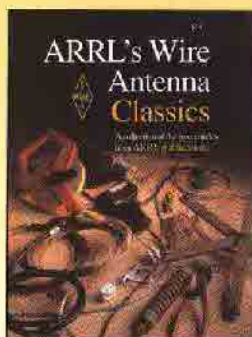
Tucson Amateur Packet Radio

8987-309 E Tanque Verde Rd #337 • Tucson, Arizona • 85749-9399

Office: (972) 671-8277 • Fax (972) 671-8716 • Internet: tapr@tapr.org www.tapr.org

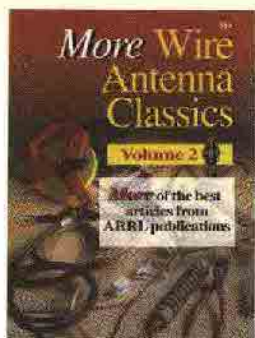
Non-Profit Research and Development Corporation

The ARRL Antenna Classics series!



The Original! ARRL's Wire Antenna Classics

So many wire antenna designs have proven to be first class performers! Here's an entire book devoted to wire antennas, from the simple to the complex. Includes articles on dipoles, loops, rhombics, wire beams and receive antennas—and some time-proven classics! An ideal book for Field Day planners or the next wire antenna project at your home station.
Volume 1. ARRL Order No. 7075—\$14 plus shipping*



Enjoy even MORE wire antennas!

More Wire Antenna Classics

This book is filled with innovative designs from the pages of *QST* and other ARRL publications. Experience the satisfaction and enjoy the benefits of building your own wire antennas. Inside, you'll find more than just creative ideas. These versatile antennas work! If you have the original ARRL's Wire Antenna Classics—you'll want MORE! ARRL Order No. 7709—\$14 plus shipping*

These versatile antennas work! If you have the original ARRL's Wire Antenna Classics—you'll want MORE! ARRL Order No. 7709—\$14 plus shipping*

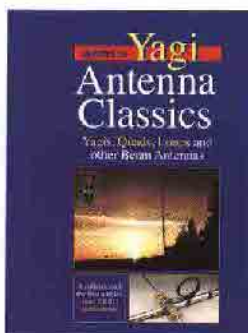
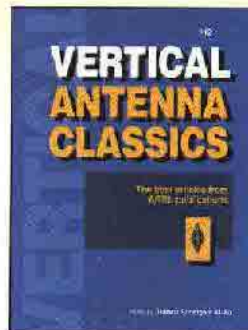
Winning Performance! Vertical Antenna Classics

Vertical antennas are everywhere — on cell phones, broadcast towers and portable radios. You'll also see them on the roofs, towers and vehicles from Altoona to Australia. And for good reason! Here are some top-notch performers from ARRL publications, brought together in one book. Vertical antenna theory and modeling, VHF and UHF, HF, directional arrays, radials and ground systems, and more.
ARRL Order No. 5218—\$12 plus shipping*

ARRL's Yagi Antenna Classics

Yagis, Quads, Loops, and other Beam Antennas

A wealth of ideas from some of the leaders in antenna design and experimentation of the last 70 years. Covers monobanders; multibanders; HF, VHF and UHF beams from 80 meters to 2304 MHz; computer modeling; towers, masts and guys. Some of the very best articles from *QST*, *QEX*, *NCJ* and other ARRL publications.
ARRL Order No. 8187—\$17.95 plus shipping*



ARRL Antenna Compendiums

More antennas
— ideas and
practical projects



Volume 6

All new articles covering low-band antennas and operating, 10-meter designs, multiband antennas, propagation and terrain assessment. CD-ROM included with propagation prediction software!

#7431 \$22.95*—Includes software

Volume 5

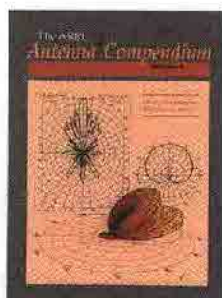
Enjoy excellent coverage of baluns, an HF beam from PVC, low-band Yagis, quads and verticals, curtain arrays, and more!

#5625 \$20*—Includes software

Volume 4 is out-of-print

ARRL
The national association for
AMATEUR RADIO

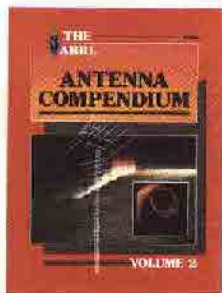
225 Main Street, Newington, CT 06111-1494
tel: 860-594-0355 fax: 860-594-0303



Volume 3

Quench your thirst for new antenna designs, from Allen's Log Periodic Loop Array to Zavrel's Triband Triangle. Discover a 12-meter quad, a discone, modeling with MININEC and VHF/UHF ray tracing.

#4017 \$14*



Volume 2

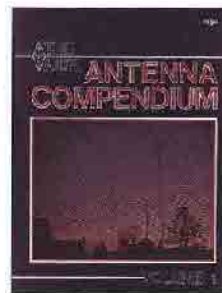
Covers a wide range of antenna types and related topics, including innovative verticals, an attic tri-bander, antenna modeling and propagation.

#2545 \$14*

Volume 1

The premiere volume includes articles on a multiband portable, quads and loops, baluns, the Smith Chart, and more.

#0194 \$10*



*Shipping: US orders add \$5 for one item, plus \$1 for each additional item (\$10 max.). International orders add \$2.00 to US rate (\$12.00 max.). US orders shipped via UPS.

Sales Tax is required for shipments to CT, VA, CA and Canada.

Order Toll Free
1-888-277-5289
www.arrl.org/shop

8 AM-8 PM
Eastern time
Mon.-Fri.

e-mail: pubsales@arrl.org

World Wide Web: <http://www.arrl.org/>

QEX 7/2002

CLOVER-2000

High Performance HF Radio Protocol

Fast, Reliable, Economical HF Data Communications

Specifically designed for high-speed data transmission over HF radio, the advanced CLOVER-2000 waveform and protocol is fast, reliable, and economical. CLOVER-2000 is the proven solution for your HF data communications problems.

High Throughput, Adaptive ARQ, & Hardware Implementation

For use with any quality HF SSB transceiver, the CLOVER-2000 waveform occupies a 2kHz bandwidth. With a data rate of 3,000 bits/sec over standard HF SSB radio channels, CLOVER-2000 delivers an "error-corrected" throughput of up to 2,000 bits/sec — *inclusive* of ARQ overhead.



Available in the HAL DSP-4100/2K DSP HF modem, CLOVER-2000 automatically adapts to real-time HF propagation conditions. The modem measures Signal-to-Noise (SNR), Phase Dispersion (PHA), and Error Corrector Activity (ECC) of each data block received. These parameters determine which of the five modulation formats should be used for the next 5.5 second transmission. In contrast, other currently available adaptive systems only use one or two modulation formats basing the format selection on past history of received errors - *not* on real-time measurements of actual HF channel parameters.

Bi-Directional ARQ

The CLOVER-2000 ARQ protocol includes real-time adaptive bi-directional transmission on the ARQ link — *without* special "over" commands. Any data, including executable programs, digital sound files, images, and text files can be sent without modification using CLOVER-2000.

Error Correction Coding

CLOVER-2000 uses Reed-Solomon error correction coding to combat burst errors that commonly occur during HF transmissions. Other ARQ modes may not include in-block error correction, or use formats that require long interleave times to combat burst errors, thereby significantly reducing throughput.

CLOVER-2000 — the proven "waveform of choice" for thousands of satisfied customers around the world!

1972 • Thirty Years of Innovation and Excellence • 2002



HAL COMMUNICATIONS CORP.

P.O. Box 365

Urbana, IL 61803-0365

Phone: 217-367-7373 • FAX: 217-367-1701

www.halcomm.com • halcomm@halcomm.com

Please call or visit our
website for more information!